Horizon 2020

Project acronym:	**LASH FIRE**
Project full title:	**Legislative Assessment for Safety Hazard of Fire and Innovations in Ro-ro ship Environment**
Grant Agreement No:	**814975**
Coordinator:	**RISE Research Institutes of Sweden**

LASH FIRE

Deliverable D09.2

Developed ro-ro spaces fire detection solutions and recommendations

August 2023

Dissemination level: **Public**

Call identifier: H2020-MG-2018-Two-Stages Starting date: 2019-09-01 Duration: 48 months
MG-2.2-2018: Marine Accident Response, Subtopic C)

Abstract

Early detection of fires on ro-ro ships can mitigate the loss of lives and cargo. Currently, heat and smoke point detectors are the most common detectors used on board ro-ro ships, but there are several technologies with the potential to decrease the time before a fire is detected, such as linear heat detectors, infrared (IR) flame wavelength detectors, IR thermal imaging cameras, and video fire detection systems. During the LASH FIRE project, the performance of traditional and new fire detection technologies has been investigated using simulations and laboratory experiments for open and closed ro-ro spaces. In addition, operational evaluations have been conducted on board a ro-ro ship for over a year, followed by fire experiments on board, making it possible to assess and demonstrate the performance of different technologies on board. The present document discusses the developed ro-ro space fire detection solutions and recommendations.

This project has received funding from the European Union's Horizon 2020 research and innovation programme under grant agreement No 814975

Document data

Document Title:	D09.2 – Developed ro-ro spaces fire detection solutions and recommendations		
Work Package:	WP9 – Detection		
Related Task(s):	T09.7, T09.8, T09.9, T09.10		
Dissemination level:	Public		
Deliverable type:	Report		
Lead beneficiary:	3 – FRN		
Responsible author:	Davood Zeinali		
Co-authors:	Reidar Stølen, Ellen Synnøve Skilbred		
Date of delivery:	2023-08-20		
References:	D04.8, D04.10, D05,6, D05.7, D05.8, D05.9, D07.7, D08.10, D09.1		
Approved by	Ola Willstrand on 08-08-2023	Maria Hjohlman on 10-08-2023	Robert Benitz on 18-08-2023

Involved partners

No.	**Short name**	**Full name of Partner**	**Name and contact info of persons involved**
3	FRN	RISE Fire Research AS	Davood Zeinali, davood.zeinali@risefr.no; Ellen Synnøve Skilbred, ellen.synnove.skilbred@risefr.no; Reidar Stølen, reidar.stolen@risefr.no
2	VTT	Teknologian tutkimuskeskus VTT Oy	Tuula Hakkarainen, tuula.hakkarainen@vtt.fi; Nikhil Verma, nikhil.verma@vtt.fi
24	DFDS	DFDS AS	Sif Lundsvig, silun@dfds.com
20	FKE	Fike Corporation	Rick Jeffress, rick.jeffress@fike.com
6	UNF	Unifire AB	Roger James, roger@unifire.com; Mattias Eggert, mattias@unifire.com
9	APS	AP Sensing	Bernd Drapp, bernd.drapp@apsensing.com; Robet Benitz, robert.benitz@apsensing.com
1	RISE	RISE Research Institutes of Sweden AB	Stina Andersson, stina.andersson@ri.se; David Schmidt

Document history

Version	Date	Prepared by	Description
[01]	2021-02-17	Reidar Stølen	Draft of structure
[02]	2023-03-15	Davood Zeinali	Draft of final report except onboard testing, circulated to reviewers
[03]	2023-08-04	Davood Zeinali	Final report circulated to reviewers
[04]	[2023-08-18]	Davood Zeinali	Final report

Content

1 Executive summary

This deliverable presents the results of simulations, laboratory tests, and onboard evaluations of the detection systems for open and closed ro-ro spaces during the LASH FIRE project. The work related to detection on weather decks is reported in deliverable D09.1 “Developed weather deck fire detection solutions and recommendations" [1].

1.1 Problem definition

Fire consequences for the ship, crew and cargo should be minimized as much as possible. For the detection system, this means that time is essential, such that the quicker the system can respond to a fire, the higher are the chances to control and extinguish the fire to minimize its consequences. Conventional heat and smoke detectors are commonly used in open and closed ro-ro spaces. These detect the conditions at their specific location and may have a delayed response to fire due to active mechanical ventilation or natural wind conditions which can dilute the smoke and direct hot smoke away from the detectors. On the other hand, optical sensors such as thermal cameras do not depend on the detection of smoke or heat but are limited by their field of view and must be able to distinguish a flame or hot spot from items of similar appearance and temperature, such as vehicle hot exhaust pipes and engines, to avoid triggering too many nuisance alarms. Linear heat detection systems offer advantages of fire location identification and monitoring the thresholds and rate of rise of temperatures, and thus they are also candidates for early fire detection but will only work for detection of fires that heat up the sensor cables enough for the system to be triggered. These technologies must therefore be fully understood for their application in open and closed ro-ro spaces in order to provide detection at the earliest stages of fire development.

1.2 Technical approach

Several detection systems detecting heat, fire and smoke have been tested for use in ro-ro spaces in this project. The systems were studied through numerical simulations, laboratory experiments, as well as operational evaluations and fire experiments on board a ship. The results from laboratory experiments and simulations were used to select the best candidate solutions to be tested on board an operational ship. The simulations also provided information on fire locations and conditions most interesting to evaluate during onboard experiments. The detector systems were left to operate and record potential nuisance alarms for one year during normal operations before the final fire tests on board were conducted to verify their ability to detect fires on board.

1.3 Results and achievements

The numerical simulations showed that for both open and closed ro-ro spaces, the traditional smoke detectors detected the fire fastest in almost all scenarios, although this assumes that the smoke detectors are fully functional. This is while point detectors tend to get damaged easily especially in open ro-ro spaces by salt spray and humidity, based on operator experience. In the simulations, the smoke detector failed to detect the fire in one open ro-ro space scenario only, and for this scenario, the linear heat detector succeeded in detection. For the open ro-ro space simulations, an unfavourable combination of fire location and wind condition could lead to fire not being detected by some detection technologies or could lead to very long activation times. Fire in the closed ro-ro space could also be detected from an exhaust ventilation duct serving the space, but much larger delays are expected than with conventionally located detectors. Among the non-conventional technologies, the simulations showed that flame wavelength detectors and video smoke detectors were the most promising for the open ro-ro spaces. However, both video analytics systems and thermal imaging cameras could have difficulty in detecting the fires when the fire location and wind conditions are unfavourable. For example, a tilted flame or smoke plume by wind in conjunction with

an unfavourable fire location can delay the detection because the heat and fire effluents are diluted and hidden from the detector's field of view. For the closed ro-ro spaces, the simulations showed that flame wavelength detectors and video smoke detectors were the most promising technologies among non-conventional detection technologies.

The laboratory tests showed how different detectors are suitable for detecting different types of fires. The smouldering fires, which produced a lot of smoke but little heat and no flames, were often detected by point smoke detectors, although these detectors were found to be less responsive in the presence of wind. The smouldering fires were also detected by thermal imaging detectors in a few cases but not by linear heat detectors and infrared (IR) flame wavelength detectors. The linear heat detection systems were superior to conventional detectors when it came to the detection of ethanol fires which produce significant heat. Optical detectors (referring in this document only to detectors that can view/see the fire from a distance, such as thermal imaging cameras) could detect some of the ethanol fires while the conventional point smoke/heat detectors were less suited for detecting this type of fires. In general, the linear heat detection system detected more of the laboratory fires than the optical detectors, but the fewer responses of the optical detectors were usually faster than those of the linear heat detection systems. As expected, the optical detectors could only detect fires when the flames were visible in their field of view. Regarding obstacles, the laboratory tests showed that the presence of beams in the ceiling can make the smoke accumulate in one area and delay the movement of the smoke towards detectors installed on the ceiling further away from the fire, and that the presence of tall and wide structures near a fire, such as a truck or a car, can make the temperature above the fire increase significantly. In laboratory tests with lithium-ion battery fires, the smoke initially dropped to the floor and the CO concentrations exceeded 40 ppm at the floor but decreased with height. It took approximately 30 min before the smoke detectors in the ceiling were triggered.

Based on the results of the simulations and laboratory experiments, installations were made on board a ro-ro ship for operational evaluations and fire testing, namely, on Hollandia Seaways (a DFDS ro-ro cargo ship). The ro-ro space installations included a linear heat detection system in the uppermost open ro-ro deck, a multi-spectrum infrared flame detector in the same open deck, and a video fire detection system in the main deck (closed ro-ro space). After a year of evaluations, it was found that implementing different (adaptive) detection settings is unnecessary for the systems because of the very low rate of nuisance alarms. The video analytics algorithm in the closed deck only produced nuisance alarms when the crew did a routine washdown of the deck. Similarly, the linear system (which was fibre-optic) produced nearly one alarm per month with the most sensitive setting above running reefer trucks, while the IR flame wavelength detector did not produce any nuisance alarm. This is considered a great improvement compared to the nuisance alarm rate of conventional detectors in the open ro-ro decks which habitually go off due to sea spray or heavy rain from the shipside according to the ship's chief officer.

Several experiments were also conducted on board the ro-ro ship at the end of the operational trial using a propane burner and a fog machine. These experiments indicated that the systems which spent over a year on board were still responsive to flame and smoke as well as they were during the laboratory experiments. Most remarkably, the conventional point heat detectors did not activate after 10-15 min during the propane fire experiments in the open ro-ro space (possibly due to the unfavourable wind direction), whereas the linear system was able to detect the fire in two of the experiments within a few minutes. Similarly, video analytics was able to detect the smoke produced by the fog machine based simply on its visual characteristics.

All in all, linear heat detection systems are found to be very useful for fire detection in ro-ro spaces, especially for open decks where linear systems can perform better than conventional heat sensors. Moreover, video analytics is found to be very useful for closed ro-ro decks where light conditions are stable and just a few cameras can be used to cover a large distance for fire detection without triggering nuisance alarms.

It is worth noting that the results of the conducted simulations, laboratory experiments, and onboard evaluations are not independent of the tested ship geometry, fire location, and environmental conditions. Therefore, each desired system is recommended to be tested in the relevant environment before major installations.

1.4 Contribution to LASH FIRE objectives

This deliverable is submitted through work package 9, i.e., WP9, the overall objective of which is to provide quicker and more reliable fire detection, localization, and confirmation in all types of ro-ro spaces by evaluation of new and advancing technologies. The present document addresses goal (9-B) which is to develop, demonstrate and evaluate, in full-scale, alternative and complementing means for quick and reliable detection on closed and open ro-ro spaces.

1.5 Exploitation and implementation

The evaluations presented in this deliverable show benefits and drawbacks with the different technologies, providing information on scenarios the detectors are most suitable for detecting. This is important information for manufacturers of the detection technologies, the suppliers, the installers, and the final users of the systems. The deliverable also demonstrates the complexities of evaluating the detectors and provides recommendations on how to test detectors and how to select a set of detectors for a specific environment.

2 List of symbols and abbreviations

B2B	Business to business, type of trade
BEV	Battery electric vehicle
CCR	Cargo Control Room (used during cargo operations)
CCTV	Closed-circuit television
C-ITS	Cooperative intelligent transport systems
CO	Carbon monoxide
DTS	Distributed temperature sensing
EV	Electric vehicle
FTP	International Code for the Application of Fire Test Procedures
FSS	International Code for Fire Safety Systems
HF	Hydrogen Fluoride
HGV	Heavy Goods Vehicles
HRR	Heat Release Rate
IACS	International Association of Classification Societies
IAMCS	Integrated Alarm, Monitoring and Control System (equipment)
ICE	Internal combustion engine
IMDG	International Maritime Dangerous Goods (dangerous cargo)
IMO	International Maritime Organization
IR	Infrared radiation
RCM	Risk control measure
RCO	Risk control option
Ro-pax	Vessel type with both roll-on roll-off cargo and passengers
RoR	Rate of rise
Ro-ro	Vessel type with cargo type roll-on roll-off
SOLAS	International Convention for the Safety of Life at Sea

3 Introduction

Main author of the chapter: Reidar Stølen, FRN

A fire on a ro-ro deck can develop and spread very rapidly, and early detection is essential for controlling the fire with the available fire extinguishing equipment and systems on board. A fire detection system that raises an alarm early in the fire development is crucial for early response, but the detection system should not be so sensitive that it triggers frequent nuisance alarms.

As per SOLAS II-2/3 [2], ro-ro spaces are defined as “spaces not normally subdivided in any way and normally extending to either a substantial length or the entire length of the ship in which motor vehicles with fuel in their tanks for their own propulsion and/or goods (packaged or in bulk, in or on rail or road cars, vehicles (including road or rail tankers), trailers, containers, pallets, demountable tanks or in or on similar stowage units or other receptacles) can be loaded and unloaded normally in a horizontal direction”.

Areas completely exposed to the weather from above and at least two sides are defined as weather decks, while open ro-ro spaces are defined by being either open at both ends or, having an opening at one end and being provided with adequate natural ventilation effective over its entire length through permanent openings distributed in the side plating or deckhead or from above, having a total area of at least 10% of the total area of the space sides. The ro-ro spaces that are not considered as open ro-ro spaces or weather decks are defined as closed ro-ro spaces. As a reference criterion, it can be considered that a vehicle space that needs mechanical ventilation is a closed vehicle space.

Both open and closed ro-ro spaces are required to have installed fire detection systems. The most common systems are point detectors which are mounted in the deckhead to detect smoke, heat, or both. The maximum distance between detectors is 9 m for point heat detectors and 11 m for point smoke detectors.

In open ro-ro spaces, the ambient conditions like wind and saltwater droplets create challenging conditions for fire detectors. In high wind conditions, the smoke and hot gases from a fire can be transported a significant distance from the origin and diluted with fresh air before reaching a detector that can trigger an alarm. Over time, the environmental conditions also cause challenges to the detectors as small droplets of salt and other pollutants may enter the detectors and cause nuisance alarms or lead to a need for replacing the detectors. Another potential challenge is the presence of ceiling beams that can both block the line of sight and obstruct the flow of smoke across the deckhead and delay the detection if the smoke needs to travel across high beams to reach the closest detector.

Conventionally, the ro-ro spaces are equipped with point smoke and heat detectors. However, the response of these detectors can be significantly delayed if ventilation is diluting the smoke or moving it away from the detectors, especially in open ro-ro spaces where there may be strong ventilation through the large openings on the sides of the deck. Accordingly, alternative detection systems must be evaluated to circumvent the issues faced by the conventional point detectors.

This deliverable presents the LASH FIRE work conducted to evaluate the potentials of alternative detection systems for use in open and closed ro-ro spaces, providing recommendations based on the results of the study. The work related to detection on weather decks is reported in deliverable D09.1 “Developed weather deck fire detection solutions and recommendations” [1].

4 Conditions in ro-ro spaces

Main author of the chapter: Sif Lundsvig, DFDS

4.1 Main fire hazards in ro-ro spaces

A general monitoring of fire hazards is essential to safety on board, but several specifically common sources of fire hazards demand special attention:

1) Faulty refrigerator trucks known as reefer units or reefers
2) IMDG (International Maritime Dangerous Goods), i.e., dangerous cargo
3) Leaking IMDG class 3, i.e., flammable liquids such as petrol and diesel, on the upper deck
4) Flammable materials such as paint or oil
5) Fires originating from hot work of all kinds and short circuits
6) Car carriers (for road transport) loaded with old cars
7) Trucks with additional equipment connected in the driver's cabin (such as heaters, kettles, or navigational equipment)
8) Alternative fuel vehicles

Note that the numbering above does not symbolize a risk assessment, nor what is more likely to occur.

Detection of faulty reefer units are currently being dealt with by a quick visual inspection during loading of cargo, when the crew on board also connects the reefer unit. The visual inspection is based on experience, and new crewmembers get instructions by colleagues if needed. However, no official job training is in place for this job, as it is up to the crew on board how they manage this. The ro-ro vessels do not have a designated fire patrol when sailing or in port, unless this is for some reason deemed necessary by the crew on board. The reefer units are nonetheless checked every 4th hour to register the temperature. To avoid short circuits in reefer units, the maintenance of reefer cables and plugs on board the vessel is important. If the mate or deckhand on board finds that the cables are not up to standards, they are sent ashore for repair or to be discarded by a shore-based unit. The plug on the reefer itself, however, is controlled and maintained by the reefer unit's owner. Improvements of cable storage could help extending lifetime of cables, as the current storage does not protect them from water or dirt.

When carrying cars, DFDS has a company standard that batteries of cars on board must be disconnected before loading. This applies only for cars transported B2B, not for private cars.

Regarding equipment in truck drivers' cabins, the drivers are instructed that it is not allowed to operate and utilize such equipment during the voyage. However, this instruction is not always followed, and besides being warned by the crew, it has no consequences to the drivers.

To minimize the fire hazard of IMDG cargo, the unit, corresponding paperwork, and any special transportation requirements are checked upon loading, and proper segregation is ensured (see section 5). Beside this, no special monitoring is provided for IMDG cargo.

Flammable materials, including paint, oils, etc., are typically concentrated in paint lockers, engine room workshop areas and in the galley. These places typically have separate fixed firefighting CO_2 systems.

4.2 Fire detection measures

This chapter gives a general description of fire detection measures on board. In this regard, it must be noted that the conditions vary from one ship to another, both as a matter of how the ships are operated and due to specific configurations on each vessel. Moreover, if the crew find that supplementary measures are needed during special circumstances (e.g., when doing hot work on board), they may dispatch a crewmember as a fire-watch or implement other means necessary given the situation and the options available on board. In addition, detection methods vary depending on what area is regarded on board. On DFDS vessels, the means of fire detection are regulated by a combination of SOLAS and national Danish authority requirements. These regulations are what the design companies use when fitting the ship with fire detectors.

The fire detection systems consist of two main parts: the Integrated Alarm, Monitoring and Control System (IAMCS), and the individual detector sensors that can identify smoke, heat, or both. IAMCS connects all the detectors with the general alarm, such that the detector signals can be processed by the fire panel to show the location of the fire alarms on the ship. The IAMCS is placed and operated on the bridge but might have slave panels in fire stations and the engine control room.

In general, it is required for the vessels to be equipped with an addressable fire detection system covering passageways, control stations, service spaces, all types of cargo decks (except open weather decks), engine rooms and machinery spaces, and so on. Systems include a computerized central unit with graphic display. The fire detection system must also include the indication and control system for fire doors and fire dampers, if any, and shall have built-in monitoring circuits that are intended to monitor that the equipment is in satisfactory order, indicating any faults that could prevent a fire alarm.

If a true alarm condition is activated by detectors, the alarm will sound. A time delay of up to two minutes is normal (for detectors only), however a pre-warning is given on the bridge. Subsequently, the general alarm will then be activated. If a push button is manually activated, it will automatically and immediately activate alarms – no time delay is permitted here. Timers for temporally disconnecting fire detectors in cargo decks are installed in the Cargo Control Room (CCR). It should be possible to disconnect each deck for up to six hours, in order to make repairs. Timer switches for loop-disconnection are fitted in the engine room workshop (not linked to manual push buttons). The power supply is 230 volt AC, from the emergency switchboard and in-built 24 volt DC batteries with charger.

All fire detectors are located so that they are easily accessible for testing. Optical and ionizing smoke detectors, rate-of-rise type temperature detectors, and infrared (IR) flame detectors are installed as seen fit and according to the Class and IMO/SOLAS rules. For ro-ro areas, a combination of smoke and heat detectors are installed. Accommodation ventilation fan stops automatically when the fire alarms go off and by the emergency stop pushbutton on the bridge. Manually operated alarm pushbuttons are installed throughout the vessel according to the regulations, and a general alarm is installed covering the entire ship.

Fire patrol is only mandatory on passenger vessels.

4.3 Desired developments for detection systems

For designing a future fire detection system, the following should be considered:

- An ideal detection system should produce no nuisance alarms but still be able to detect fires at an early stage such that they can be extinguished easily.
- The system should be as simple as possible in terms of setup, maintenance, and use.

- The system must be approved by SOLAS and classification societies.
- The system should require a minimum amount of space and not interfere with the cargo space.
- A good fire detection system must be easy to install on board and should be able to integrate all means of fire detection on board, so that one, and only one, system covers all fire detection as well as remotely released fire extinguishing systems.
- If a new fire detection system is to be implemented on board, it should either completely substitute the existing system, so that this can be un-installed, or be integrated with the existing system.
- Any new fire detection system is expected to be made of a material that does not worsen the situation of a developing fire if caught on fire itself.
- For setting up equipment on board, it should be considered that pulling cables is extensive work and expensive, as metalwork is to be expected, and that cables going through watertight departments complicates the setup.
- With regards to maintenance, the less manual inspections and care are needed the better. When all smoke detectors on board are to be tested, this takes 2 persons around 2-4 weeks to complete depending on the size of the vessel. Accordingly, a self-testing system would save a lot of time and can make sure that no detector is missed or unchecked. Such a system must notify the crew in case of errors or sabotage.
- With regards to alarms, it is important that a fire detection system send a clear signal to the bridge indicating where the source of the fire is located. It is also important that if a fire starts and begins to spread, the system does not keep sending alarm messages that disturbs the already stressful work on the bridge of taking control of the situation. Instead, the system should support the officers to make informed choices and to keep an overview of the situation. This does *not* mean that the system should stop giving feedback on the development of the fire, just that it could be done in a better way than current procedures.
- Spare parts should be easy and cheap to attain, and repairs should be easy to make. It is also expected that the components are made of sufficient quality to ensure a long life for the system, taking life cycle assessments into account. In this regard, materials with the least environmental footprint should be preferred.
- A fire detection system should be able to run without downtime or have a back-up solution if downtime should occur.
- A new fire detection system should take less of the crew's time than the systems in place today.
- A new system that could enable inspection of cargo holds to be done from the bridge in a thorough manner without adding to the number of sensors and cameras installed could add value and safety on board.
- Digital manuals for all equipment and systems, so that it is easy to search for specifics of the equipment or system, would reduce time used to gather necessary information in a critical situation.
- The fire detection system should never rely on any kind of shore connection or internet access. It should always be fully functional when using onboard systems.
- Decision support from AI. An interesting improvement to look further into, would be to train an AI system to sort out which detectors are active, show it on a 3D map, and come up with an attack plan, including where cooling should be applied and what means of fire extinguishing should be used depending on what type of cargo have caught fire.

- Detection systems should ideally be able to localize the fire accurately and be able to provide the location information to autonomous fire suppression systems. Such systems will improve the safety of fire confirmation and suppression by reducing the need for crew members close to the fire area. Moreover, the system components are expected to be much more resistant towards heat and smoke compared to crew members.
- For the detection of thermal runaway events in electric vehicles, it must be investigated what gases are emitted first and what time delay is expected for detection using detectors mounted along the ceiling.
- The impact of ventilation must be considered.
- Heat detection should be investigated, even if a build-up of heat may happen well after smoke generation. It might be needed to look into detection options in locations closer to the fire sources.

4.4 Conclusion

The perfect fire detection system does not exist, but there are some functions that could have other shapes and ways to operate than current systems do, including new non-conventional technologies. However, simplicity, reliability and costs are the most important factors for a new fire detection system if it is to be useful to the maritime industry.

Further clarifying the limits of official regulations and where the ship company's own demands start is of further interest for the development of new systems because company specifications for vessels do not distinguish between the two.

It is critical to keep the fire detection systems up to date because cargo with new materials and technologies enter the cargo space continuously, thus requiring upgrades in the capabilities of the fire detection systems on board.

5 Fires in open and closed ro-ro spaces

Main author of the chapter: Sif Lundsvig, DFDS

5.1 Combustible materials on board

Vehicles contain the main combustible materials available in ro-ro spaces, including their motor fuel or source of power, as well as their cargo, especially the cargo of trucks and trailers that can represent a large amount of combustible material.

Presently, the main motor fuel or source of power for vehicles is either petrol or diesel. Alternative fuels and power sources, which may be more ubiquitous in the future, currently include batteries, liquified or compressed methane or hydrogen, as well as liquified propane and ethanol [3] [4]. These power sources have different elements and characteristics, so each behaves differently in a fire.

Batteries are comprised of cells that generate electricity using electrolytes and electrodes placed in designated sections. Under certain circumstances, e.g., a physical damage to the battery sections, undesirable chemical reactions may be triggered that can generate heat, oxygen, and flammable gases, leading potentially to combustion and thus generation of more heat. This could create a state of uncontrolled self-heating known as a thermal runaway event, which is difficult to extinguish as it does not require external oxygen or heat to sustain itself. Such an event sometimes happens after a fire is thought to be extinguished. Most battery electric cars today use lithium-ion batteries [5], and it is of great interest to detect their thermal runaway at an early stage. An overview of the literature in this area has been made as part of the LASH FIRE project and is included in Annex A.

Liquified hydrogen and methane are cryogenic liquids, so they will evaporate rapidly when they are released. This is while ethanol, petrol and diesel are liquids under ambient conditions. Propane can be liquified when pressurised, but it flashes to gas when it is released. Moreover, compressed hydrogen and methane are kept in a gaseous form. The initial stage of a fire for each of these fuels will be different, which affects how they can be detected. For instance, a pure hydrogen jet flame from a fuel cell vehicle can be hardly visible and will not produce any soot or visible smoke. However, in a real fire scenario, due to the close vicinity of cargo on ro-ro ships, it is likely that a real fire will include different combustible materials and fuels. This will make the flame more visible.

Gases leaking from vehicles can also be detected before they ignite. Gases that are heavier than air, like propane, will flow down and accumulate in low points. Sensors for these gases should hence be placed low. Lighter gases like hydrogen and methane will rise and the respective sensors should be placed on the deckhead to be able to detect these gases. However, regardless of the initial fuel source, a vehicle fire will likely include several other combustible materials like plastic which can be detected using smoke detectors.

Considering Battery Electric Vehicles (BEVs), it has been reported that the heat release rate and total heat release of BEV fires are comparable to those of similar-sized Internal Combustion Engine (ICE) vehicles, but the peak of the heat release rate is increased by the bursting of the gasoline tanks in the case of ICE vehicles and by the ignition of the battery packs in the case of BEVs [6]. Moreover, a spillage or splash of the liquid fuel from an ICE vehicle makes it easier for the fire to spread to nearby vehicles. Jet flames from the battery packs of BEVs can also promote fire spread, but they last only tens of seconds or shorter. In a small under-ventilated environment, the accumulation of unignited gases released from a decomposing battery can become explosive, but the spaces on board ro-ro ships are very large and well-ventilated, such that explosive conditions cannot be created easily, even though a sudden burst of flames will still happen when the unignited gases find a source of ignition.

Trucks, formally referred to as Heavy Goods Vehicles (HGVs), i.e., freight vehicles of more than 3.5 tonnes, are designed with larger fuel tanks and more combustible materials than regular passenger vehicles, e.g., because of their bigger tires, cargo hold cover, etc. However, the most significant difference of HGVs compared to smaller vehicles comes from their significant amount of cargo. Each truck may contain several tonnes of combustible material in solid, liquid or gas state. The combustible material in trucks may be classified as dangerous goods but may also be any other combustible material. The dangerous goods are declared at loading and placed with the proper segregation according to the category of the cargo.

5.2 Ignition sources

Refrigeration units, known as reefers, and power connections serving these units are reported to be the main fire causes on ro-ro decks according to a survey of fires between 2005 and 2016 made by DNV-GL [7]. The survey studied 35 fires and listed the cause of fires where this information was known. The cars transported as cargo are assumed to be in poorer condition than cars that roll on the ship by their own power. There was also one case with a fire starting in a new car, but considering the large number of new cars that are transported, the ignition risk of new cars is very low on average.

Reefer units carry sensitive cargo such as medicine or fish that must be kept cold under refrigerated conditions. Given that the engines of the vehicles are stopped during the voyage, reefer units are connected to the ship's power supply to maintain refrigeration without relying on the motor engine power. Short circuits or other faults in the related connections and units are known to represent a fire hazard on board [7]. Moreover, in cases where there are too many reefer units on board such that the number of charging points is not sufficient, some units may be allowed to have their engine running in an idle mode during the voyage. Such units will therefore maintain a hot engine and keep producing exhaust fumes, which could be considered a potential fire hazard.

Electric Vehicles (Evs) may rarely be ignition sources, and they are not charged on board as a common practice today. However, even if they are to be charged on board, the ignition probability of Evs while charging is very low. Only 4 cases of fires in charging Evs were found globally in a recent survey [8]. Three of these fires started while charging at high power and the fourth fire started in an extension cord. It is expected that ignition is more likely linked with higher charging currents. Accordingly, to charge several electric vehicles simultaneously, the ship needs to regulate the charging current appropriately to be able to distribute the available power to the connected vehicles safely and efficiently. If the duration of the voyage is long, the charging power can be relatively low to make the charging process safer. Moreover, the charging process can be made safer if the battery capacity, state of charge, and desired power of each vehicle can be communicated automatically to the charging system. This type of system can also be used for billing each car owner according to the delivered energy and/or power [8].

Other vehicles can also represent an ignition source caused by faults in their engine or electric system. Such faults that can cause a fire are more likely in old vehicles than new ones. The diverse cargo of the vehicles can also contain ignition sources, e.g., cooking appliances in camper vans or loose batteries stored improperly that could initiate or contribute to a fire in the event of a fault or external source of heat. Moreover, when the vehicles are loaded, they can have hot engines, exhausts, and brakes, which are sources of heat. However, these parts will normally cool down to ambient temperature soon after the vehicles are switched off.

5.3 Fire development

5.3.1 Fires in car parks

Recent fires in car parks have shown that it can be difficult to limit the spread of fires between cars in such closed environments. The fire in Kings Dock car park in Liverpool, in December 2017, is one of the large fires that have occurred in car parks recently. In this fire, approximately 1150 cars were burnt. From the time smoke was first visible in the car park CCTV, it took 14 minutes until the fire alarm was manually activated and an additional 13 minutes until external firefighting from the fire brigade began. The assumptions on the fire spread in the car park were based on an old paper stating that the fire would most likely not spread between vehicles and, if it did, the fire brigade would be in attendance within 3 to 4 minutes. Two hours after the start of the fire, the fire brigade evacuated, unable to control the fire. The evaluation of this fire concluded that the risk of fire spreading between vehicles were underestimated and that the vertical spread of fire between levels was aided by the burning fuel dripping through floors via the central drainage system [9].

A similarly large car park fire broke out at Stavanger airport Sola in Norway in December 2019 [10]. The fire was able to spread dramatically. Both the municipal fire service and the airport fire service responded, but they were not able to control the fire for several hours. A large part of the building structure collapsed and approximately 300 cars were destroyed in the fire [11]. Based on the subsequent investigations [10], there was no automatic fire alarm system present in the car park. Moreover, strong wind helped accelerate the spread of fire. At the time of the fire, the wind was 10-13 m/s from the south [12], which could influence not only the speed but also the direction of fire spread between vehicles. The fire brigade from the airport was on site in nearly 10 minutes after the fire was reported, but they quickly realised that they were unable to control the fire [13], as the fire had already spread to several vehicles before the fire brigade was on site [10].

The width of the parking space dedicated to each car at the Stavanger airport Sola car park was 2.5 m, and a comparison of other indoor parking spaces shows that they are in the same range or slightly narrower [14]. This reveals that the average distance between the parked cars is small, such that flame spread is a significant issue to consider.

None of the said car parks had automatic fire suppression systems at the time of the fire incident. This is while experiments have shown that extinguishment systems such as sprinklers could have significantly delayed the development of fire and its spread to other vehicles before the attendance of the fire service [15]. Moreover, the parking houses were naturally ventilated, and the initial fire started in a part of the parking that was under a roof. Therefore, the fire scenario is very comparable to that in an open ro-ro space on a ro-ro ship (discussed in the next section).

5.3.2 Comparison of ro-ro deck and car park fires

Compared to car parks, ro-ro ships have the vehicles parked much closer to each other. This is to maximize the capacity of the ships for carrying vehicles. The distance between cars, from bumper to bumper, can be as low as 0.6 m according to measurements made as part of the LASH FIRE project on several Swedish and Danish ro-ro ships following local regulations. Moreover, the typical lane width for a ro-ro deck is approximately 3 m for trucks and 2.2 m for passenger cars. Accordingly, the possibility and speed of fire spread from one vehicle to several other vehicles is higher compared to those in car parks where each car has free access to drive out of the parking space. Such free passageways inside the car parks will serve as fire barriers that can limit or slow down the spread of fire between the different sides of the car park. The lack of such free passageways on ro-ro ships contribute to easier and quicker fire spread in ro-ro spaces.

The fire on board the Urd that occurred in 2014 is an example of a fire in a closed ro-ro space that did not spread to more than one vehicle. A light fixture had failed, ignited, and fallen on top of the tarpaulin of a truck below. The fire was manually detected at an early stage and the sprinklers were activated within 10 minutes after the fire was observed. The fire was detected by smoke detectors 6 minutes later than the first manual observation. These smoke detectors were located approximately 20 m away from the fire, but still responded faster than the heat detectors that were installed in the section of the ship where the fire started. Within 30 minutes, the fire was extinguished by the sprinkler system and manual firefighting with hoses. Only limited damages to the truck and the tarpaulin were observed after the fire [16].

Some types of dangerous goods are only allowed in open ro-ro spaces. These dangerous goods may or may not be combustible, but it would lead to a higher concentration of dangerous goods vehicles than on the closed ro-ro spaces. The containers for dangerous goods are designed to contain the cargo safely, but in the event of a fire, the contents may be released, for example, through a pressure relief device. If these systems are working as intended, these releases would not be expected until the container has been exposed to a significant fire for a certain time. Hence, detecting a fire at an early stage is critical for initiating firefighting before the fire has reached an uncontrollable size, so that fire spread can be mitigated.

The most important lesson from the fire incidents is that the fire can rapidly spread between vehicles and that within a short amount of time the fire can become difficult to control. This means that it is important that the fire is detected at an early stage when it can still be controlled and prevented from spreading to other vehicles.

6 Detection technologies

Main author of the chapter: Davood Zeinali, FRN

6.1 Reviewed detection methods

There are several types of detection principles for detection of fires available on the market. An overview of available detector types that were reviewed in the LASH FIRE project is given in Table 1. These detectors can sense the presence of flames, smoke, convective or radiative heat, or a combination of these elements.

Table 1: Fire detection principles reviewed in the LASH FIRE project.

Type of detector	**Measurement parameter**	**Covered area**	**System architecture**
Video detection of smoke/flame	Visual characteristics of flame/smoke	Field of view of camera	Raw video signals processed and analysed by software in a central server. Different algorithms are used for the detection of smoke and the detection of flames.
Infrared thermal imaging detection	Emitted infrared radiation	Field of view of camera	Local or centralised processing
Flame (wavelength) detection	Emitted Infrared (IR) radiation from flames	Field of view of detector	Sensors detect radiation in the full field of view. Array detectors use several sensors to be able to localize the flame within the field of view.
Light beam linear smoke detection	Attenuated infrared (IR) light absorbed/reflected by smoke along the light beam.	Straight line of light beam, up to about 100 m	Some signal processing is required to avoid nuisance alarms due to blocked light beam, etc.
Acoustic detection	Characteristic sound from a fire	Depends on background noise and type of fire	Requires signal processing and analyses of the sound
Point detectors	Smoke particles, and temperatures	Measures single point	Sensors, data processing and communication in each unit
Linear heat detection	Temperature	Along a cable, up to 16 km [17]	Central detection unit. Only cable mounted throughout the ship.
Aspirating smoke detection	Smoke particles and/or gases	Gas sampled and mixed through a network of pipes with small holes	Central detection unit with high sensitivity sensors. Only pipes aspirating air is mounted throughout the ship

The most common types of fire detectors in ro-ro spaces are point smoke and heat detectors. These sensors detect local conditions where they are installed, such that they will only detect levels of heat or smoke in the immediate vicinity of the detector device, even though the heat or smoke may be coming from a distant fire source (e.g., due to wind effects).

The overhead of the open and closed ro-ro spaces acts as a barrier for smoke and heat rising from a fire. This means that the smoke and hot gases will accumulate close to the overhead and make them easier to detect. The assumption for this to happen is that the combustion products from the fire are hot and lighter than the ambient air so they will rise from the origin of the fire. In cases where the heat release from the fire is small, or when the smoke is cooled or blown away, this might be less effective. Moreover, the overhead is in most cases uneven due to the beams and girders spanning the ro-ro space. This will obstruct the horizontal spread of hot smoke across the overhead, thereby delaying the transport of smoke towards the nearest detector which might be several beams away.

Optical detectors (referring in this document only to detectors that can view/see the fire from a distance, such as thermal imaging cameras) can identify fires from far away, as long as the fire is within the field of view of the detector. Most of such optical sensors rely on infrared (IR) or ultraviolet (UV) light emitted from the fire source. For example, thermal cameras use infrared radiation to measure high temperature regions. Triple-IR flame wavelength detectors look at three thresholds of IR radiation and can identify flames from a long distance. Visible light is also used by detection systems such as video analytics algorithms that can recognise the visual characteristics of smoke or flame, e.g., colour, size, shape, flicker pattern, motion, and transparency.

The ventilation conditions in closed ro-ro spaces are predictable and controlled by the ventilation system. In open ro-ro spaces, however, the ventilation conditions are affected by the wind and by the openings on the sides of the ship. This makes the ventilation conditions unpredictable, with potentially very high air flows. These air flows can influence both the development of fire and the spread of smoke. If the smoke is transported away from the detectors or diluted to an extent where it is not able to trigger a detector, the activation of the fire alarm will be delayed significantly.

Several flag states require smoke detectors exclusively or in combination with other detectors. Standard heat detectors are considered less efficient because of the large space and height of the deck. On DFDS ro-ro spaces, a combination of smoke and heat detectors are installed as mentioned in section 4.1.

In open and closed ro-ro spaces, the available space between the top of the cargo and the overhead is limited. This means that the effective field of view of optical detectors will be narrower than what can be expected on weather decks where the sensors can be mounted high above the top of the cargo with no obstructions between the cargo and the sensors. Still, the space between the overhead and the top of the vehicles can be monitored by optical sensors. The detection of flame and smoke in between the vehicles would be challenging this way, but as soon as the heat, flame or smoke rises above the top of the vehicles, it may be detected in the same way as on a weather deck.

6.1.1 Optical detectors

The term "*optical detectors*" is used in the present document to refer to detectors that can view/see the fire from a distance. Because infrared (IR), ultraviolet (UV), and visible light emitted by the fire are electromagnetic waves traveling with the speed of light, they can be used for the quick detection of fire at a large distance using optical detection methods such as video detection, thermal imaging detection, flame detection, and light beam linear smoke detection. Such optical detectors do not need to be placed near the fire, smoke, or elevated gas temperatures to be able to respond quickly. This is much more efficient than the response of conventional smoke detectors and heat sensors that relies on the transport of smoke and hot gases to the vicinity of the detector for detection. Optical attenuation from smoke particles is also used as an optical detection principle in point smoke detectors, but these are categorized as point smoke detectors in the present document as they cannot detect optical fire signatures from a distance.

The term "*flame detector*" [18] is classically used exclusively for detectors that have sensors for detecting IR or UV light expected of flame radiation wavelengths commonly associated with combustion products such as carbon dioxide. Such detectors are not to be confused with other flame detection sensors that employ different technology such as video flame detection relying solely on visible light. Accordingly, to avoid confusions hereafter, the present document refers to classic flame detectors as "*flame wavelength detectors*," and especially uses it to focus on multi-band IR flame detectors which have long-range detection capability suitable for ro-ro spaces, as opposed to UV/IR detectors which have short-range detection capability.

Among all optical detectors, the light beam smoke detector stands out because it measures the attenuation of an emitted light beam due to a fire, whereas the other detectors sense the optical output from the fire itself. Video smoke detection is also somewhat different because it requires a certain level of ambient light and contrast to be able to see the smoke in the visual spectrum. Most video detection methods are suitable in closed ro-ro spaces more than they are in open ro-ro spaces as they need stable light conditions in the background. Some video detection systems can use images from ordinary CCTV cameras that are already installed on board which makes their implementation easier.

In open and closed ro-ro spaces, as compared to weather decks, the sensors cannot be placed high above the deck with a good overview of the vehicles. This restricts the field of view of optical detectors and limits the possibility to detect fires in between the vehicles in open and closed ro-ro spaces. However, the optical detection systems are less influenced by elements such as sunlight and precipitation in open and closed ro-ro spaces than those on the weather deck. Therefore, even with the restricted field of view and the limited coverage between vehicles, the optical detection systems could be useful in open and closed ro-ro spaces, as they may detect reflected light from a fire, smoke, and hot gases that rise above the top of the vehicles faster than conventional point detectors of smoke and heat.

6.1.2 Acoustic detection

Acoustic detection is based on analysing the characteristic sound that is emitted from a fire. Different materials in a fire will emit characteristic sounds that can be detected by sound sensors. As the sound can be transmitted both through open air and through solid materials, the fires can be detected even without direct line of sight from the detector. Experiments have been reported to give early detection of fires in a small room with low ambient noise [19].

In a ro-ro ship, the ambient noise from other sources will most likely be a major challenge for acoustic detection systems, such that it is not expected for such systems to be able to detect a small fire at an early stage on board a ro-ro ship with a large variation in the potential fire sources. No available commercial products have been found that use this type of technology, making it difficult to assess for ro-ro ships. Moreover, no recent research on the topic is found, indicating that this principle of fire detection is still not practical for real world applications. Therefore, acoustic fire detection is not considered in the LASH FIRE project.

6.1.3 Aspirating smoke detectors

Aspirating smoke detectors collect samples of the air through a system of pipes with holes that allow aspirating the gases into a central detector. Sample extraction smoke detection systems are not allowed for open ro-ro spaces and closed decks with passenger access according to SOLAS II-2/20.4.2. Therefore, these detectors are not considered for ro-ro spaces in the LASH FIRE project.

6.1.4 Point smoke/heat detectors

Point detection of heat and smoke is the most used method in open and closed ro-ro spaces. The point detectors detect high temperatures or the presence of smoke, but other versions can also detect specific gases such as CO. Detectors are placed in the overhead at a specific spacing and raises an alarm when the condition at that point exceeds a defined limit. These detectors communicate with an alarm central that gives an overview of which detector(s) has triggered an alarm. A significant number of detectors is needed to cover a ro-ro deck. However, each of the detectors is a small unit with its own sensors, electronics, and communications, which results in many detector units to maintain and test. The estimated time for testing all the detectors on a large ro-ro ship is 2-4 weeks for 2 persons.

6.1.5 Linear heat detection

A linear heat detection system uses a single sensor cable to detect the temperatures over a long distance. In its simplest form, this can be an electric cable where the insulation between two wires melts at a specific temperature, and the alarm is triggered by recording the short circuit that has occurred. However, the relevant systems for use in ro-ro spaces are sensing cables that are resettable and can continuously measure and record temperatures at addressable locations along a sensing cable as described in EN 54-22 [20].

Two different addressable linear heat detection systems have been evaluated and tested through laboratory experiments in the LASH FIRE project (see section 10). One system is based on a fibre-optic cable allowing laser pulses transmitted and reflected through the cable to be used for monitoring the temperatures along the entire cable in a continuous way. The other system is an electric sensing cable with embedded electronic temperature sensors at predefined intervals inside the cable. The working principles of the two systems are different, but the resulting outputs are temperature recordings along the cable. Both the fibre-optic and the electric sensor cables can cover a large ro-ro space, providing more extensive measurements compared to point heat detectors mounted with maximum spacing, albeit the fibre-optic system can offer a higher resolution of measurements along the cable given its continuous nature without individual sensors.

The sensor cable needs to be fixed on the ceiling along the deckhead of the ro-ro space (see Figure 1), whereby temperature recordings are made along the cable. As the longitudinal and transversal girders on the deckhead create many compartments along the ceiling, the ideal configuration for fire detection is achieved when the sensing cable goes through all the compartments.

The detection criterion for alarm triggering can be a certain temperature limit at any single point, a certain temperature rise with time, or a local temperature rise compared to the average temperature of the rest of the cable. The length of the sensor cable can be up to 16 kilometres [17], and this makes it possible to monitor the temperatures along a very long line with one system. For the use in a ship, the cable could be mounted in a pattern across the overheads of several decks to give an overview of the temperature distribution with better resolution than what would be feasible with conventional point heat detectors. As the detector part of the unit can be mounted in a well shielded and clean place, the system is robust and can withstand dirt, dust, corrosive environments, organic vapours, extreme temperatures, and radiation. Moreover, in the case of a fibre-optic sensor cable, temperatures up to 1000 °C can be withstood without losing monitoring capability, i.e. 2 hours testing with a minimum flame temperature of 750 °C is achievable according to IEC 60331-25 [21].

Redundancy design is a safety factor that can be achieved using a linear system, such that the system can continue its functionality even if one sensor cable is damaged or broken completely at a certain spot, while an error message will be generated in such cases that will identify the failure point along

the cable. In the case of fibre-optic linear heat detection systems, detection redundancy can be considered both at the level of sensor cable and at the level of acquisition system, i.e., Distributed Temperature Sensing (DTS) instrument. For the sensor cable, it is possible to have either double-ended or single-ended measurement setups. In a double-ended configuration, a DTS instrument with two channels is used to make measurements from both ends of the cable. This means that light is sent alternately from both ends into the fibre-optic cable. This way, the system maintains its full functionality even if the cable is damaged at any single spot. In a single-ended setup, a DTS channel is used to make measurements from only one end of the cable. Therefore, for a fully redundant design with a single-ended setup, two DTS channels are needed to make separate measurements from either end of the cable. If these two DTS channels are provided by the same DTS instrument, the system relies on this instrument for its functionality. If the two DTS channels are provided by two separate DTS instruments, the system relies less on each given DTS instrument for its functionality. In addition, it is noteworthy that each standard sensor cable carries two fibre-optic cables inside, offering “cable redundancy”, although it is normally expected that both these inner cables are likely to be damaged at the same time in cases where the cable is damaged by a strong mechanical force.

Figure 1: LASH FIRE installation of a fibre-optic heat detection cable on Hollandia Seaways. The cable is isolated from pipes using spacers.

6.1.6 Previous studies

The FIRESAFE II project studied several detection systems for ro-ro decks [22]. The detection methods discussed in the final report of the FIRESAFE II project are listed in Table 2.

Based on initial evaluations and cost-effectiveness assessments, fibre-optic linear heat detection system was selected for tests in the open ro-ro deck of Stena Scandinavica during the FIRESAFE II project [22]. In the ro-ro deck where the fibre-optic linear heat detection was installed for testing, there were point heat and smoke detectors already in place. This allowed for comparing these detection methods. The fibre-optic linear heat detection system triggered the alarm faster than the conventional detectors in all the tests, although the tested fire was in favour of thermal detection,

because it was a gas burner which burned with little smoke and without any initial smouldering stage. A real fire is expected to likely include a combination of several combustible materials such as plastics that release more smoke than the gas burner used in the tests. In such fires with a smoky stage in the beginning, the smoke is expected to be detected before the heat release becomes strong for thermal detection.

The system was left on the ship for one month after the fire tests to collect information on nuisance alarms. No nuisance alarms were triggered in this period.

Table 2. Detection systems evaluated in the FIRESAFE II project [22].

Type of detector	Suitable for open ro-ro decks	Suitable for closed ro-ro decks
Linear heat detection	Yes	Yes
Aspirating smoke detection	No, if passengers have access	Yes
Gas detection with ASD	No, if passengers have access	Yes
Video detection of smoke/flame	Yes, if overhead space is sufficient	Yes, if overhead space is sufficient
IR thermal imaging detection	Yes, if overhead space is sufficient	Yes, if overhead space is sufficient
Flame (wavelength) detection	Yes, if overhead space is sufficient	Yes, if overhead space is sufficient
Light beam linear smoke detection	Yes, if beam deflections can be accounted for	Yes, if beam deflections can be accounted for
Acoustic detection	No available systems are known	No available systems are known

6.2 Challenges for detection on open and closed ro-ro spaces

6.2.1 Visual obscuration

The limited space between the top of the cargo and the overhead is a restricting factor for the position of optical detectors that require a clear field of view for optimal fire detection. If a camera is placed relatively low compared to the height of the vehicles, the closest vehicles may block most of the field of view.

6.2.2 Light

Video smoke detection requires a certain ambient light to be able to see the smoke. Moreover, the contrast between the smoke and the background objects will influence how well the smoke can be detected by these systems.

Sensors that detect the IR radiation emitted from the flames do not require any ambient light. For instance, thermal imaging cameras detect IR radiation and thus they can indicate any abnormal temperature increases caused potentially by a fire, but they would require a heated surface or its reflection that is visible to the thermal camera. The reflection may come from any surfaces which are specular (mirror-like) reflectors, e.g., a shiny metal surface.

Smouldering fires (i.e., flameless fires) will not emit any visible light and, in the early stage, very limited amounts of smoke. These fires can be difficult to detect based on visible light, if not impossible. Using infrared radiation, however, such fires can be detected more easily, e.g., using a thermal imaging camera with a field of view to the smouldering area.

Video detection methods use only the visible light spectrum and need to differentiate a flame from other types of light by using video analytics algorithms. This is because unhazardous light sources may also exhibit some characteristics which are like those of a fire. For example, direct sunlight or that reflected from the sea surface or other moving surfaces may look like the flickering light from a flame.

In closed ro-ro spaces, the light conditions will be controlled by the installed light fixtures alone. In open ro-ro spaces, the light conditions are also influenced by the sun. Compared to weather decks, these challenges will be easier to handle for open and closed ro-ro decks with the right placement of the detectors and masking or blocking certain zones in the detection software. For example, the parts of the field of view that include the sea or the sky may be masked to avoid triggering nuisance alarms. Reflections from surfaces on the vehicles is more difficult to mask as they are in the areas that must be covered for fire detection.

Flame wavelength detectors may detect flame radiation at several wavelengths at the same time to differentiate between radiation from sunlight and that from fires which have characteristic wavelengths such as hot carbon dioxide radiation.

Thermal imaging cameras monitor IR radiation in their field of view to detect hot spots, but this can cause nuisance alarms due to sunlight and its reflections.

Direct light from the sun or other powerful light sources may also dazzle or blind optical detectors (e.g., due to overexposing the sensor or causing flaring and reduced contrast). This problem applies to almost all optical detectors. Accordingly, dazzling tests and certifications are included in some standards, e.g., see annex D in EN 54-10 [18].

6.2.3 Distance to detector

For detectors that require combustion products or hot gases to physically travel from the fire to the detector, a large distance will mean a longer detection time. Therefore, the maximum spacing of the detectors is limited according to the regulations. However, the distance requirement does not fully account for the deck height or the wind that may blow the smoke away from the closest detector.

The optical detectors may see the fire, smoke, or heat from great distances as the radiation travels through the air with very little attenuation. However, the effective detection distance of the detector is defined by the size of the fire and the sensitivity settings of the detector. Only small amounts of rain or snow will be able to get into the open ro-ro spaces, but fog or condensation on the lens of the detection sensors can increase the attenuation and reduce the effective range of the optical detectors. For light beam linear smoke detectors, this will lead to a reduction in the light intensity that reaches the receiver and may trigger frequent nuisance alarms. The different wavelengths that each type of sensor uses are absorbed differently by molecules in the air. For instance, water will block more of the infrared light than the light in the visible spectrum.

Tests of two different video flame detector systems show that the detection time increases with distance for a given fire source [23]. This is because the flame appears smaller at longer distances, so the used video analytics algorithms need more time and data from the images before they can identify the flame.

When flame wavelength detectors are tested and classified, they are certified for a certain flame size and distance in a controlled environment [18]. In challenging conditions, such as rain, snow or fog, the fire must be closer or larger before an alarm is raised.

6.2.4 Rain, snow, ice, and salt

When a detector is installed outdoors and close to the sea, rain, salt, and ice can cover the detector and absorb or deflect incoming signals from a fire. This can increase the maintenance needs for detectors in such conditions. As the open and closed ro-ro spaces are better shielded from the ambient conditions than the weather deck, the sensors mounted in these areas will be less exposed to rain, snow, ice, and salt. Still, the environment is somewhat harsh, and some cleaning of the sensors may be required.

6.2.5 Wind and ventilation conditions

On open ro-ro spaces, the ventilation is determined by the ambient wind conditions. In strong wind conditions, the smoke and hot gases from a fire can spread, be diluted, and be deflected from the detectors above. At the same time, the wind can increase the horizontal speed of fire spread causing the growth of fire and its rate of heat release to increase via the supply of fresh air. Closed ro-ro spaces have mechanical ventilation and hence a more predictable air flow over the deck.

6.2.6 Cargo characteristics

Fires inside steel containers are challenging to detect, because the smoke and heat are trapped inside for an extended period, thereby delaying detection using conventional point heat/smoke detectors. Similarly, fires inside trailers may be detected with extended delays because many trailers have waterproof covers for their freight, and the cover can contain the smoke for a considerable amount of time. Fires inside vehicles can also go unnoticed for an extended period. For example, abnormal heat build-up in the traction battery of an electric car can be extremely difficult to detect from outside the vehicle using regular smoke/heat detectors installed along the deckhead, because the battery pack is inside a tightly sealed compartment placed under the vehicle. Similarly, the smoke and heat from smouldering fires developing inside the passenger compartment of a car can be trapped for many minutes before leaking out to be detectable by smoke/heat detectors along the deckhead.

6.2.7 Nuisance alarms

Some ships have nuisance alarms from too much humidity in the cargo space when it is raining or snowing. Moreover, exhaust fumes from the vehicles during loading and unloading are sources of nuisance alarms. However, as normally the exhaust fumes are released only during loading and unloading operations, the detectors may be deactivated during this period, which could result in another problem if detectors are not re-activated directly when an area is left unattended. Moreover, in cases where there are too many reefer units on board such that the number of charging points is not sufficient, some units may be allowed to have their engine running in an idle mode during the voyage, which can be a source of nuisance alarms.

6.2.8 Other challenges

Apart from the factors discussed earlier relating to the challenges of fire detection on board ro-ro ships, there are other general factors that may challenge the detectors less frequently to different extents, such as radiated electromagnetic fields, vibrations, and cyclic damp heat. A non-exhaustive list of standard test methods for the evaluation of detectors against such factors can be found in Table 1 of EN 54-10 [18].

7 Development considerations

Main author of the chapter: Reidar Stølen, FRN

The fire detection methods and their functionality can be improved via new system developments to suit the environment and requirements on board ro-ro ships. Some promising developments are discussed in this chapter and the feasibility of their implementation is evaluated.

7.1 Moving sensors

Different types of sensors can be mounted on a platform that is able to move and navigate through the ship. The platform for the sensors may be moved around in the ship through the air with a drone, on a rail system, or freely on the deck like a small car. This will allow for sensors to be moved across the different areas to scan the environment for abnormal conditions. Compared to stationary sensors, this will allow each sensor to cover a larger area resulting in fewer sensors required in total. The sensor vehicle may be programmed to follow a defined route to patrol and cover the area of interest, or it may be sent directly to a certain point of interest based on input from operators or other sensors.

For a moving sensor to be able to detect a fire at an early stage, it is essential that each point be covered at regular and short intervals. The system would also need to have redundancy on all essential parts of the system to be able to achieve a similar level of reliability as stationary permanently mounted detectors. If the moving sensor is used as a supplement to an existing fire detection system, it may be used for confirmation of fire or investigation of any interesting event that calls for an inspection. This application would only require the sensor platform to be standing by and be ready to go to a defined position on board. This can be both faster and safer than sending crew members to confirm a fire, gas leakage, or other potentially dangerous events.

Ground sensors moving on the floor are currently not compatible with the infrastructures and protocols of ro-ro decks, such that the implementation of these sensors is expected to be highly challenging for closed and open ro-ro spaces. Aerial applications are under development for weather decks. For example, as part of LASH FIRE efforts in work package 7, a prototype drone system for aiding fire patrol, search and rescue operations, and fire resource management has been evaluated [24]. For open and closed ro-ro spaces, however, this type of drone system will be more complex in terms of navigation, data communication, power supply, etc., especially if it is to replace fixed detectors in the future. Accordingly, the number of possible failure modes will be higher, thereby requiring several parallel systems to be able to reach an acceptable level of reliability, making the solution very challenging to implement (refer to [24] for the details of future work required in this area). Given that the systems are not expected to be easily exploitable for fire detection in ro-ro decks, the evaluation of moving sensors is not considered as part of this document.

7.2 Vehicle sensors

Modern vehicles have sensors monitoring the temperature inside their engine and other relevant parts. These sensors are expected to be connected to each other and to road infrastructures in the future. This will allow the road users and road managers to share useful information. Cooperative Intelligent Transport Systems (C-ITS) is the overall term used for this type of communication. If the sensor data can be collected, mapped, and monitored throughout the ro-ro decks, this could give very early warnings on fires that start in the internal parts of the vehicles, although fires starting in the vehicle's cargo cabin may be detected with a longer delay, unless sensors are included there by design to detect abnormal temperature developments.

This type of communication is being developed for traffic management and it is not clear whether the sensor information will be available from parked vehicles. If it is possible to extract this data from the vehicles during the voyage, it can be included in the fire detection system interface together with the other detector data (see delivered guidelines of LASH FIRE work package 7 for fire detection system interface design and those of work package 8 for electrical connections of reefers and electrical vehicles in ro-ro spaces). If this type of information is only available when the vehicles are running, this information may be used during the screening of cargo before the vehicle goes on board (see LASH FIRE deliverable D08.10 [25] regarding the prototype for the automatic detection of potential ignition sources via cargo screening).

7.3 Video detection improvements

To improve the performance of video-based fire detection algorithms, they should be adapted to the normal situations on board ro-ro ships to be able to detect fires as quickly as possible in all stages of the ship's journey with as few nuisance alarms as possible. Accordingly, the video detection systems are assessed in the operational conditions on board. Moreover, onboard experiments have been performed to assess the performance of the systems against a reference fire.

7.4 Linear heat detection

Live temperature data from linear heat detectors can be used to generate a heatmap of the deck head as shown in Figure 47. This map can be included in the fire resource management system and provide a useful overview of the temperature distribution in case of fire or in other events that can cause higher or lower temperatures in certain areas. Temperature data from other sensors, like point heat detectors can also be used to provide such heatmaps, but the resolution of the map will be limited by the number of detection points.

7.5 Conclusions

The open and closed ro-ro spaces on ships are normally equipped with point heat and smoke detectors. The detection solution requires service on many detectors throughout the ship, a task that is highly time consuming. Accordingly, an alternative or supplementary detection system could introduce a tangible improvement if it offers easier maintenance and better long-term performance with equal or shorter detection times.

Optical detection methods are suggested primarily for weather decks, but they could also be used in open and closed ro-ro spaces. Limitations in available space above the vehicles is a challenge and the systems will have to demonstrate that they can detect fires at least as quickly and reliably as the currently used point detectors.

New and improved detection methods have been developed, tested in the laboratory environment, and validated on board a ro-ro ship during the project. Quick detection of real fires, few nuisance alarms, and the ability to operate in the relevant environment without too much maintenance are key factors in the evaluation of the systems.

8 Evaluation criteria

Main author of the chapter: Davood Zeinali, FRN

Any alternative detection technology to be used in open and closed ro-ro decks must: (1) provide effective detection performance better than or equal to that of conventional systems, (2) be compatible with the operational conditions on board, and (3) be cost-effective.

The performance criteria are assessed firstly through simulations and subsequently through experiments in a corresponding laboratory environment and then on board an operational ship.

The compatibility and cost-effectiveness criteria are studied in cooperation with work package 5 of LASH FIRE which deals with ship integration (see deliverables D05.6 [26], D05.7 [27], D05.8 [28], and D05.9 [29]).

8.1 Performance

First and foremost, it must be noted that detection systems have various applications and standards (e.g., see [18] and [20]), and thus the focus of the present project is not to assess the working mechanism of the systems or their compliance with standards. Rather, the goal is to assess the suitability of the underlying technology for the detection of fires in the environments of open and closed ro-ro decks given the challenges discussed in section 6.2. Among other elements, the following main factors are considered critical to assess:

- **Wind and ventilation:** the dispersion of smoke and the tilting of the fire plume due to wind and/or ventilation can make in-situ fire detection difficult. This is assessed via simulations and experiments to quantify how alternative detection systems are affected by such phenomena.
- **Light:** both artificial and natural sources of light can hinder fire detection and are considered in the evaluation of alternative detection systems via experiments.
- **Other environmental factors:** weather conditions (rain, snow, frost, condensation, sunlight, vibrations, wind, etc.) can affect the performance of the detection systems. This is assessed through operational evaluations on board a ship for one year.
- **Cargo:** the normal operations related to cargo loading/unloading as well as the emission of (direct/reflected) light from the cargo surfaces can pose a detection challenge and lead to nuisance alarms. The obstruction of field of view could also be a problem. These factors are assessed through operational evaluations on board a ship for one year.

8.2 Operational aspects and cost assessment

LASH FIRE deliverable D05.6 [26] discusses the ship integration requirements for the fire detection systems in ro-ro spaces, while deliverables D05.7 [30] and D05.8 [28] discuss the corresponding integration evaluations and cost assessment of the promising detection technologies based on the input provided by the lead author of the present document. Therefore, the information is not repeated here in detail. Instead, two examples are presented in this document to demonstrate the main concepts and to discuss the related insights.

8.2.1 Video fire detection for a generic ship

Just as other optical detectors, regular cameras used for video detection rely on a free line of sight to the flame or smoke. Moreover, the detection range for the cameras follows the square law between distance and the area of detection as long as the distance is high compared to the characteristic length of the object to be detected, such that detection at twice the distance requires nearly four times the area, as illustrated in Figure 2. Moreover, the area is proportional to the fire size in terms

of radiant heat output (RHO). Therefore, if a flame detector can detect a fire with RHO = 40 kW at 30 m, detection at 60 m is expected to require a fire with RHO = 160 kW.

Using a video fire detection system, each camera can cover a large area for fire detection. However, the use of cameras below the deckhead of ro-ro spaces limits their view to the free height above the cargo when the deck is fully loaded.

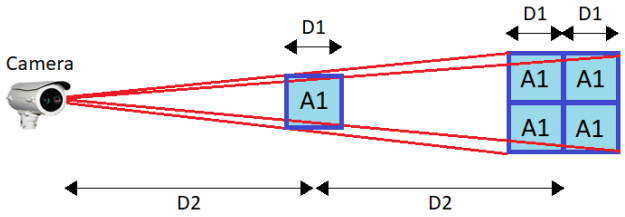

Figure 2: Square law between distance and area of detection (applicable when D2 >> D1): if an object that has an area of A1 is detectable at the distance of D2, detection at a distance of 2 x D2 requires nearly an area of 4 x A1.

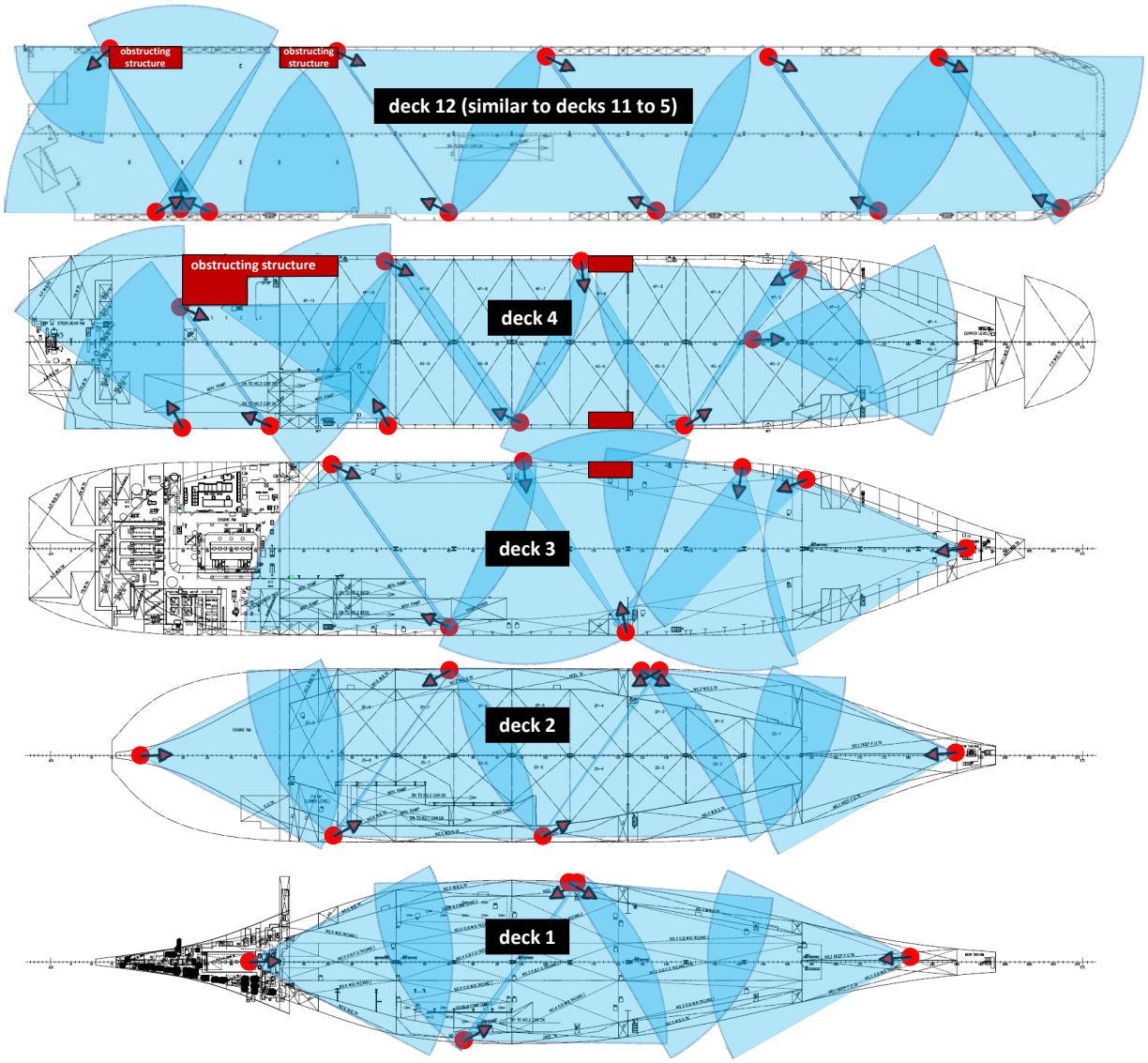

Figure 3: Integrated example of a video fire detection system for the closed ro-ro spaces on Torrens (generic vehicle carrier).

Figure 3 illustrates an example video fire detection system integrated into the closed ro-ro spaces on Torrens (generic vehicle carrier), consisting of 129 cameras: decks 12 to 5 are similar and each require 12 cameras, while deck 4 requires 10 cameras, deck 3 requires 7 cameras, deck 2 requires 7 cameras, and deck 1 requires 5 cameras. The long-range cameras in this example have medium sensitivity settings allowing effective detection range of nearly 40 m at 54° horizontal angle and 40° vertical angle, while the low-range cameras (used in decks 12 to 5) have a wider lens allowing effective detection range of nearly 20 m at 85° horizontal angle and 63° vertical angle. A total of 8800 m of power and signal cables is estimated for the proposed design. The cost estimate for this system is presented in Table 3. Examples for other generic ship types can be found in deliverable D05.8 [28].

Table 3. Estimated costs for the proposed video detection system shown in Figure 3 for Torrens (generic vehicle carrier).

Investment item	**Cost in EUR**
Purchase of system	951 760
Integration design and validation	16 000
Assembly/installation	304 000
Commissioning	5 000
Administration	8 000
Operator training	500
Total maintenance cost (assuming lifetime for existing ship is 22.9 years)	78 565
Total*	**1 363 825.00**
* This cost estimate is highly conservative. Increasing the detection sensitivity settings may allow the use of fewer cameras, thereby reducing the costs significantly. However, the level of sensitivity must not be too high such that it leads to frequent nuisance alarms.	

8.2.2 Linear heat detection for a generic ship

The linear heat sensing cable needs to be fixed on the ceiling along the deckhead of the ro-ro space, whereby continuous temperature recordings can be made along the cable. As the longitudinal and transversal girders on the deckhead create many compartments along the ceiling, the ideal configuration for fire detection is achieved when the cable goes through all the compartments.

One challenge with the installation of linear heat detection systems is the requirement for cable fixings at regular intervals [31]. In addition, metallic cable clips or saddles are required at regular distances to retain the cable during a fire if the cables are not laid on top of horizontal cable trays or supports. This requirement increases the time and cost of installation because the cable cannot be in direct contact with any cool/hot surfaces which might interfere with the functioning of the heat sensing cable. Hoistable decks may also pose some challenges for the implementation of linear systems, as the wires on the hoistable decks need to partly go along the sides of the ship to be joined with the rest of the decks. Installation details and recommendations are provided in section 12.2.

Figure 4 shows an integrated example of a fibre-optic linear heat detection system for the uppermost ro-ro space of Torrens (generic vehicle carrier). For the uppermost ro-ro space which offers space for 708 cars, the full coverage using the proposed design requires approximately 1205 m of cables, offering a measurement resolution of 2 m with redundancy. Converting this cable length proportional to the deck capacity for the other decks, it can be estimated that the entire ship will require 11200 m of cables. The cost estimate for this system is presented in Table 4. Examples for other generic ship types can be found in deliverable D05.8 [28].

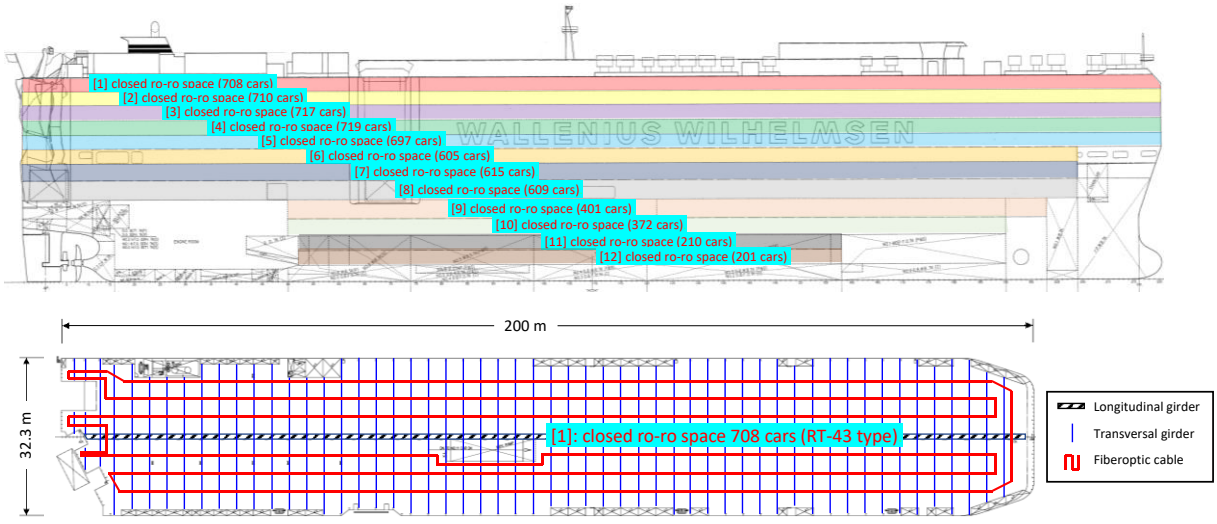

Figure 4: Integrated example of a fibre-optic linear heat detection system for Torrens (generic vehicle carrier): the different ro-ro spaces are shown above, while the example detection system is shown at the bottom for the uppermost ro-ro space (requiring approximately 1205 m of fibre-optic cable).

Table 4. Estimated costs for the proposed linear heat detection system shown in Figure 4 for Torrens (generic vehicle carrier).

Investment item	**Cost in EUR**
Purchase of system	168 400
Integration design and validation	55 000
Assembly/installation	478 000
Commissioning	30 000
Administration	15 000
Operator training	5 000
Total maintenance cost (assuming lifetime for existing ship is 22.9 years)	168 915
Total*	**920 315**
* This cost estimate is for a fibre-optic design and may be highly different from that of other linear systems such as electric ones.	

8.3 Conclusions

Video fire detection systems offer a good potential for ro-ro cargo decks which commonly incorporate CCTVs. However, for existing ships, integrating a video analytics algorithm with the existing CCTV may require supplementary hardware such as a computer that serves as a server for the in-situ analytics.

A big operational advantage provided by the linear heat detection systems is that they require minimal maintenance from the crew compared to traditional point detectors, which require cleaning and inspection for each individual unit. Another advantage is the improved detection coverage provided by the sensor cable and the short distances between cable routes compared to the spacing between traditional detectors as per the FSS code [32]. A critical limitation of the linear systems is that only heat is detected, not smoke.

The solution of adaptive threshold settings for detection is expected to be only integrable for new builds due to potential difficulties with system software adjustments and approval issues, while the integration potential for existing ships highly depends on the systems installed on board.

The cost estimations suggest that the installation of a linear heat detection system on ro-ro ships is especially cost-effective for very large ships, such that the overall cost is significantly lower than that of a video fire detection system. For smaller ships, however, the overall cost of a linear system is

much higher than that of a video fire detection system installation. Nevertheless, linear systems provide the advantage of being usable for both open and closed decks, whereas video fire detection systems are only recommended for closed decks where light conditions are stable. Moreover, the installation cost for a video fire detection system is more dependent on the ro-ro space arrangement, since the deck geometry and structural obstructions can increase the number of camera units needed.

The most significant system costs are those related to the purchase of the components and the installation work, while lower costs are associated with inspection, testing, and maintenance. Considering the scalability of the costs for different ships, the costs for the linear heat detection systems can be scaled per deck area with acceptable accuracy, but the costs of video fire detection systems must be calculated on a case-by-case basis.

9 Numerical simulations

Main author of the chapter: Nikhil Verma, VTT

Included in Annex B are numerical simulations that have been carried out using Fire Dynamics Simulator (FDS) software as part of LASH FIRE WP09 to evaluate and compare the performance and detection time of different detection technologies on ro-ro spaces. The simulations considered different fire properties, fire locations, and ventilation conditions. The LASH FIRE generic ship model of Stena Flavia was used in the simulations, with conventional detectors like point detectors of smoke, heat, and carbon monoxide (CO) as well as non-conventional detectors like flame wavelength detectors, video-based smoke and flame detectors, and linear heat detectors. The performance of the detectors has been evaluated in various scenarios, and their promptness in activation with respect to different environment and fire conditions has been outlined.

The results obtained in this work are highly qualitative in nature and have not been validated against any experimental results. The results are meant to give insight into the general conditions resulting potentially in good or poor performances for the detection technologies. The activation times presented in this report are dependent on the chosen alarm sensitivities, detector types, fire locations, fuel types, environmental conditions, and many other factors.

9.1 Modelled technologies and settings

The theoretical approach and numerical implementation of FDS have been documented in detail in the software's technical reference guide [33, p. 1]. FDS has been validated for simulating both smoke and heat transfer in enclosure fires, but also its capability for producing correct wind profile has been assessed [34, p. 3]. The modelling of some detection technologies is restricted by the limited models available in the FDS software. Primarily, the software includes the models for conventional detectors like heat detectors (point sensors) and smoke detectors (point sensors). The software also provides an option to position devices in a computational domain to measure carbon monoxide concentration and temperatures at various points. Such temperature measuring devices have been used to replicate the functionality of linear heat detectors. Moreover, to cater for the need of other non-conventional detectors like video flame detectors, video smoke detectors, flame wavelength detectors, and thermal imaging cameras, certain related outputs are chosen as shown in Table 5. These outputs are assessed to evaluate the response of such non-conventional detection technologies.

The video flame detector was assumed to activate when there are visible flames above the trucks, and the video smoke detector was assumed to activate when there is visible smoke above the trucks (optical density value of 0.1 m^{-1} . The flame wavelength detector was assumed to activate when it was receiving more than 0.5 kW/m^2 radiation, which is estimated to correspond to a detector activating in 3–5 s at 10 meters from a 0.1 m^2 heptane fire. These values are supposed to represent a robust detector device, which has a relatively low sensitivity to prevent nuisance alarms. The thermal imaging camera was assumed to activate when the temperature, either gas or surface, in the field of view was above 200 °C. Such numerical values are generalized based on a general discussion with the fire and smoke detection companies keeping their identification and detection thresholds in confidentiality.

For other detection technologies, activation times were estimated based on the quantities shown in Table 6. Note that upper and lower activation limits are used to cover a range of activation possibilities.

Table 5. FDS outputs provided for the evaluation of response from some non-conventional detection technologies.

Detection technology	FDS output
Video flame detector	Heat release rate per unit volume for flame height (kW/m^3)
Video smoke detector	Optical density (m^{-1})
Flame wavelength detector	Radiant heat flux (kW/m^2)
Thermal imaging detector	Gas temperature and surface temperature (°C)

Table 6. Activation limits of point heat and smoke detectors and linear heat detectors

Detector	Lower activation limit	Upper activation limit	Remark
Point heat detector	54 °C	78 °C	Activation is based on temperature
Smoke detector	2% (m^{-1})	12.5% (m^{-1})	Activation is based on optical density
Linear heat detectors (fixed temperature)	57 °C	60 °C	Activation based on fixed temperature
Linear heat detectors (rate of rise)	8 °C/120 s	14 °C/120 s	Activation based on rate of rise of temperature
Carbon monoxide	40 ppm	400 ppm	Activation based on parts per million

9.2 Design fire

A heavy goods vehicle (HGV) fire is considered as the design fire in the simulations. Generally, such vehicles carry goods made of a combination of plastics (PE pallets, plastic toys, polystyrene cups etc.) and wood (wooden pallets, furniture, paper cartons etc.) [35]. Moreover, based on Swedish statistics and professional goods transport agents, an 80% cellulose and 20% plastic fuel load is a reasonable division to allocate goods transport on the road [36]. Thus, to represent the fire of wood and plastics, based on data provided in [37] (table B.1-2), a T-squared fast fire curve is used in the simulations. Table 3.6 of [38] also presents the fast growth rate for various stuff made of wood and plastics. The fast fire curve has a growth constant of 0.047 kW/m^2, and it is shown in Figure 5. The figure also includes the T-squared slow fire curve (growth constant of 0.003 kW/m^2), which have been used for the sensitivity study with the T-squared fast fire curve. The simulations mainly considered design fires with the fast growth rate, while only a few simulations considered design fires with a slow growth rate for a sensitivity analysis (not included here). The fuel had either high wood and low plastic contents (low soot and carbon monoxide yield), or low wood and high plastic contents (high soot and carbon monoxide yield). For open ro-ro space, different wind speeds in different directions have been used in the simulation, whereas in case of closed ro-ro space, mechanical ventilation with supply and exhaust points have been used. For both the spaces, fire locations have been varied in simulations to check the swiftness of various detection technologies in conjunction with the ventilation condition as shown in Figure 6 and Figure 7.

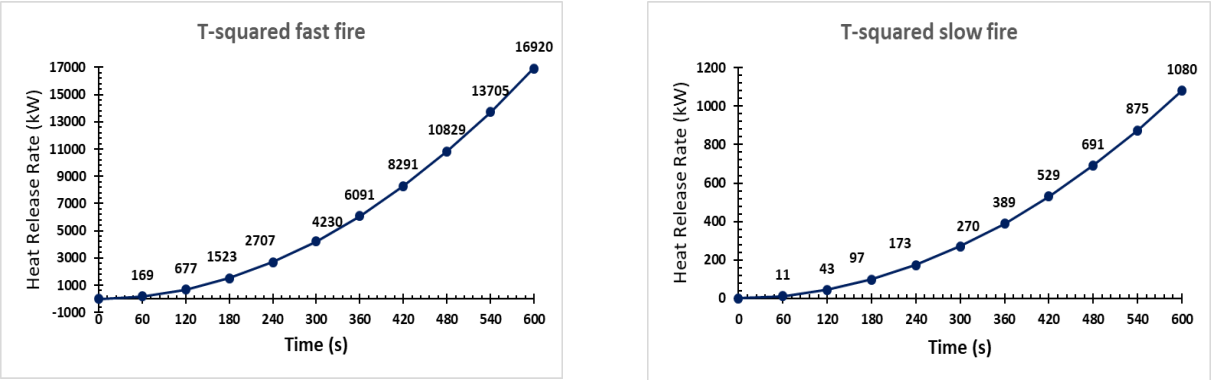

Figure 5. The fire growth rates considered in the simulations: (left) fast fire growth rate (right) slow fire growth rate.

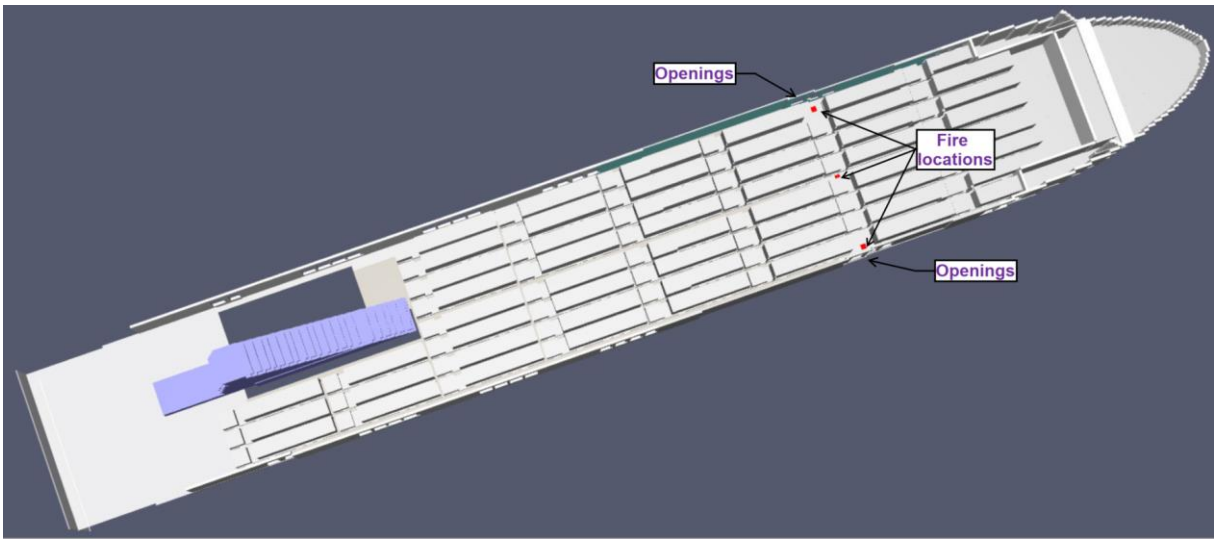

Figure 6. A view of open ro-ro space in Stena Flavia simulation model from above. Locations of fires are marked with red rectangles. Two fires are located near openings, and one is along the centreline of the space.

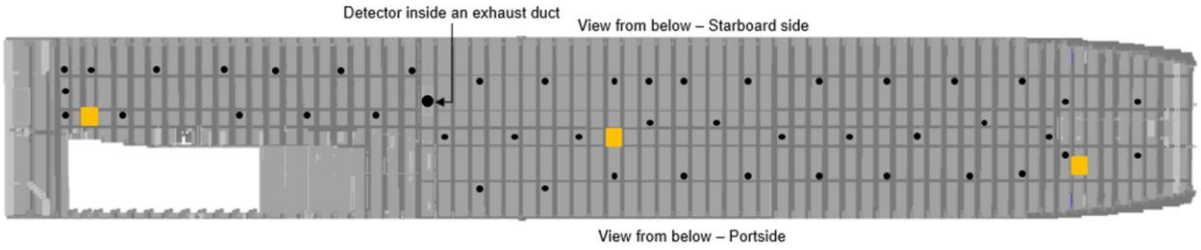

Figure 7. A view of closed ro-ro space in Stena Flavia simulation model from below. Locations of the fires are marked with orange rectangles. A fire located near a ventilation supply point is located in the forward part of the ship, and a fire located near a ventilation exhaust point is located in the aft part of the ship.

All the inbuilt FDS devices, excluding Linear Heat Detectors, are plotted in the simulations as per the point detectors layout provided for Stena Flavia drawing for open and closed ro-ro space.

9.3 Simulation scenarios

Tables 7 and 8 show the considered simulation scenarios with different conditions for open and closed ro-ro spaces, respectively. Different fire locations, wind speeds, wind directions, soot yields, and carbon monoxide yields have led to different activation times of detectors. Furthermore, channelling of smoke by girders, formation of smoke pockets in between girders and immediate obstructions (vehicles, trucks) around the vicinity of fire have affected the smoke movement and transportation and thus the activation of detectors also.

Table 7. Open ro-ro space simulation scenarios.

ID	Fire growth rate	Fire location	Wind	CO & soot yield
S1	Fast	Starboard side opening	3.75 m/s starboard side wind	Low
S2	Fast	Starboard side opening	7.5 m/s starboard side wind	Low
S3	Fast	Centreline	7.5 m/s headwind	Low
S4	Fast	Centreline	7.5 m/s tailwind	Low
S5	Fast	Portside opening	7.5 m/s starboard side wind	Low
S6	Fast	Portside opening	3.75 m/s starboard side wind	High
S7	Fast	Starboard side opening	7.5 m/s starboard side wind	High
S8	Fast	Centreline	7.5 m/s headwind	High
S9	Fast	Centreline	7.5 m/s tailwind	High
S10	Fast	Portside opening	7.5 m/s starboard side wind	High

Table 8. Closed ro-ro space simulation scenarios.

ID	Fire growth rate	Fire location	CO & soot yield	Note
S11	Fast	Centreline	Low	
S12	Fast	Ventilation exhaust point	Low	
S13	Fast	Ventilation supply point	Low	
S14	Fast	Centreline	Low	Fire moved ½ beam span
S15	Fast	Centreline	Low	No openings in girders
S16	Slow	Centreline	Low	
S17	Slow	Ventilation exhaust point	Low	
S18	Slow	Ventilation supply point	Low	
S19	Fast	Centreline	High	
S20	Fast	Ventilation exhaust point	High	
S21	Fast	Ventilation supply point	High	

9.4 Main findings

As discussed in Annex B, in almost all the simulations, the conventional smoke detectors detected the fire fastest, although this assumes that the smoke detectors are fully functional. This is while point detectors tend to get damaged easily especially in open ro-ro spaces. A smoke detector failed to detect the fire only in one open ro-ro space simulation whereas the linear heat detector succeeded in detection in all the simulations of open, and closed ro-ro spaces.

It is important to note that for open ro-ro space simulations, an unfavourable combination of fire location and wind condition could lead to fire not being detected by some detection technologies or could lead to very long activation times. Fire in the closed ro-ro space could also be detected from an

exhaust ventilation duct serving the space, but much larger delays are expected than with conventionally located detectors. However, the results are dependent on the ship arrangement, and results for spaces with different ventilation or girder arrangements could be significantly different.

In the open ro-ro spaces, the flame wavelength detectors and video smoke detectors seemed to be the most promising non-conventional technologies. However, the success of the detectors is dependent on their location in the ro-ro space. Both video analytics systems and thermal imaging cameras could have challenges in detecting fires when the fire location and wind conditions are unfavourable. For example, the tilting of flame or smoke plume by wind in conjunction with an unfavourable fire location can lead to no visible flames or too much diluted smoke plume above cargo height, which can affect the detection.

For the closed ro-ro spaces, among non-conventional detection technologies, flame wavelength detectors and video smoke detectors seem to be the most promising technologies. Based on the qualitative assessment, the obstructed spaces might not be the best working environment for video analytics systems, but similarly, as for the open ro-ro spaces, the result is highly dependent on the fire location and the existing environmental conditions during the fire. The use of thermal imaging cameras should also be given further consideration. Their use for effective fire detection seems to be dependent on how low their alarm threshold can be set without excessive number of nuisance alarms. The thermal imaging cameras can identify hot surfaces, which could enable detecting developing fires before ignition. However, crowded ro-ro spaces can make noticing such hotspots quite challenging, as the cameras cannot see most of the cargo.

Based on the findings, the following points are outlined for consideration via experiments and operational evaluations:

1. For open ro-ro spaces, scenarios where the fire is located near the side openings must be included. If possible, this fire location should be tested for the following two wind conditions: (1) wind scenario orienting the fire products and hot gases out of the opening; (2) wind scenario orienting the fire products and hot gases toward the inside of the ro-ro space. Based on the simulation results, the fire can be difficult to detect in these scenarios.
2. At least linear heat detectors and video smoke detectors are suggested to be included in the large-scale studies, as they were the most promising alternative detection technologies based on the simulations (linear heat detectors were the only detection system among conventional technologies being successful in detection in all the scenarios, whereas video smoke detectors also being successful in detection in all scenarios among non-conventional technologies were the fastest in detection among such technologies).

10 Laboratory experiments

Main authors of the chapter: Ellen Synnøve Skilbred, Reidar Stølen, and Davood Zeinali (FRN), Robert Benitz (APS)

10.1 Fire detection experiments with four ISO 8ft containers

Thirteen types of fire detectors were tested in a variety of fire scenarios with four ISO 8ft containers in two separate test series, where the first was in November 2020 and the second in June 2021. The detectors included point detection of smoke, gas and temperature, linear heat detection and optical detection systems including video detection, IR flame wavelength detectors, and IR thermal cameras. The full list of detectors tested is given in Table 9. Some detectors gave only an alarm signal, others gave only sensor data, and some sensors provided both. The devices were tested with their default sensitivity settings for detection. The point detectors were supplied from four manufacturers. One of the detector types could not be compared with the other detectors, and the data was also difficult to interpret as several different detectors were connected and gave a signal that could not be traced to the specific detector reaching the alarm criteria. These detectors are therefore not included here. Linear heat detectors were supplied from two manufacturers, IR flame wavelength detectors from three manufacturers, IR thermal cameras from three manufacturers, and a video detection system from one manufacturer. The PD1 detectors detected smoke, heat, and CO, and were connected in a hub. The alarm would go off if one of the PD1 detectors reached the alarm criteria, but the system did not tell which of the PD1 sensors had met the alarm criteria. Therefore, the results show one detection time for the PD1 sensors, which is the time before the first sensor reached the alarm criteria. The PD3 sensors did not have alarm criteria and were only used in the battery tests. A prototype of a deck-mounted linear heat detector was tested in the first test series, but the initial experiments showed that the detector only gave alarm when the fires were very close to it, and it was therefore taken out of the experimental matrix.

Table 9: List of the tested detectors in the two series of laboratory experiments for open and closed ro-ro spaces.

Detector ID	Detector type	Test series
PD1	Point smoke, heat and CO (multi-)detector	1 and 2
PD2 a/b	Point visibility sensor (two identical units used)	1 and 2
PD3	Point CO sensor	1 and 2
LHD1 a	Electric linear heat detector* pre-alarm	1
LHD1 b	Electric linear heat detector* full alarm	1 and 2
LHD2 a	Fibre-optic linear heat detector** pre-alarm	1 and 2
LHD2 b	Fibre-optic linear heat detector** full alarm	1 and 2
FD1	Flame wavelength detector with IR array (16x16 IR sensors)	1 and 2
FD2	Flame wavelength detector with triple IR	2
IR1	IR thermal camera	1 and 2
IR2 a/b***	IR thermal camera (one unit with two settings)	1 and 2
IR3	IR thermal camera	2
VSD	Video smoke detection	2
VFD	Video flame detection	2

* The electric linear heat detector had individual temperature sensors at every 1 m along the cable with measurement cycles of 10 s, while the alarm settings were as follows: pre-alarm at a maximum temperature of 45°C, or a temperature differential of 1.4°C in proprietary system correlation; full alarm at a maximum temperature of 50°C, or a temperature differential of 2.8°C in proprietary system correlation. The system had standard certification based on EN 54-22 [20].
** The fibre-optic cable was used with a spatial resolution of 1 m using sampling intervals of 0.5 m, measurement cycles of 10 s, and alarm settings as described in section 10.1.3.2. The system had standard certification based on EN 54-22 [20].
*** IR2a used settings that allowed vehicle nuisance source discrimination. IR2b used default settings without this feature.

10.1.1 Experimental setup

The two series of tests were conducted in the large fire test hall at RISE Fire Research in Trondheim, Norway. The hall has an adjustable ceiling height which was set to either 3 m or 5 m during the experiments relevant for ro-ro spaces (see Figures 8 and 9). During the same test series, experiments were also conducted with 16 m ceiling height to simulate a more relevant distance for detectors for weather decks, but these tests are presented in deliverable D09.1 [1].

During the tests without wind, the fans were inactive, and the gates of the test hall were closed, such that the only air circulation in the room was that created by the fires. In the tests with wind (conducted only during the first test series), windy conditions were generated by extracting air using ventilation fans and by opening the test hall's western gate (measuring 4.5 m wide and 4.3 m high as shown in Figure 8), creating wind blowing from west to east across the test hall. The maximum wind velocity achieved was with both ventilation fans active and a ceiling height of 3 m, which was approximately 5 m/s at 3 m upstream of the 8ft containers and 1.5 m height near the centre of the hall (see central wind sensor location shown in Figure 16), where the total airflow through the gate was 106 m^3/s. The wind velocities reported in the next section through Table 10 are for this central location. In addition, the velocities were characterised along the transversal wind measurement plane shown in Figure 9 across the height and in the transversal direction, the results of which are presented in Figure 10.

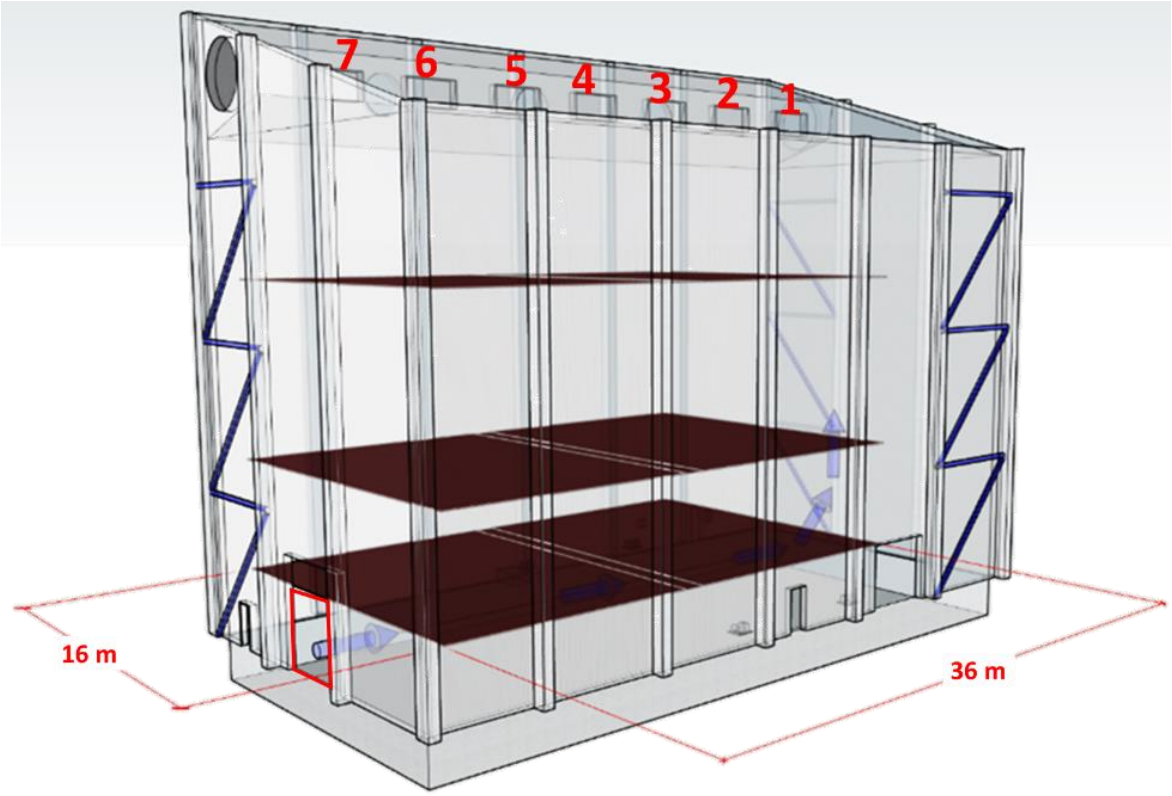

Figure 8: The large fire test hall at RISE Fire Research in Trondheim, Norway. The purple arrows indicate the wind direction across the test hall when using an open western gate measuring 4.5 m wide and 4.3 m high (marked with a red rectangle) and ventilation fans at the top of the hall (numbered 1 to 7 with red digits). The adjustable ceiling measuring 25 m long and 16 m wide was fixed at the heights of 3 m and 5 m during the ro-ro space tests.

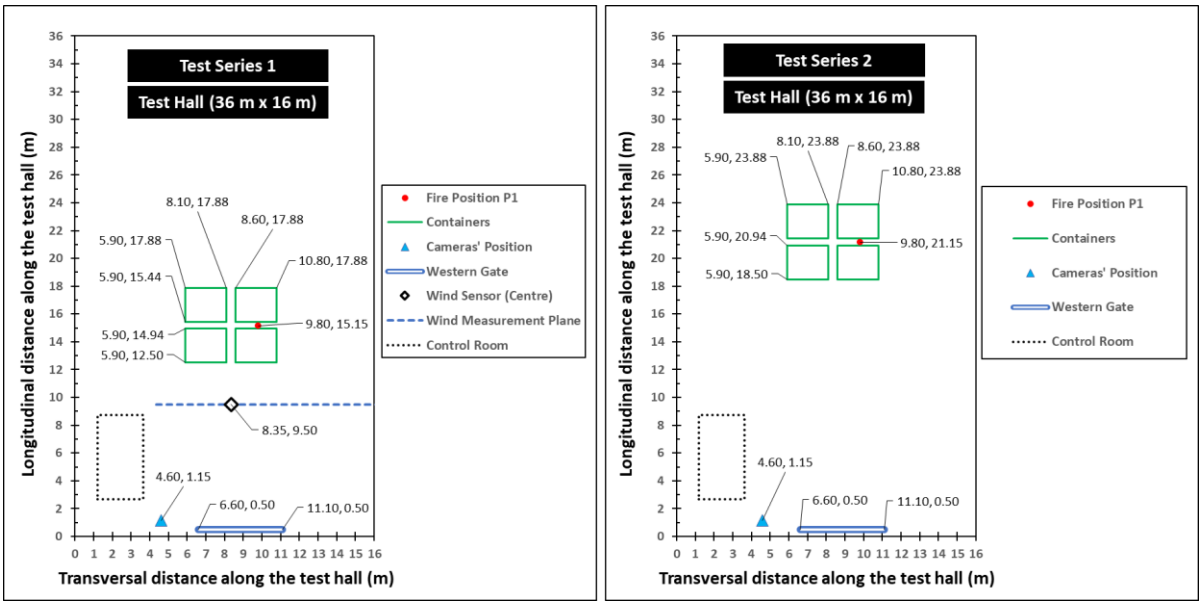

Figure 9: Top view of setup used in the two series of tests. The container setup was moved 6 m further away from the position of detectors in the second test series. The numbers indicate the X and Y positions of items in the test hall. The four green squares indicate the outlines of the ISO 8ft containers. During the first test series, the detector cameras were mounted at the height of 2.5 m while the ceiling height was 3 m. During the second test series, the detector cameras were mounted at the height of 4 m while the ceiling height was 5 m.

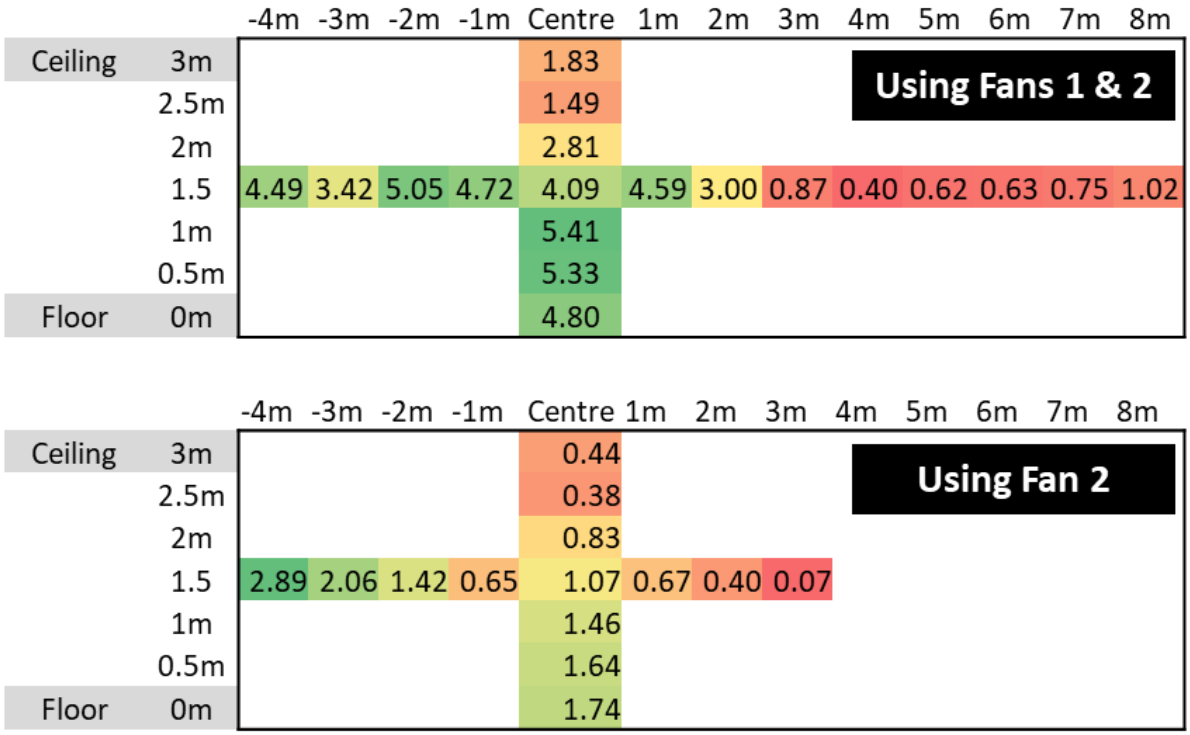

Figure 10: Wind velocities (m/s) along the wind measurement plane shown in Figure 9 with active fans 1 & 2 (top) and only fan 2 (bottom). The fan locations are shown in Figure 8.

The detectors were installed on the adjustable ceiling placed above four steel ISO 8ft containers measuring 2.43 m x 2.2 m x 2.26 m (Length x Width x Height) which were spaced 0.5 m apart, as shown in Figure 11. Wind conditions were generated by opening a gate to the outdoors and

ventilation fans. The first test series was conducted with a flat ceiling, while the second test series was conducted with vertical barriers mounted on the ceiling to simulate the beam constructions that are common in ro-ro decks. The vertical barriers were wooden beams covered by welding cloth and divided the ceiling into two rectangular compartments measuring 3 x 6 x 1 m. Experiments with ceiling barriers were conducted both with these barriers sealed and with openings measuring 10% of the total area of each of the barrier walls. These dimensions are found to be typical for many ro-ro ships and corresponds well with for example deck 3 on the ship Stena Flavia, as shown in Figure 12 where ceiling beams are sketched in blue lines and smoke detectors in red dots. In addition, the star shows the worst-case point of ignition where the smoke needs to pass the most beams to reach smoke detectors. The star indicates the primary beam compartment to be filled with smoke, while the yellow rectangles will be filled next, and the green compartments that contain smoke detectors will be filled lastly.

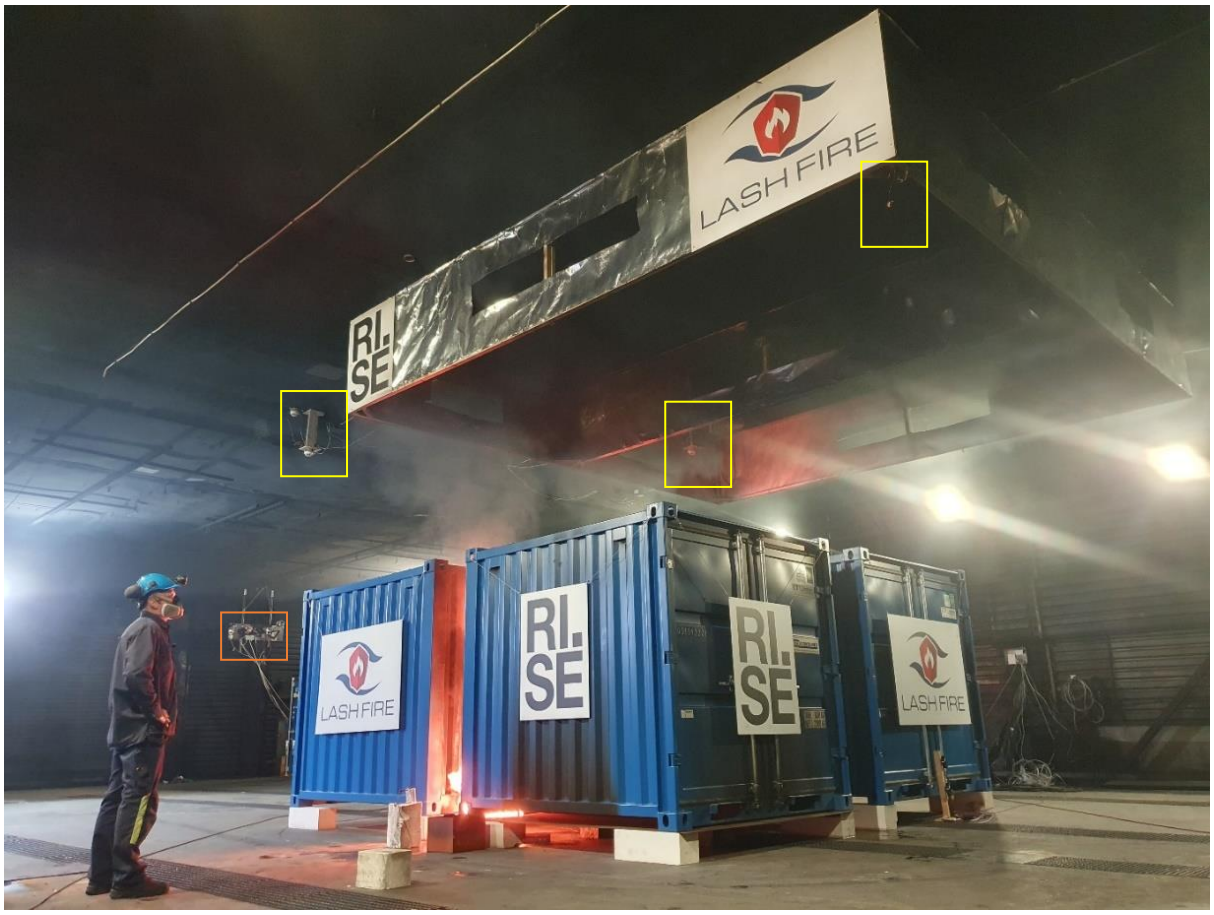

Figure 11. The experimental setup with 5 m ceiling height and beam compartments with 10% openings. Detectors mounted on the wall can be seen in the background marked with orange rectangle. Ceiling mounted point detectors are marked with yellow rectangles. One of the linear heat detection cables can be seen as a white line across the ceiling in the top left part of the picture.

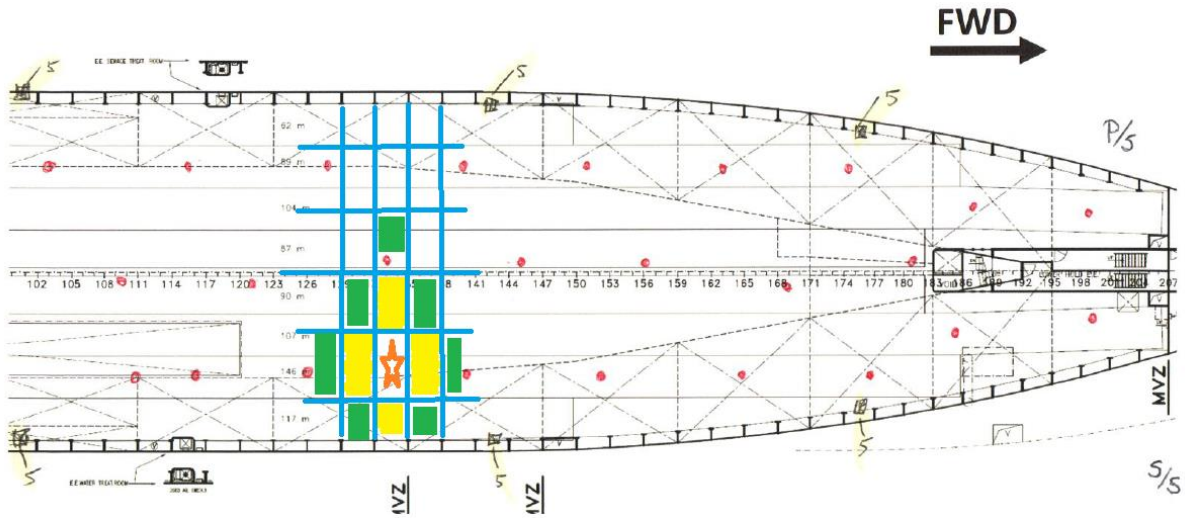

Figure 12: Sketch of deck 3 in Stena Flavia with ceiling beams drawn in blue and smoke detectors marked with red dots. A star indicates a worst-case fire position where the smoke would need to pass the most beams to reach smoke detectors.

The positions of ignition sources and detectors relative to the containers and ceiling beams are shown through Figures 13, 14, 15, and 16.

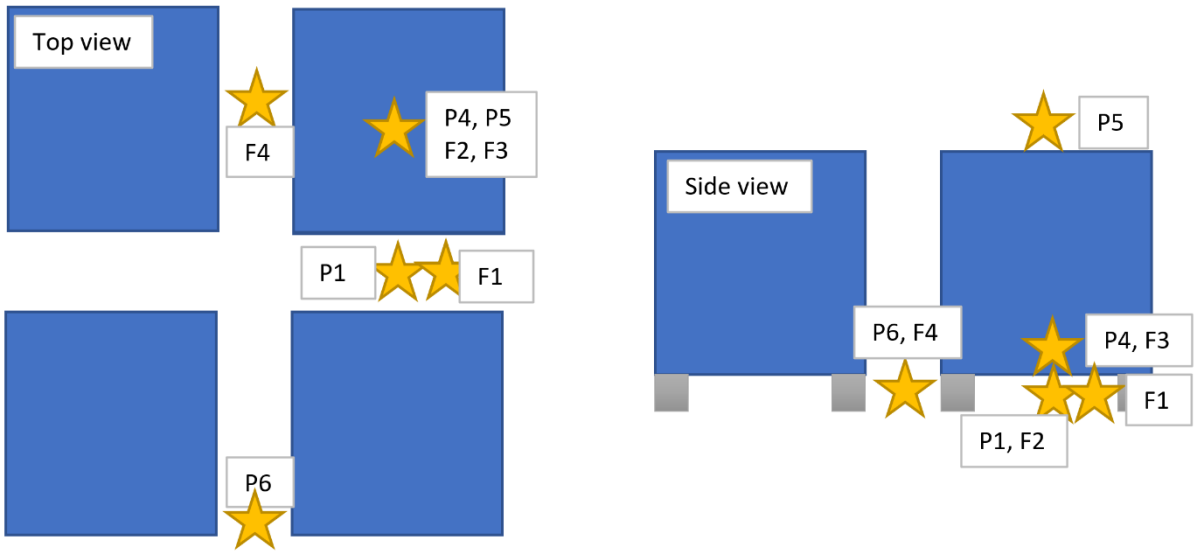

Figure 13: Positions of the ignition sources relative to the steel containers. Positions used in test series 1 is marked with P1, P4, P5 and P6, and positions used in test series 2 is marked F1 – F4.

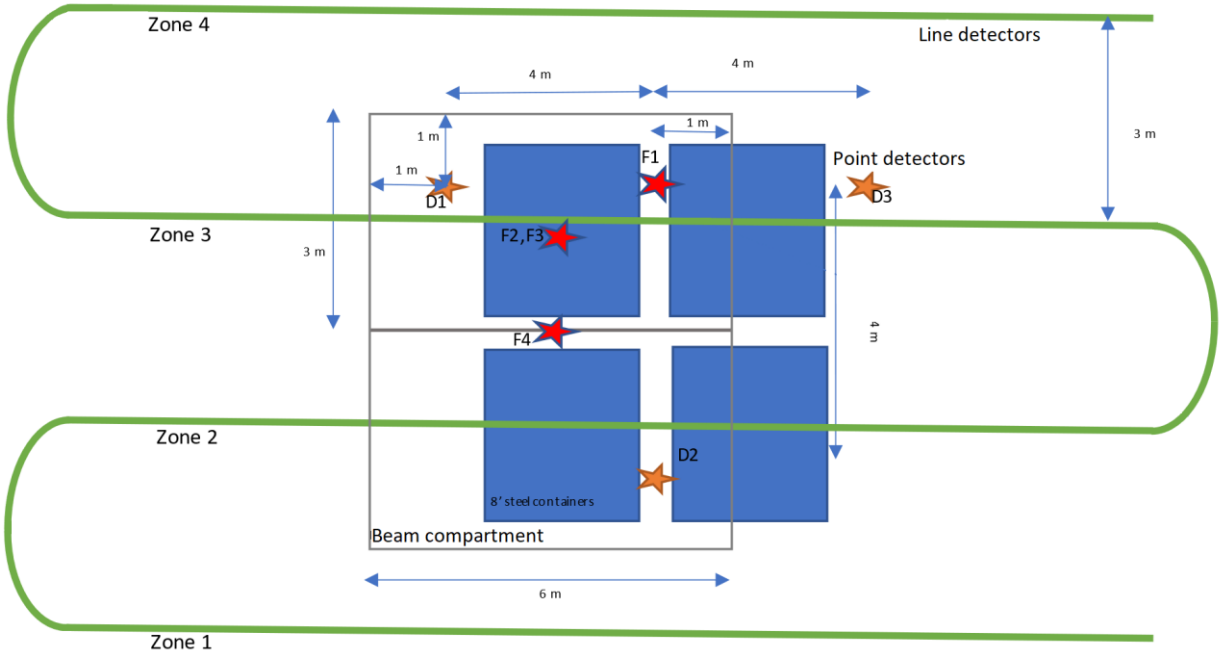

Figure 14: Top view of the test configuration with ceiling beam compartments as tested in June 2021. The linear heat detectors are marked with green lines that form detection zones 1 to 4, the point detectors are marked with orange stars and the fire source positions are marked with red stars.

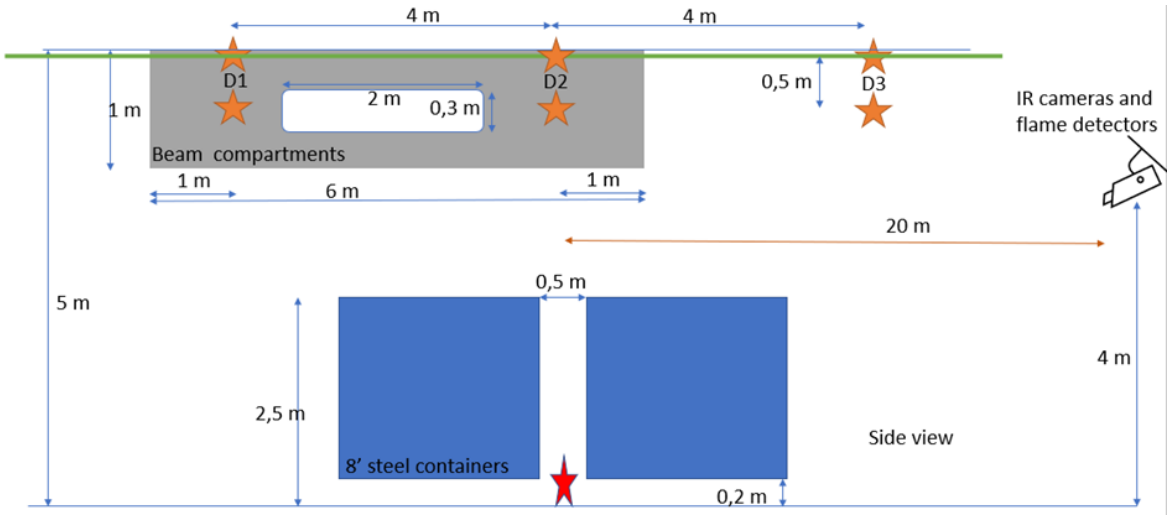

Figure 15: Side view sketch of the experiment configuration in the second test series. The detectors were placed both in the ceiling of the beam compartments and 0.5 m down from the ceiling.

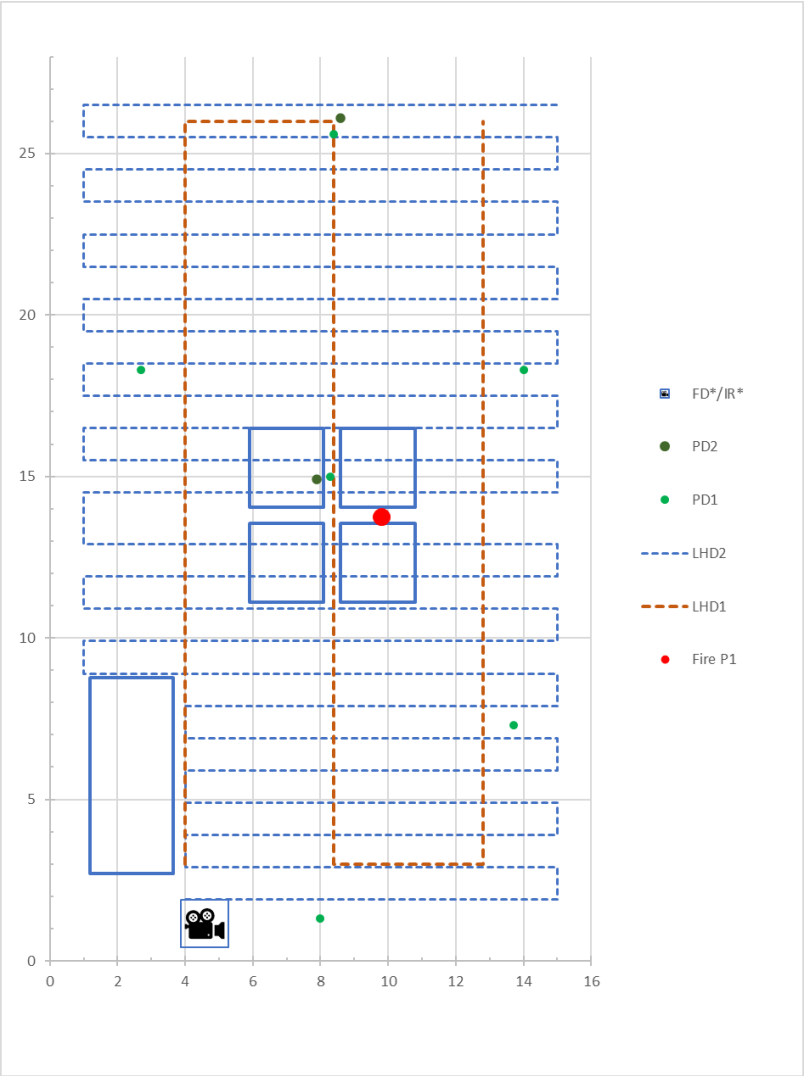

Figure 16: Detector positions in the test series conducted in 2020. Each dot represents a point detector. The four blue squares in the centre mark the outlines of the test containers and the large rectangle in the lower left corner marks the outline of the control room container. The different point detectors are located at different positions and their detection times are therefore not comparable. Detector PD2a is the one in the centre of the test area, and detector PD2b is the one near the top of this figure. All the IR thermal cameras and Flame wavelength detectors (IR/ FD*) were mounted in the same position and these results are therefore comparable.*

10.1.2 Ignition sources

The laboratory experiments were conducted with three types of ignition sources: beechwood sticks on a hot plate, liquid pool fire tests, and lithium-ion batteries.

The beechwood sticks on hot plate ignition source is based on the test setup described in EN 54-29 annex I of a smouldering wood fire [39]. The beechwood sticks are sized 20 mm x 25 mm x 75 mm and are heated on a hot plate to release a light grey smoke without igniting as shown in Figure 17. The heater had a maximum temperature of 420°C and a linear heat ramp such that it could reach 350°C in 4 minutes.

Figure 17: Beechwood sticks on a hot plate generating light grey smoke without flames.

Liquid pool fires with methylated spirits and n-Heptane were used according to the guidelines of EN 54-10 [18]. The fuel was added to a water base in pool trays of different dimensions. In the 2020-tests, a square tray measuring 30 x 30 cm^2, a circular tray with a diameter of 10 cm, and a circular tray measuring 15 cm in diameter were used. In the 2021-tests, only heptane was used as a fuel, and rectangular pools of three sizes were used, namely 30 x 30 cm, 50 x 50 cm, and 60 x 60 cm. The corresponding heat release rate of each fire was calculated to 65, 302 and 364 kW based on burn duration and fuel contents, respectively. The maximum flame height is shown in Figure 18. The flames from the smallest pool fire did not reach above the top of the containers, while the flames of the medium sized pool extended above the top intermittently, and the largest pool fire extended above the top of the containers for most of the time. Hence, only the two larger fires were visible from the location of the wall-mounted optical detectors. Both the heptane fires and ethanol fires produced visible smoke and luminous flames, but the smoke was more visible and light intensity higher for the heptane fires.

Figure 18: Maximum extension of the flame lengths for the three heptane pan fires of 30 x 30 cm (left), 50 x 50 cm (middle) and 60 x 60 cm (right).

The lithium-ion battery experiments in the first test series involved initially two experiments with a battery module containing 24 cells (each being a 3.63-Volt, 60-Amp hour, 218-Watt hour LGY LGCHEM li-ion pouch cell, measuring 35.3 cm x 10.0 cm x 1.6 cm), connected to a short-circuit device employing several hundred ampers of current through a coil around a pipe with internal water

cooling, but this scenario did not produce much overheating or smoke because the short-circuit of the battery broke within a second. Therefore, a third experiment was conducted, including heating a single cell (235-Watt-hour LG JP3 NMC pouch cell), namely by placing it over the heater shown in Figure 17 until the end of the experiment. During the second test series, two experiments were conducted using a steel box containing three battery cells (each being a 235-Watt-hour LG JP3 NMC pouch cell as in the first test series), heated with two 500-W electric heating elements until the end of the experiment as shown in Figure 19. The battery cells were placed inside the test container, 60 cm above the floor, and with the container door fully open. This corresponds to position P4 in Figure 13. CO detectors (PD3) were placed in front of the open container door at a horizontal distance 2 m away from the battery cells at three heights: floor level, 25 cm, and 50 cm above the floor level.

Figure 19: Overheating three lithium-ion battery cells in a steel enclosure with electric heating elements. The steel box was open in the front. Insulation was placed on top of the box during tests to get a more uniform heating of all three cells.

10.1.3 Results and discussion

10.1.3.1 Time from ignition to detection

The time from ignition to detection for detectors tested in the two test series is shown in Table 10 and Table 11. Some of the tests and detectors were not included in the analysis, as they were not comparable due to differences in fire visibility or data output from the detection systems. Detector PD3 did not produce any alarms and is therefore not included in these tables. The tests are sorted according to the type of fuel used for and the location of the fire.

The results from different detectors cannot be directly compared as the detectors were in different positions relative to the fire and the detectors have different sensitivity settings which were not fixed in the same way. Thus, the detection times cannot be compared between different detectors in this test setup.

The test results show how the different types of sensors are suitable for different types of fires. The beechwood hot plate fuel fires produced smoke which was detected by at least one of the point detectors in all the experiments. The beechwood hot plates did not create flames and have little spread of heat and were therefore harder to detect by IR cameras and linear heat detectors. The times before triggering were higher for the beechwood hot plate scenario since these fires developed slower than the pool fires.

Both the heptane fires and ethanol fires produced visible smoke and luminous flames but only the heptane fires, which had higher light intensity and more visible smoke, were detected by the point detectors, even though detector PD1 was a combined heat, smoke, and CO-detector. Linear heat detectors installed at the ceiling could detect all the ethanol fires except the fires in position P5, which had the smallest pool size (Ø 10 cm) and were above the containers. The optical detectors could also detect some of the ethanol fires. In general, however, the linear heat detection system detected more fires than the optical detectors, although the fewer responses of these detectors were usually faster than those of the linear heat detection systems.

Table 10: Results from the first test series (ceiling height = 3 m), sorted based on ignition position. The numbers given for each detector in each test is the number of seconds passed from ignition to detection. 'ND' indicates 'No Detection', i.e., the detector did not detect the fire. The wind velocities were measured at the central wind sensor position shown in Figure 9.

						Point detectors			Linear heat detectors				Flame detector	IR cameras		
Test no	Fuel	Fuel amount (l)	Pool size	Ignition position	Wind (m/s)	PD1	PD2a	PD2b	LHD1a	LHD1b	LHD2a	LHD2b	FD1	IR1	IR2a	IR2b
8	Beech hot plate	6 Sticks		P1	0	520	713	613	ND	ND	ND	ND	ND	ND	ND	ND
19	Ethanol	1	30 x 30 cm	P1	0	ND	ND	ND	148	ND	44	44	ND	ND	ND	ND
30	Ethanol	1	30 x 30 cm	P1	1	ND	ND	ND	283	ND	43	43	ND	ND	ND	ND
13	Heptane	1	30 x 30 cm	P1	0	33	112	82	96	263	31	31	ND	ND	ND	ND
42	Heptane	1	30 x 30 cm	P1	0	47	129	32	165	ND	37	37	ND	ND	ND	ND
10	Heptane	0.1	Ø 10 cm	P1	0	ND	133	297	ND	ND	100	90	ND	ND	ND	ND
22	Heptane	1	30 x 30 cm	P1	1	31	77	19	69	107	32	42	ND	97	ND	ND
39	Heptane	1	30 x 30 cm	P1	5	ND	85	49	164	ND	64	64	ND	125	ND	ND
6	Beech hot plate	6 Sticks		P4	0	422	271	ND	ND	ND	ND	ND	ND	ND	ND	ND
21	Beech hot plate	6 Sticks		P4	1	ND	671	ND	ND	ND	ND	ND	ND	ND	ND	ND
38	Beech hot plate	6 Sticks		P4	5	ND	448	ND	ND	ND	ND	ND	ND	ND	ND	ND
31	Ethanol	1	30 x 30 cm	P4	1	ND	ND	ND	76	127	59	59	ND	ND	ND	ND
1	Heptane	0.3	15	P4	0	ND	173	203	ND	126	95	95	ND	ND	ND	ND
2	Heptane	1	30 x 30 cm	P4	0	ND	45	94	61	70	40	39	ND	75	ND	ND
5	Heptane	1	30 x 30 cm	P4	0	60	38	116	61	79	44	44	ND	74	ND	ND
4	Heptane	0.3	Ø 15 cm	P4	0	ND	124	370	145	ND	102	102	ND	ND	ND	ND
7	Heptane	0.2	Ø 15 cm	P4	0	ND	104	413	136	ND	107	98	ND		ND	ND
20	Heptane	1	30 x 30 cm	P4	1	62	53	ND	53	73	41	41	ND	185	ND	ND
37	Heptane	1	30 x 30 cm	P4	5	ND	51	ND	109	152	61	61	ND	ND	ND	ND
33	Li-ion module	24 cells		P4	0	ND	ND	ND	ND	ND	ND	ND	ND	ND	ND	ND
34	Li-ion module	24 cells		P4	0	ND	ND	ND	ND	ND	ND	ND	ND	ND	ND	ND
35	Li-ion cell	1 pouch		P4	0	ND	ND	ND	ND	ND	ND	ND	ND	ND	ND	ND
18	Ethanol	0.01	Ø 10 cm	P5	0	ND	ND	ND	ND	ND	ND	ND	ND	9	ND	23
29	Ethanol	0.01	Ø 10 cm	P5	1	ND	ND	ND	ND	ND	ND	ND	ND	117	ND	ND
9	Heptane	0.01	Ø 10 cm	P5	0	ND	276	ND	ND	ND	ND	ND	ND	10	ND	ND
27	Heptane	0.01	Ø 10 cm	P5	1	ND	ND	ND	ND	ND	ND	ND	ND	0	ND	ND
11	Beech hot plate	6 Sticks		P6	0	726	630	302	ND	ND	ND	ND	ND	82	338	256
24	Beech hot plate	6 Sticks		P6	1	ND	335	ND	ND	ND	ND	ND	ND	474	376	156
32	Ethanol	1	30 x 30 cm	P6	1	ND	ND	ND	258	ND	162	333	6	9	20	18
17	Ethanol	1	30 x 30 cm	P6	0	ND	ND	ND	45	72	42	42	5	10	8	6
41	Heptane	1	30 x 30 cm	P6	0	54	97	ND	43	52	33	33	4	9	3	7
25	Heptane	1	30 x 30 cm	P6	1	64	93	17	89	126	61	61	6	9	4	26
40	Heptane	1	30 x 30 cm	P6	5	ND	ND	ND	121	ND	64	64	5	9	9	6

Most of the heptane pool fires with pool size 30 cm × 30 cm were not detected by FD1, IR2a and IR2b, as the flames from these fires did not reach the top of the containers, see Figure 18. Detector IR1 detected more of these fires than the other optical detectors. All the optical detectors were mounted on the same position on the wall, which makes these results comparable. The lower time before detection for sensor FD2 compared to FD1 shows that this sensor is more sensitive. For tests where both sensors detected the fire, the difference in sensing time between the detectors varied from 3 s to 24 s. This shows how difficult it is to predict the effect of changing the sensitivity settings of a detector. Among the IR-detectors, IR3 was the most sensitive and detected almost all the 50 cm × 50 cm and 60 cm × 60 cm heptane pool fires. IR1 and IR2 detected some of the same fires and some different fires. A slight difference appears for heptane pool fires in position F2, F3 and F4,

where IR1 detects most of the fires while IR2 does not, most likely due to differences in sensitivity settings for the detection threshold.

The number of point detectors detecting the fire was lower in the tests with wind than in the tests without wind in various scenarios (but not all). However, the detection performance of the other systems shows no clear trend of effects from the tested wind speeds (0 to 5 m/s). Therefore, it seems that the wind sensitivity of point detectors is higher than that of the other detection systems tested. Moreover, it is expected that wind speeds higher than 5 m/s will be needed to cause a noticeable effect in the detection performance of the other systems (see section 10.3).

Table 11: Test results from the second test series with heptane pool fires and lithium-ion batteries (ceiling height = 5 m). The numbers given for each detector in each test is the number of seconds passed from ignition to detection. 'ND' indicates 'No Detection', i.e., the detector did not detect the fire. 'Yes' indicates detection happened while the timing was not recordable. Empty fields indicate that the detector was not active during the test.

							Point detectors			Linear heat detectors		Flame detectors		Video detection		IR cameras		
Test no	Fire size	Fuel amount (l)	Position	Beam	Burn time (s)	Average HRR (KW)	PD1	PD2a	PD2b	LHD1	LHD2	FD1	FD2	VDS	VDF	IR2	IR3	IR1
16	30 x 30 cm	1	F1	10% open	522	63	ND	67	135	152	56	ND	ND	186	ND	ND		ND
20	30 x 30 cm	1	F1	10% open	478	69	ND	59	134		60	ND	ND		ND	ND		81
3	30 x 30 cm	1	F1	Closed	533	62	ND	52	121	116	55	ND	ND		ND			
4	30 x 30 cm	1	F1	Closed	469	70	257	54	94	117	45	ND	ND	203	ND	ND		
9	30 x 30 cm	1	F1	Closed	530	62	ND	80	147	190	61	ND	ND	199	ND	ND		ND
17	50 x 50 cm	3	F1	10% open	371	267	25	7	24	53	27	28	11	43	ND	yes	22	yes
18	50 x 50 cm	3	F1	10% open	378	262	26	12	28	48	29	25	20	60	ND	yes	19	
2	50 x 50 cm	1,5	F1	Closed	131	378	25	10	21		26	27	17		151		22	
5	50 x 50 cm	3	F1	Closed	304	326	31	13	26	50	33	33	19	64	ND	ND	21	
6	50 x 50 cm	3	F1	Closed	310	319	25	12	24	43	36	35	13	42	ND	yes	13	
10	50 x 50 cm	3	F1	Closed	378	262	26	7	21	50	24	20	17	43	ND	ND	11	yes
19	60 x 60 cm	4	F1	10% open	359	368	25	10	28	45	31	20	14	ND	ND	yes	16	12
7	60 x 60 cm	4	F1	Closed	367	360	23	9	20	40	30	17	12	154	ND	yes	11	
8	60 x 60 cm	4	F2	Closed	1098	120	33	17	28	ND	ND	ND	ND	78	ND	ND	ND	yes
11	30 x 30 cm	0,5	F3	Closed	402	41	ND	ND	ND	ND	ND	ND	ND	ND	ND	ND	193	yes
13	30 x 30 cm	1,5	F3	Closed	722	69	ND	ND	ND	ND	ND	ND	ND	ND	ND	ND	172	yes
12	50 x 50 cm	1,5	F3	Closed			ND	ND	ND	ND	ND	ND	ND	ND	ND	ND	yes	yes
14	30 x 30 cm	1	F4	Closed	465	71	226	64	59	228	68		58	155	ND	ND	ND	ND
15	50 x 50 cm	3	F4	Closed	371	267	27	11	11	52	34	26	2	30	86	ND	9	157
27	3 Li-ion cells		F4	10% open			2047	2010	2045	ND	ND	ND	ND	1516	ND	ND	ND	ND
28	3 Li-ion cells		F4	10% open			1714	1633	2073	ND	ND	ND	ND	2912	ND	ND	ND	2132

10.1.3.2 Alarm criteria settings for the fibre-optic linear heat detection systems

The time of detection for linear heat detectors depends on the thresholds fixed in the alarm criteria settings of the detector. The detector cables of LHD1 and LHD2 in test series 2 had four detection zones along the ceiling (see Figure 14). To evaluate the effect on the alarm activation time, several different threshold settings were considered to post-process the raw data captured by the fibre-optic linear heat detector LHD2 in test 17 of the second test series. The corresponding times of alarm activation for the different criteria are presented in Table 12. Three types of thresholds were used:

- Temperature-rise threshold settings. These range from 6 °C in 120 s to 20 °C in 240 s.
- Individual point measurements that are above the average temperature of the zone. For example, "ZoneAvg+15°C" is triggered when the temperature at one location is at least 15 °C higher than the average temperature of the zone.
- Static maximum temperatures. These thresholds trigger an alarm when the temperature measurements of one location exceed a given limit. For example, "Max_50°C".

The first threshold that was reached was the temperature rise of 6 °C in 120 s in alarm zone 3. Approximately 30 s after the first alarm, the threshold was reached in zones 2 and 4, and after another 20 s, zone 1 reached its threshold. Zone 3 had the detection point closest to the fire source,

and this point was positioned 0.5 m horizontally from the fire source. The detection points closest to the fire source for Zones 4 and 2 were 2.5 m and 3.5 m away from the fire, respectively. This means that the detection delay may be caused by the increased distance from the fire, but it can also be affected by the obstructions caused by the beams along the ceiling.

Table 12: Time elapsed before different alarm criteria were reached for the linear heat detector LHD2 in test 17. The cycling time for each temperature measurement was 10 s.

Alarm Zone #1	Alarm Zone #2	Alarm Zone #3	Alarm Zone #4	Seconds from ignition	Seconds from first alarm
		6°C/120s		**27**	**0**
		8°C/120s		**37**	**10**
		10°C/120s			
		14°C/120s			
		20°C/240s		**47**	**20**
		ZoneAvg+15°C			
	6°C/120s	26°C/360s	6°C/120s	**57**	**30**
	8°C/120s		8°C/120s		
		Max_50°C	10°C/120s	**67**	**40**
		ZoneAvg+25°C			
6°C/120s	10°C/120s	Max_57°C	14°C/120s	**77**	**50**
		Max_60°C			
8°C/120s	14°C/120s	ZoneAvg+30°C		**97**	**70**
10°C/120s				**107**	**80**

10.1.3.3 Effect of ceiling beams on smoke spread

In the second test series, beams were attached to the ceiling as the ceilings in ro-ro spaces often have such beams and the beams can cause a delay of the smoke transport across the ceiling. An example of this delay is shown in Figure 20 where the measurements from four of the point detectors PD1 in test 17 of the second test series are given. The detectors were installed 4 m from the fire in positions D1 and D2 as shown in Figure 14 and Figure 15, at ceiling height (5 m) and 0.5 m below the ceiling (4.5 m). Detector position D1 is inside the same ceiling beam compartment as the fire, while position D2 is in the next ceiling beam compartment. The smoke concentration in the primary compartment stabilizes at a level almost twice as high as that in the next compartment. The smoke level registered by detectors in position D1 starts to increase almost immediately after ignition, while the smoke level registered by the detector in position D2 at ceiling level starts to increase after 15-20 s, and the smoke registered by the detector in position D2 at 4.5 m starts to increase after approximately 50 s. This indicates that the smoke is first filling up the beam compartment directly above the fire before the smoke starts flowing over to the next compartments through the openings and below the beams.

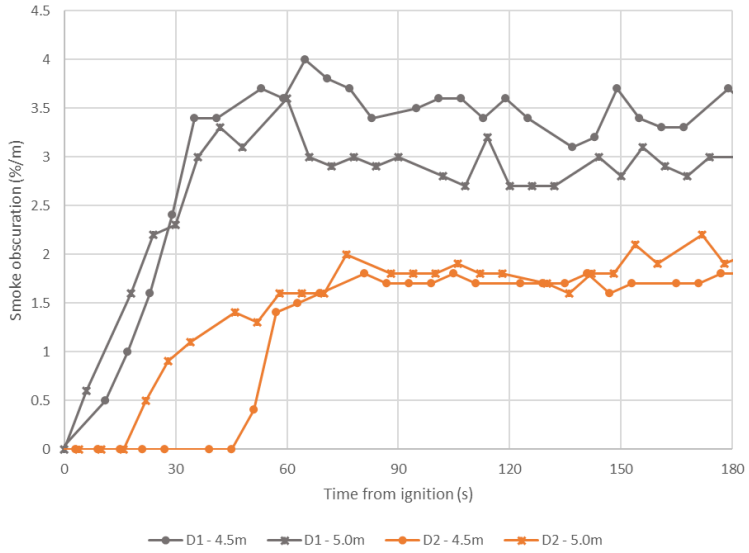

Figure 20: Smoke density measurements from point detectors PD1 mounted in two different positions and two different heights, namely position D1 (above the fire) and D2 (4m horizontal distance from the fire) and heights 4.5 m and 5m. Data from test 17 in the second test series.

10.1.3.4 Lithium-ion battery tests

In the first test series, the short-circuit of the battery module broke within a second and did not produce much overheating or smoke, such that the temperature inside the battery module did not go above 60°C. However, the heat from the short-circuit device itself which produced steam and had glowing hot parts was detected in the first experiment by the thermal cameras and then the linear heat detection systems because the short-circuit device was outside the container (see Figure 21). Similarly, the overheating of the single pouch cell on the hot plate did not produce much flame or smoke to be detected by any of the detectors.

In the second test series, the overheating of three pouch cells in a steel box produced heavy smoke which was visible from the battery cells 20 min after the heating was initiated (t = 0 s). In test 27, the video smoke detection algorithm triggered the alarm at ~25 min, i.e., nearly 2 minutes after the battery cells had caught fire (t = 1376 s), followed by alarms from the point detectors, while they battery cells were still aflame until ~45 minutes (t = 2713 s). In test 28, point detector PD2a triggered the alarm at ~27 min, i.e., nearly one minute before the battery cells caught fire (t = 1690 s), followed by alarms from the other point detectors, then thermal camera IR1, and then the video smoke detection algorithm, while the battery cells were still aflame until ~44 minutes (t = 2631 s).

The measurements from the carbon monoxide (CO) detectors in tests 27 and 28 with three pouch cells heated in a steel box are shown in Figure 22. The concentrations of CO at the floor level exceeded 40 ppm, but the concentrations at 25 cm and 50 cm above the floor level were much lower. It was only after an initial period of heavy smoke dropping to the floor that the smoke started rising and triggered the point smoke detectors in the ceiling (detection times ranging from ~27 min to ~35 min). This suggests that an overheated battery (e.g., under an EV) may release heavy smoke containing detectable CO at the floor level several minutes before the smoke starts rising towards the smoke detectors on the ceiling. However, this lower layer of smoke is thin and its concentration decreases rapidly with height.

Figure 21: The short-circuit device used in the two first lithium-ion battery tests is shown to the right (red rectangle). The unit produced steam and had hot glowing parts which triggered the IR detectors and the linear heat detection system.

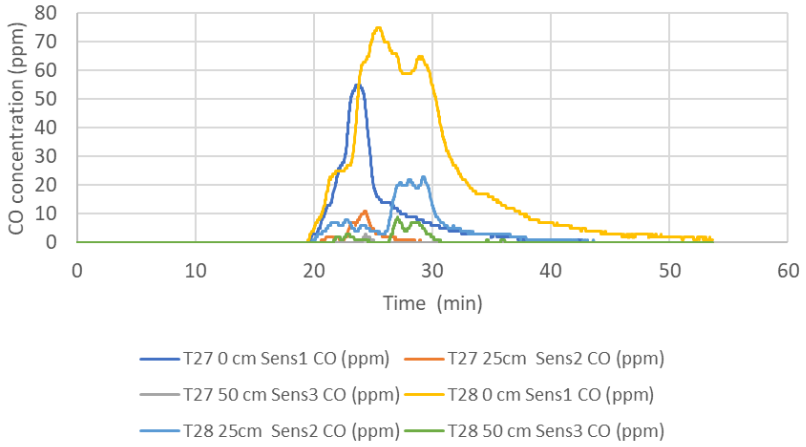

Figure 22: CO concentration measurements from three detectors mounted at different heights during tests with lithium-ion batteries. The data is collected from test 27 and 28 of the second test series.

10.2 Fire experiments with side walls simulating vehicles

The behaviour of a fire is affected by the presence of walls and other obstructions nearby, such as cars and trucks. To prepare for assessing such effects using onboard testing, laboratory experiments were performed to gain confidence in the experimental design for onboard tests.

10.2.1 Experimental calibrations

According to EN 54-10 [18], a heptane pool fire can be used for the testing of flame wavelength detectors. However, an equivalent gas burner had to be produced during the LASH FIRE project after receiving feedback from DFDS because the standard testing method using a heptane pool fire was not practical for onboard tests. The designed gas burner measures 30 × 30 × 30 cm^3 operated using a small 11 kg propane bottle (see Figure 23). The inside of the gas burner was filled with lightweight clay aggregates that disperse the propane uniformly, creating a flame that looks very much like that of the heptane pool fire source described in EN 54-10 [18].

The gas burner was calibrated such that its heat release rate (~120 kW), flame height (~0.9-1.1 m), and heat fluxes (~5 kW/m^2) were comparable to those of the standard heptane pool fire (see data shown in Figure 24).

The heptane burner used for the calibrations was almost identical in construction, except the inside of it contained water at the bottom and heptane at the top during the test. This was to make sure that the heptane pool surface had the same free height from the top edge of the tray as mentioned in EN 54-10 [18], i.e., 45 mm after adding 500 ml heptane with 3% toluene.

Figure 23: Tray for the heptane pool fire (left) and the equivalent gas burner (middle) used with a propane bottle (right).

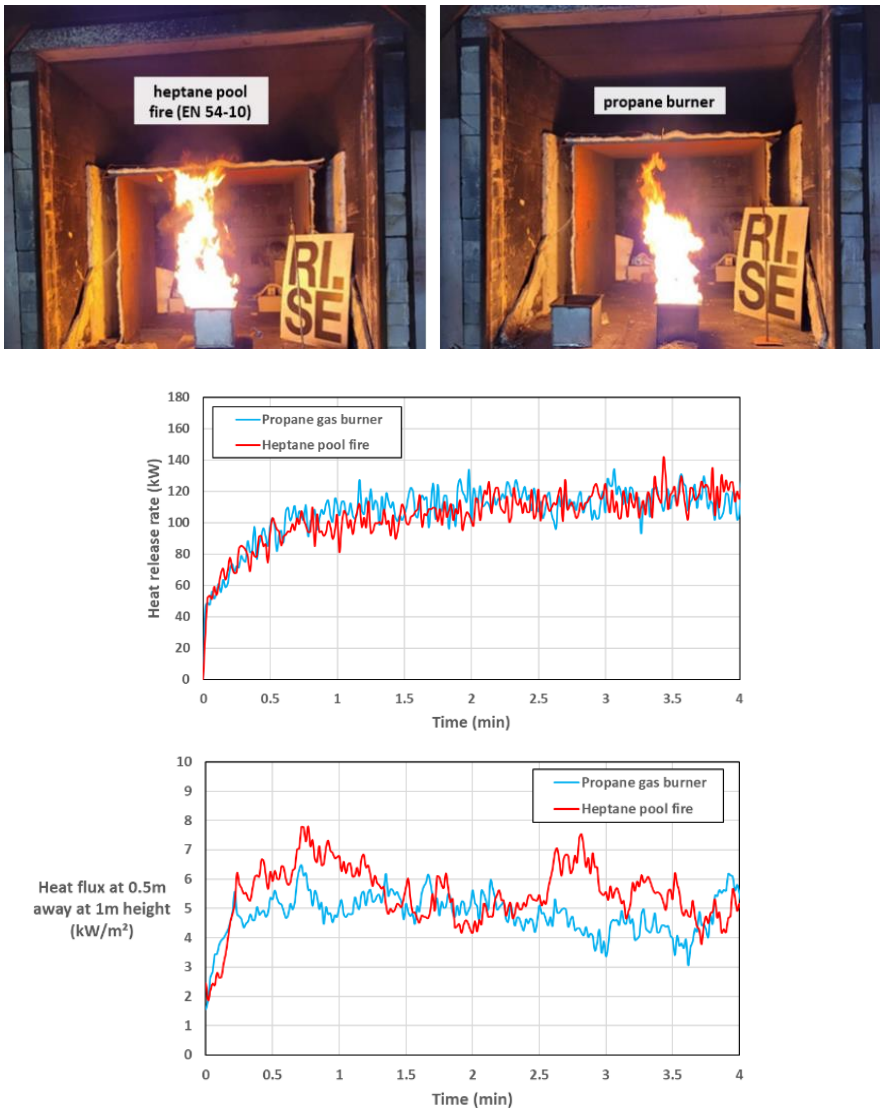

Figure 24: Snapshots of standard heptane fire versus the propane fire (top), heat release rate of each fire (middle), and heat fluxes (bottom) measured at 0.5 m horizontal distance from the edge of each burner at the height of 1 m.

10.2.2 Test setup with side walls simulating cars and trucks

For the truck test, two gypsum panels were used, each measuring 4 m high (average truck height) and 1.2 m wide. The panels were fixed upright and placed 0.5 m apart from one another as shown in Figure 25 to simulate two trucks parked next to each other in the ro-ro space. In the middle of the two panels, a fire was created using the propane burner discussed in section 10.2.1, although a higher peak heat release rate was used (see Figure 28). This was to see how a fire on the floor between two trucks is detectable based on the temperature rise along the ceiling at 7.5 m height (note that the detection time determined this way is conservative given that the actual deck height is 5.8 m on board the ship used for the trials). A thermal camera and a thermocouple installed on the ceiling were used to monitor the temperature rise along the ceiling above the burner. On the back side of each panel, three thermocouples were installed at heights 1 m, 1.5 m, and 2.5 m to monitor whether the level of temperature rise is safe for onboard tests.

For the car test, the gypsum panels measured 1.5 m high, but the panels were clamped between concrete blocks such that the top of the panels was at the height of 1.7 m (average car height), while the width of the panels was 1.2 m. The panels were placed 0.5 m apart from one another as shown in Figure 26, simulating two cars parked next to each other in the ro-ro space. In the middle of the two panels, a fire was created using the propane burner discussed in section 10.2.1, although a higher peak heat release rate was used (see Figure 28). A thermal camera and a thermocouple installed on the ceiling were used to monitor the temperature rise along the ceiling above the burner. The height and width of the flame were monitored by video recording. On the back side of each panel, a thermocouple was installed at 1 m height to monitor whether the level of temperature rise is safe for onboard tests.

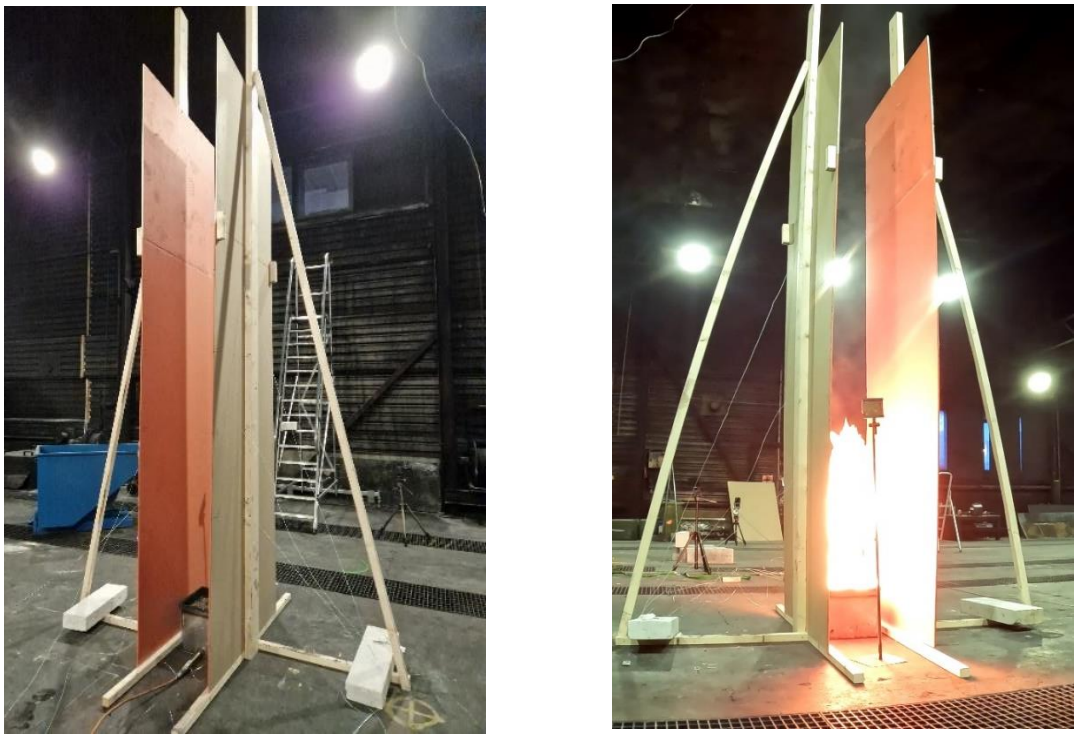

Figure 25: Test setup for fire test with gypsum panels simulating the effect of two trucks parked near the ignition source.

For both the truck test and the car test, the temperature at the surface of the burner was also measured to identify ignition, and the test lasted 10 min after the registered ignition.

Apart from the truck and car tests, a test with no panels was also conducted as a reference case (Figure 27).

Figure 26: Test setup for fire test with gypsum panels simulating the effect of two cars placed near the ignition source.

Figure 27: Reference fire test conducted with no panels.

10.2.3 Results and discussion

Figure 28 shows the heat release rate of the burner which was operated at the maximum possible power using the propane bottle shown in Figure 23. The ceiling temperature rise (with respect to the ambient temperature) is shown in Figure 29 as measured by the thermocouple on the ceiling at 7.5 m above the burner. Thermal images of the ceiling are also shown in Figure 30.

The temperature rise measured along the ceiling was below 25 °C for all the tests, while the ambient temperature in the test hall was about 4 °C. Generally, the temperature increased equally fast in the first 60 s of the three tests, but later the truck test displays a temperature rise that is about 5 °C higher than the reference test conducted with no panels. The car test displayed a temperature rise trend like the reference test with no panels for the first 150 s, but the temperature rise values in the car test after the first 150 s are about 2 °C higher than those of the reference test.

In all the scenarios, the temperature rise reaches 14 °C within 30 s. Comparing this to the alarm criteria suggested for the linear heat detectors in Table 12 and a logging interval of 10 s, the first four criteria are met. This means that the linear heat detection system is expected to raise a fire alarm within 30 s, but this may vary depending on wind speed. The fifth alarm criterion in Table 12 is 20 °C temperature rise within 240 s which was met only during the car and truck tests, but not during the reference test without any panels.

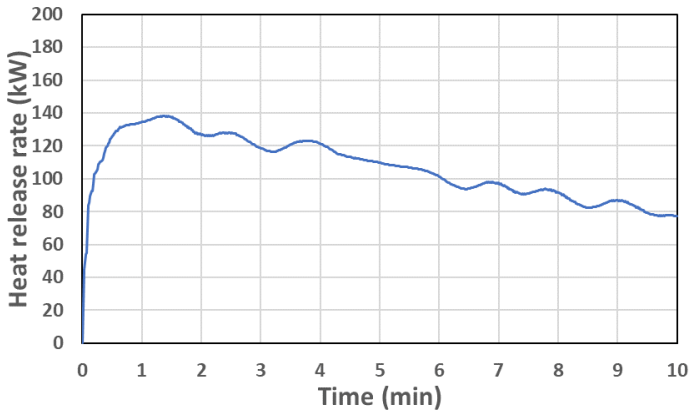

Figure 28: Heat release rate of the burner operated at the maximum possible power using the bottle shown in Figure 23.

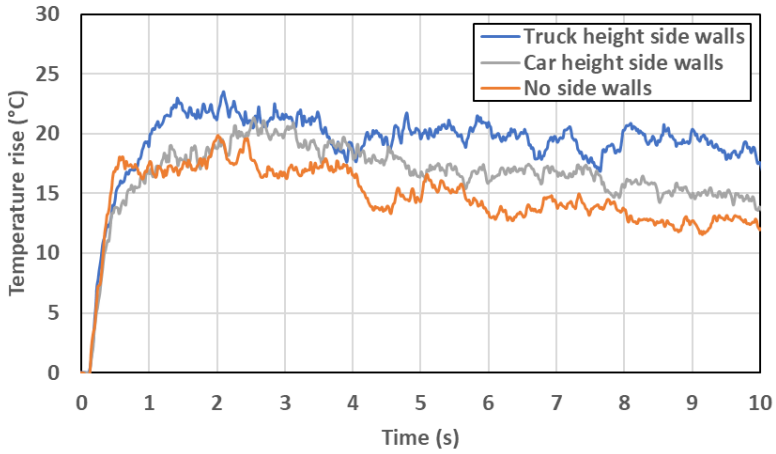

Figure 29: Ceiling temperature rise (with respect to the ambient temperature) measured by the thermocouple placed on the ceiling at 7.5 m above the burner for the tests with truck height side walls (4 m height), car height side walls (1.7 m height), and with no side walls.

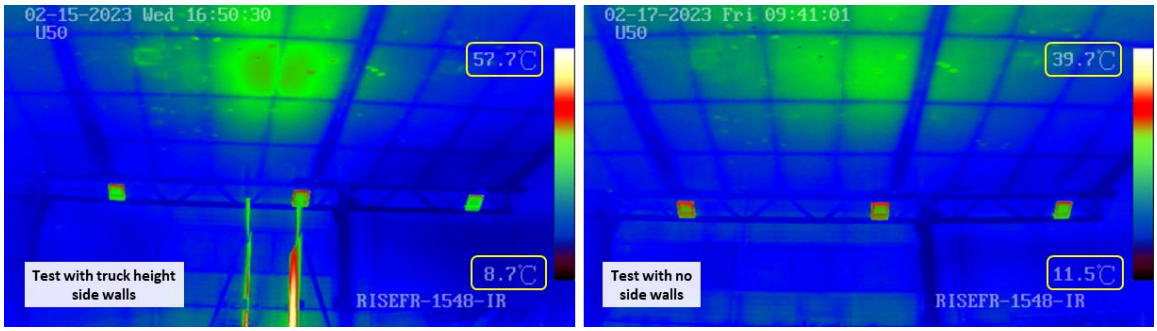

Figure 30: Thermal images of the ceiling showing temperatures at the end of the tests (t = 10 min) with truck height side walls (left) and with no side walls (right). Note that the colour bars generated automatically and recorded in the thermal footage of the infrared camera are different for each case, namely, the maximum temperature range of the colour bar in the left image is higher because the hot truck-height walls are visible in the image.

It is noteworthy that the flame tip from the 140-kW fire was high enough to be visible above the car height (see Figure 26). Therefore, optical detectors such as video fire detection systems and flame wavelength detectors are expected to detect this flame within seconds if the camera/detector sees

the fire area or the flame reflections. However, the flame height was not high enough to be visible above the truck height (see Figure 25). Therefore, optical detectors are not expected to see the fire in the latter scenario unless the fire gets bigger or it is reflected toward the detector.

10.3 Wind experiments

High wind speeds can affect fire dynamics and thereby the ability of detection systems in open ro-ro spaces to detect the fire. Several tests were conducted to investigate this effect. These tests complement the lower wind speed tests discussed in section 10.1.3.1.

10.3.1 Experimental set-up

The wind experiments were conducted using the propane gas burner discussed in section 10.2.1 with the heat release rate shown in Figure 28. Fans were placed at 3.45 m distance from the burner, and a wind speed sensor was placed in between at 1.5 m from the burner and 1.95 m from the fans at the height of 0.5 m as shown in Figure 31. A CCTV camera and a thermal camera were used to monitor the flame. These were installed on a tripod placed on a scaffolding at 10 m height as shown in Figure 32. The horizontal distance between the burner and the cameras was 27.1 m. Nine experiments were conducted in total with wind speeds ranging from 4.5 to 11 m/s.

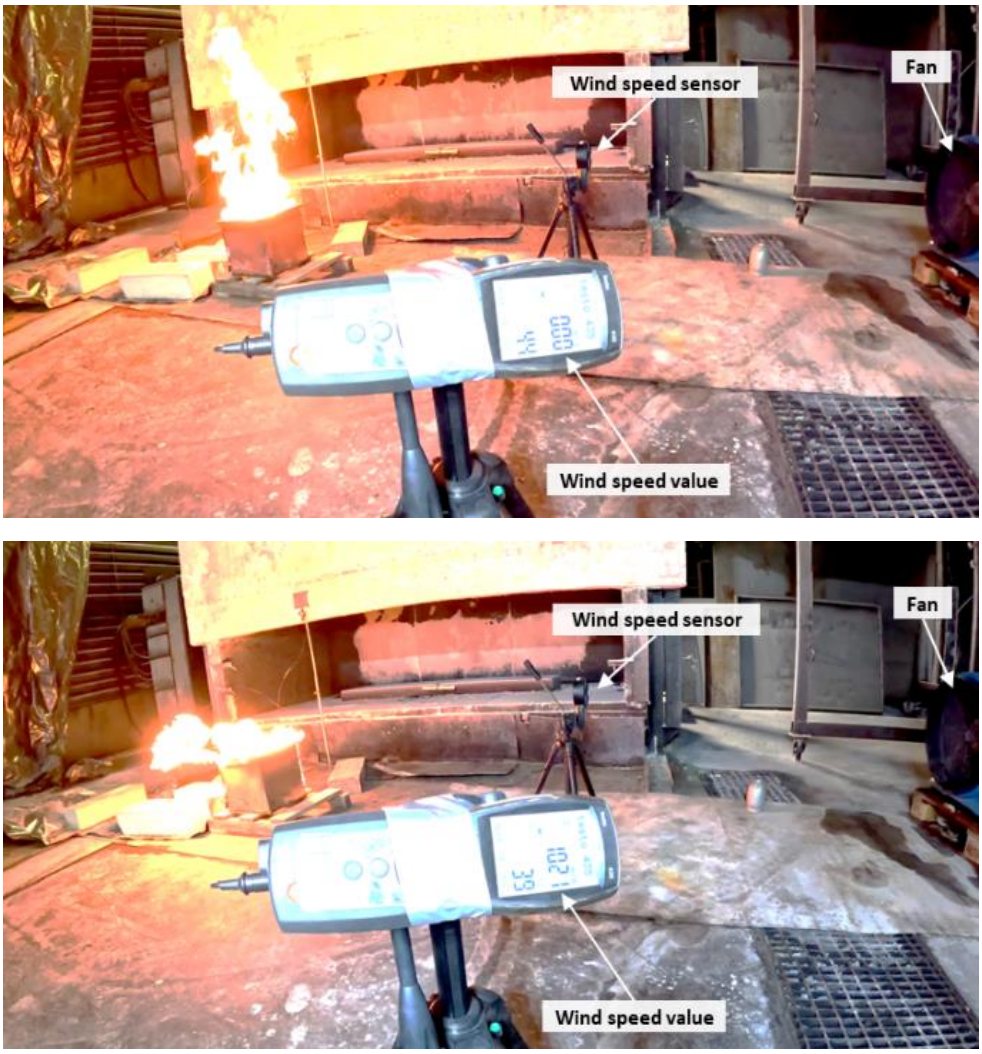

Figure 31: Snapshots showing a wind test with the propane burner before and after fan activation (wind speed = 10.21 m/s).

Figure 32: Thermal imaging (IR) camera and regular CCTV camera installed at 10 m height and 27.1 m horizontal distance from the burner shown in Figure 31.

10.3.2 Results

Figures 33 and 34 show snapshots that illustrate the effect of wind on the flame shape recorded in the footage of thermal imaging and regular video cameras. The wind usually makes the flame occupy fewer pixels in images from both regular video and thermal imaging cameras, but the reflections of the flame on nearby surfaces could sometimes make the fire appear much larger in images captured by regular video cameras. This effect is quantified in Table 13, which presents the average number of footage pixels occupied by the flame obtained based on the data of 20 random footage frames for each camera type.

The quantitative results shown in Table 13 suggest that lower wind speeds (in the order of 4.5 m/s) cause the biggest amount of change in the recorded size of the flame, whereas the highest wind speeds (in the order of 11 m/s) cause the smallest amount of change in the recorded size of the flame. This is because the higher speeds cause the flame to pulsate back and forth more chaotically, such that the overall recorded size of the flame on average is still considerable compared to the original flame size recorded without wind. This is while lower wind speeds cause more regular flame tilting that keeps the size of the flame smaller than that with no wind. As a result, it is expected that lower wind speeds cause more challenge for fire detection than high wind speeds.

Figure 33: Wind effects visible in footage snapshots of a flame captured by a camera at 27.1 m horizontal distance and 10 m height: the wind causes the fire to appear smaller sometimes (middle photo) and bigger at some other times (right photo) due to the image saturation and flame reflections from nearby surfaces.

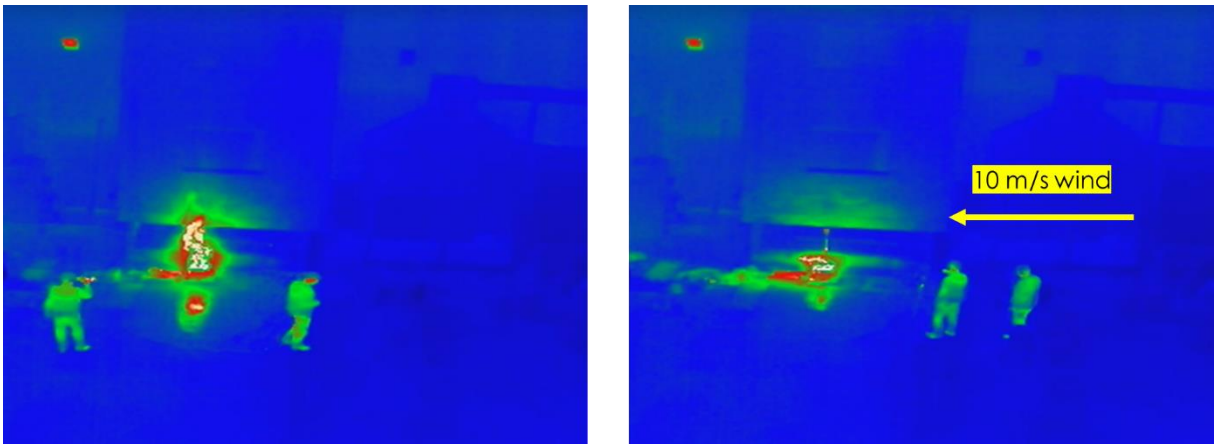

Figure 34: Wind effects visible in footage snapshots of a flame captured by a thermal imaging camera at 27.1 m horizontal distance and 10 m height: the wind causes the flame to occupy fewer pixels, which makes it more difficult to detect.

Table 13: Average number of image pixels occupied by the flame in thermal imaging and regular video footage from the wind tests.

Wind source	Regular video footage		Thermal imaging footage		% of change with wind for regular video camera	% of change with wind for thermal imaging camera
	Flame pixels without wind	Flame pixels with wind	Flame pixels without wind	Flame pixels with wind		
Small fan (~4.5 m/s)	24054	6840	5921	1758	-72%	-70%
Big fan (~10 m/s)	27288	12797	4692	1518	-53%	-68%
Both fans (~11 m/s)	23322	18719	3066	1941	-20%	-37%

The results also suggest that the change in flame size due to wind is bigger in thermal images than in regular video images for all cases with wind, except the case with the small fan where both image types have the same level of change. This is because regular video images tend to get saturated by highly luminous sources such as flames. Reflections over shiny surfaces are also perceived more strongly in regular video images. In contrast, thermal images tend to be more precise in their localization of the actual flame boundaries, with minimal image saturation. This precision quality of thermal images is usually beneficial for surveillance of hot areas, but it may make manual detection of fires more difficult in occasions with windy conditions, especially with lower wind speeds which reduce the flame size the most (note that overwhelming image saturation and high-speed changes due to strong wind can also confuse some video analytics algorithms). However, systematic fire detection based on temperature thresholds in the thermal image is still highly reliable. To the contrary, video detection systems that rely on flame flicker patterns across a certain number of pixels may have more difficulty detecting the fire in a systematic way under windy conditions.

10.4 Main findings from laboratory tests

The point detectors of smoke were found to be superior in detecting the beechwood sticks on the hot plate which produced a lot of smoke, whereas neither the linear heat detection systems nor the optical detectors detected these smouldering fires, with the exception of infrared optical detectors which detected the hot plate in several cases. This suggests that point detectors are a good option for the detection of smouldering fires, although wind and ventilation in open ro-ro spaces are expected to make the detection much more difficult. The laboratory experiments also showed that

the beam compartments along the ceiling cause the smoke to accumulate in one area, and this significantly delays the movement of smoke towards detectors further away from the fire.

Ethanol fires, which produce much less visible smoke compared to heptane and beechwood stick fires, were not detected by point detectors, but the linear heat detection systems installed on the ceiling could detect all the ethanol fires except the fires starting below the containers. The optical detectors could also detect some of the ethanol fires. In general, however, the linear heat detection systems detected more fires than the optical detectors, although the fewer responses provided by the optical detectors were faster than those of the linear heat detection systems. As expected, the optical detectors could only detect the fire when the fire was visible in their field of view.

Heptane fires, which produce more smoke, were more often detected by linear heat detection systems than optical detectors. This can be linked to the limited number and field of view of the optical detectors. The larger the ro-ro space, the more optical detectors are needed to ensure good coverage and field of view, while a linear heat detection system can more easily cover large areas and is less affected by visual obstacles, as long as the generated heat from a fire can reach the overhead where the cable is installed.

In tests with lithium-ion batteries, the CO concentrations at the floor level exceeded 40 ppm, but the concentrations just 25 cm above the floor were much lower. The smoke initially dropped to the floor level before rising and triggering the smoke detectors on the ceiling. This suggests that installing smoke detectors near/on the floor in areas where lithium-ion batteries are placed may reduce the smoke detection time significantly. However, such installations on the floor are not expected to be practical in ro-ro spaces.

The tests with and without side walls displayed how the presence/absence of tall structures near a fire, such as trucks or cars, can change the fire detection along the ceiling. This is an important factor to consider when designing a detection system, as the placement of the sensors with respect to the cargo items can strongly affect the detection time.

Based on the fire tests conducted with wind speeds from 0 to 5 m/s, it seems that the wind sensitivity of point detectors is higher than that of the other tested detection systems, such that fewer point detectors detect the fire as wind is introduced, whereas no clear trend of effects from wind can be seen for the other detection systems. Therefore, it is expected that the alternative detection systems tested can improve detection to a greater extent in open ro-ro spaces where there are wind effects. For optical detectors relying on thermal imaging or regular video analytics, experiments with wind blowing against a propane burner fire showed that the flame size in the footage of cameras changes more dramatically for lower wind speeds (~4.5 m/s) than for high wind speeds (~11 m/s). Moreover, the change in flame size was more dramatic for thermal imaging cameras than for regular video cameras. As a result, manual observations of the flame in the footage are expected to be more challenging in windy conditions. As for systematic fire detection, it is expected that thermal imaging systems based on temperature thresholds can detect the fire more reliably than video fire detection systems, although it is noteworthy that thermal imaging systems can be prone to frequent nuisance alarms if the maximum temperature or rate of rise detection criteria are not fixed with the right sensitivity thresholds.

11 Onboard evaluations

Main author of the chapter: Davood Zeinali (FRN), Robert Benitz (APS)

Based on the conducted simulations and laboratory evaluations, several candidate detectors were selected and tested on board Hollandia Seaways (DFDS ro-ro cargo ship) between February 2022 and July 2023. The present chapter discusses the operational evaluations as well as the fire experiments performed on board to test the sensitivity of the sensors in the beginning and after one year on board.

11.1 Objective and selection of detectors

The main objective of the evaluations on board Hollandia Seaways is to provide a realistic validation for the operational performance of the detection systems. Another important objective is to evaluate how the alarm threshold settings can be optimized for the different systems to balance early detection with a low number of nuisance alarms during normal operations.

For open ro-ro spaces, linear heat detection was selected for onboard evaluations based on the results of conducted simulations and laboratory experiments, as it was found suitable for well-ventilated and windy environments. One available system was based on a fibre-optic cable, and the other option was an electric sensing cable with embedded temperature sensors at discrete intervals. With the default sensitivity settings in the laboratory experiments, the fibre-optic system detected a higher number of fires and had shorter detection times compared to the electric system, although changing the sensitivity settings may make the two systems more comparable. Due to the limited resource available, however, only the fibre-optic system was selected for the onboard evaluations. The system was installed on the upper most open deck of Hollandia Seaways in February 2022. A triple-IR flame wavelength detector was also installed. This was to see how the flame detector performs with the limited field of view available in the open ro-ro space and whether there are any nuisance alarms.

For closed ro-ro spaces, video detection was selected for onboard evaluations, as it was found cost-effective and suitable for average-sized closed decks where the light conditions are stable. Accordingly, a system was installed on the main deck of Hollandia Seaways in February 2022.

The existing point smoke and heat detectors onboard were used as a point of reference to determine whether the newly installed detection systems are able to provide better detection and less frequent nuisance alarms.

11.2 Installations and initial testing

The first system studied on board was the fibre-optic linear heat detection system, with approximately 180 m sensor cable length, installed as part of the LASH FIRE trials in the uppermost open ro-ro space (deck 7) of Hollandia Seaways as shown in Figures 35, 36, and 37. After installation, the boundaries of the rows along the deckhead were marked on the sensor cable using frost spray (see Figure 38). This allowed to virtually split the cable into several alarm zones, each zone covering two or three deck rows. Subsequently, the live measured temperatures along the cable could be visualized in the form of a thermal map as illustrated in Figure 39. The settings of the fibre-optic linear heat detection system were fixed as follows:

- Measurement time per channel: 10 s.
- Spatial resolution: 1 m.

- Confirmation cycle enabled: an alarm is only triggered if the alarm criteria is fulfilled for two consecutive measurement cycles.
- DTS instrument setup: two DTS instruments were used, first DTS monitors the fibre-optic cable only from one end (single ended configuration, no fibre break protection) with a total measurement time of 10 s. Second DTS monitors the fibre cable successively from both ends (loop configuration, fibre break protection), with a total measurement time of 20 s.
- Different alarm criteria are considered simultaneously as explained in section 10.1.3.2.

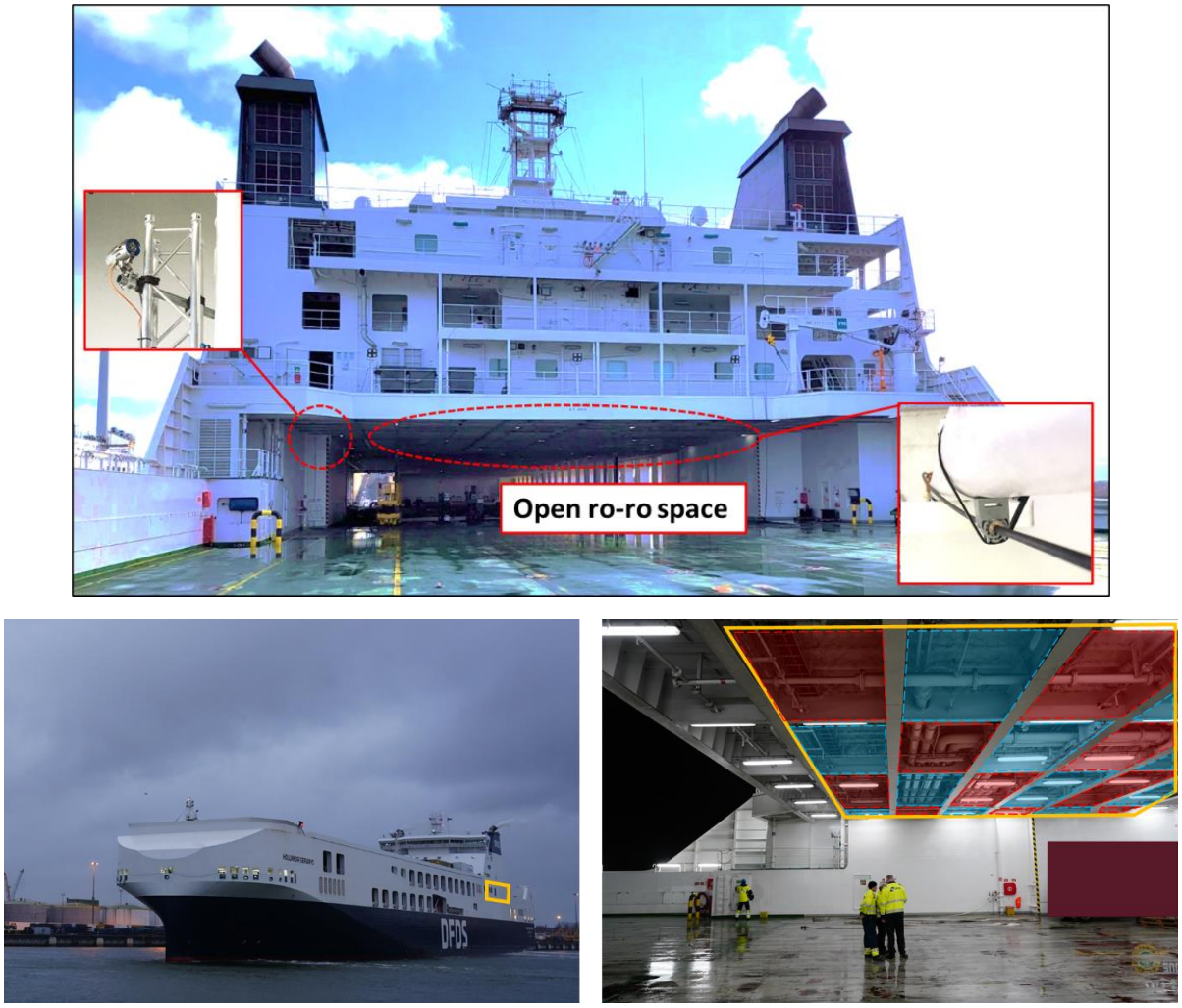

Figure 35: Detector installations in the uppermost open ro-ro space (deck 7) of Hollandia Seaways for the LASH FIRE trials, including a triple-IR flame wavelength detector with triple IR technology that overlooks the aft part of the deck, as well as a fibre-optic linear heat detection system installed along the deckhead in the same area. The geometry of the cable route and the ceiling compartments are shown in Figures 36 and 37. The ship itself has conventional heat detectors in this area.

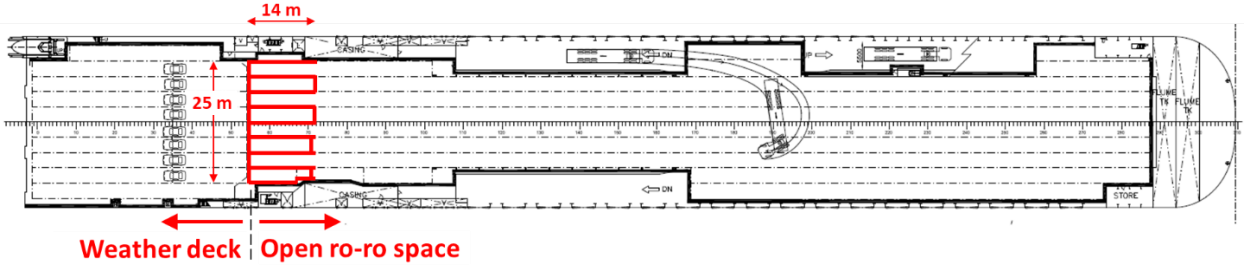

Figure 36: Sketch showing the route and location of the installed fibre-optic linear heat detection cable (thick red line).

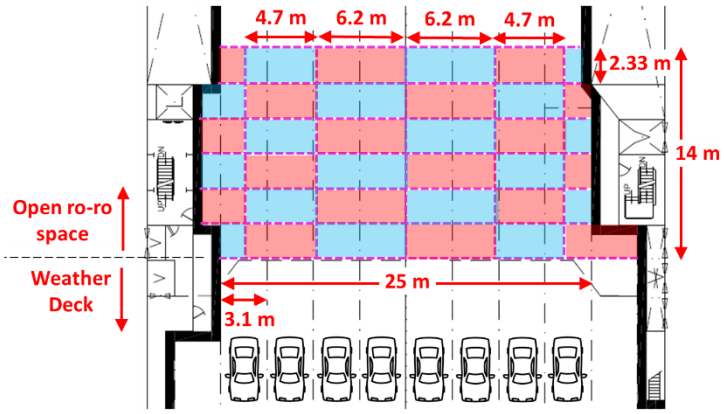

Figure 37: Sketch showing the ceiling compartments created by the transversal and longitudinal girders along the deckhead of the open ro-ro space where the fibre-optic linear heat detection system is installed on Hollandia Seaways. The ceiling compartments are coloured with consecutive shades of blue and red (also illustrated in Figures 35 and 41).

Figure 38: System expert using a frost spray to pinpoint the locations of the different rows of fibre-optic cables installed along the deckhead.

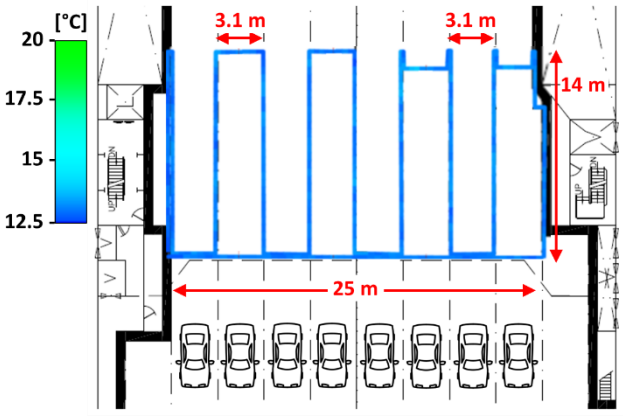

Figure 39: A thermal map from the fibre-optic heat detection cable installed on Hollandia Seaways for the LASH FIRE trials (thermal data provided by AP Sensing).

The second system studied on board was a triple-IR flame wavelength detector configured using its default medium sensitivity settings and a pre-defined 5-s delay for detection. This detector overlooked the aft part of the deck as shown in Figures 35, 40, and 41. After installation, the detector was tested using a flare with flames which was detected within a few seconds (see footage snapshot in Figure 42).

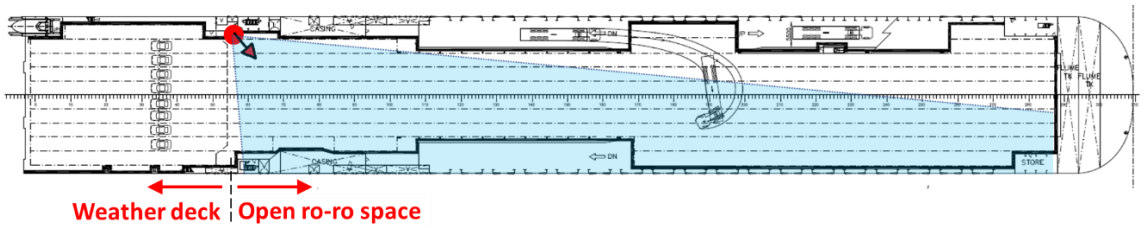

Figure 40: Triple-IR flame wavelength detector installed in the uppermost open ro-ro space (deck 7) of Hollandia Seaways for the LASH FIRE trials. A photo of the installation is shown in Figure 41.

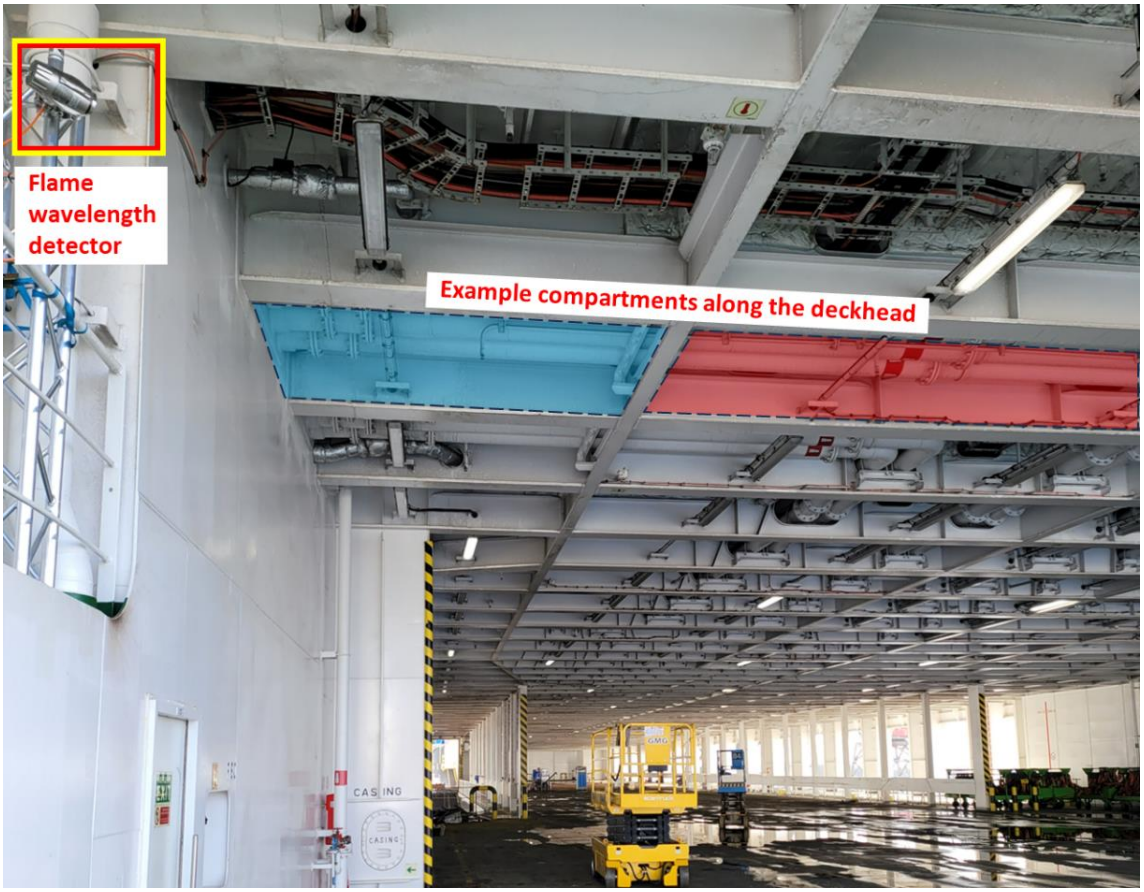

Figure 41: Triple-IR flame wavelength detector installed on Hollandia Seaways for the LASH FIRE trials. The photo also shows examples of compartments along the deckhead which are arranged as shown in Figure 37.

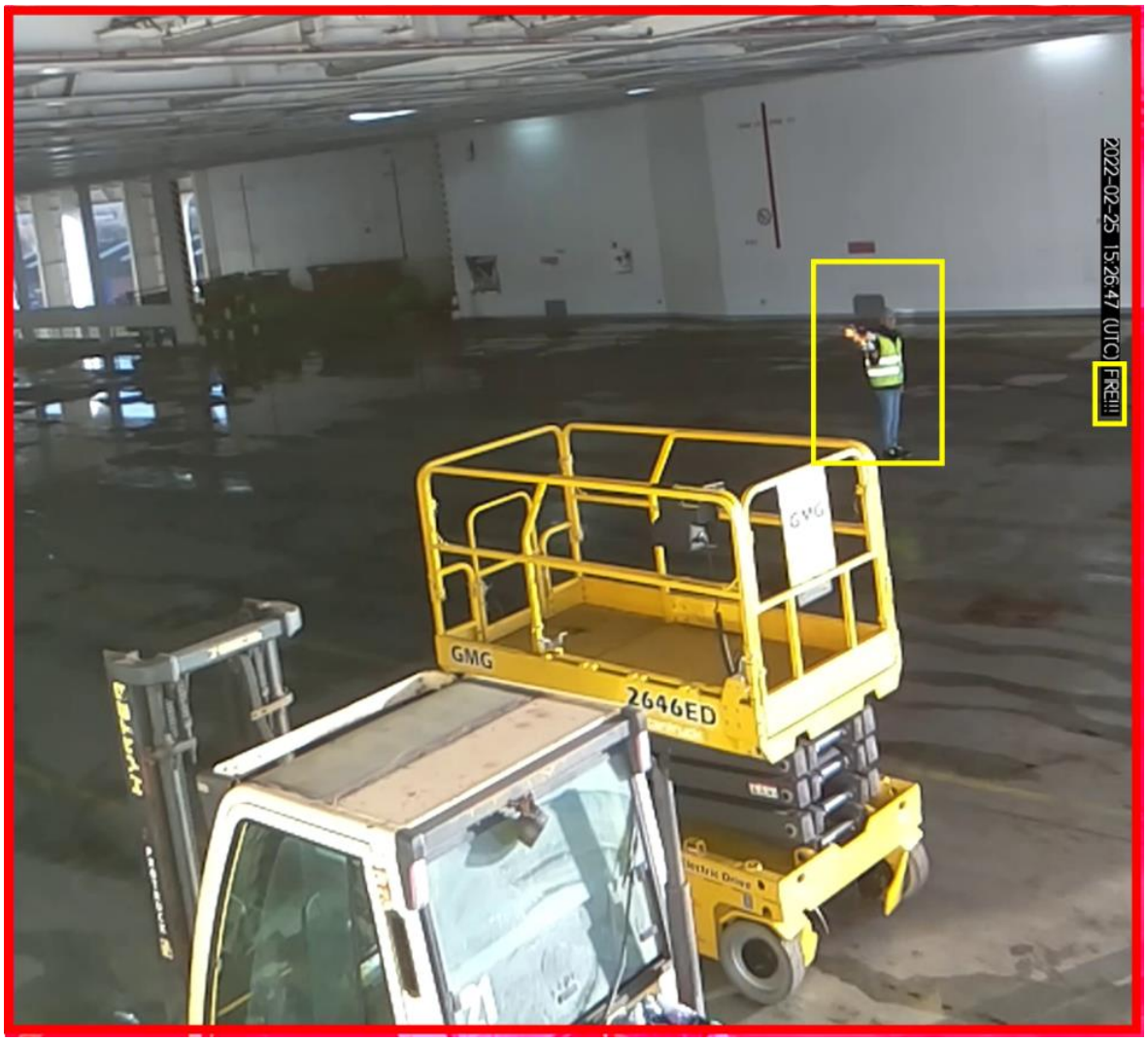

Figure 42: Snapshot from footage recorded by the built-in camera of the triple-IR flame wavelength detector as the presence of flame is confirmed by the detector. The person holding the flare and the "fire" message are highlighted using yellow rectangles.

The third system studied on board Hollandia Seaways was the video fire detection system tested during the laboratory experiments. This system was installed on the main deck, i.e., in the closed ro-ro space in deck 3, as shown in Figure 43.

The video fire detection system was configured with default low sensitivity settings and a pre-defined 5-s delay for detection. Moreover, two detection zones were defined, namely, one for smoke and one for flames, as shown in Figure 43. This was to avoid nuisance alarm sources at lower heights, such as moving vehicle lights, which could be misinterpreted as fire sources. It is noteworthy, however, that the system does monitor the lower heights for the purpose of its analyses, while alarms are only triggered when the detected smoke/flame reaches the pre-defined detection zones. More precisely, the system monitors the light levels across all the footage pixels, and when a group of pixels has a certain light level change and moves in an organized pattern consistent with learned smoke/flame examples, the system triggers an alarm. This is a very basic analogy and there are more nuisances to each proprietary software used for video analytics, which could be useful for monitoring engine rooms for oil mist and smoke as well as large spaces such as vehicle decks for fires.

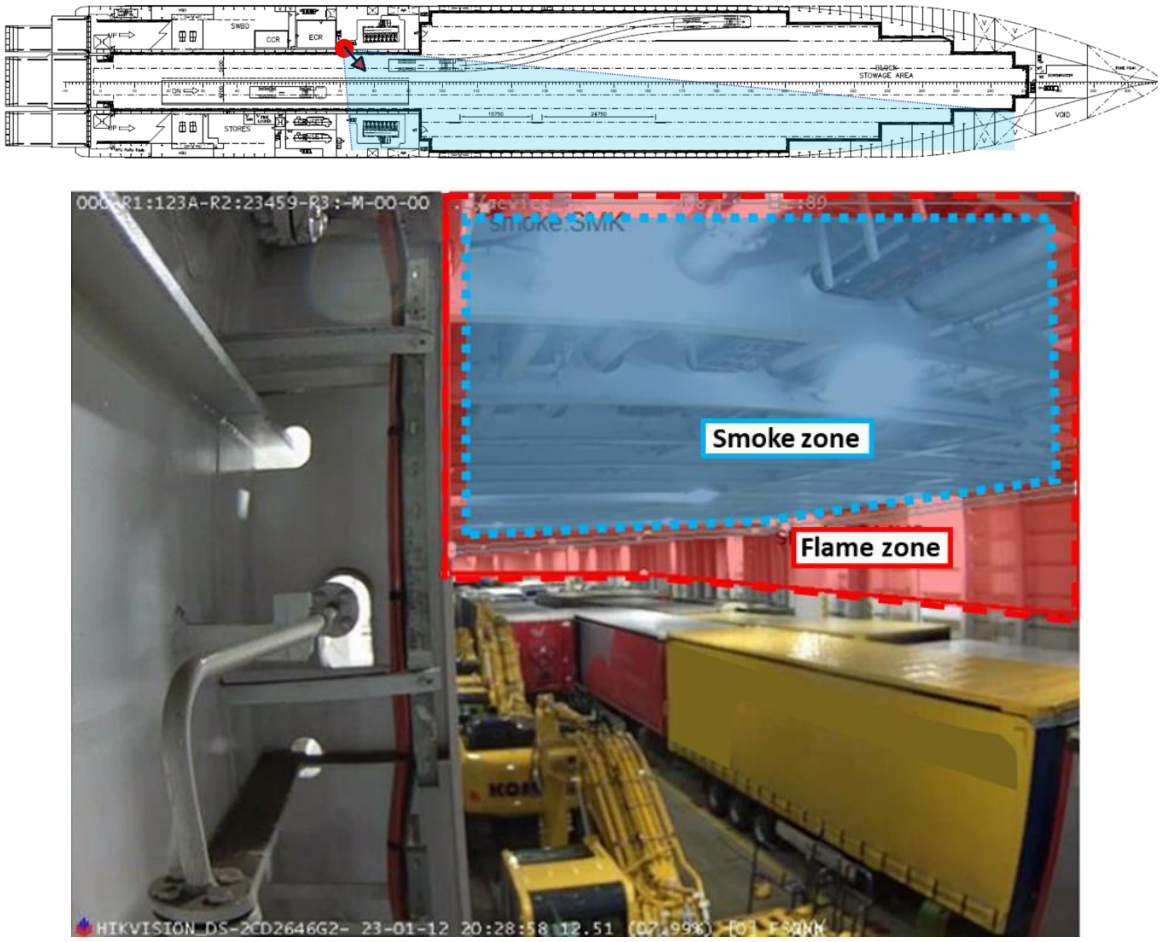

Figure 43: Location of video fire detection camera installed in the closed ro-ro space of deck 3 on Hollandia Seaways (top figure), and snapshot from footage recorded by the camera showing the defined detection zones (bottom figure). The ship itself has conventional smoke/heat detectors on this deck.

11.3 Alarms during normal operations on board

The history of nuisance fire alarms from the new systems installed on Hollandia Seaways is shown in Table 14 for the period from February 2022 to July 2023 while the ship operated as usual. Note that although a low number of nuisance alarms is considered beneficial, the performance of the systems cannot be judged solely based on these results, because a low number of nuisance alarms might be linked to a low sensitivity and thus less ability to detect a real fire.

There were no real fires during the trials, and the triple-IR flame wavelength detector had no nuisance alarms during the normal operations, but both the fibre-optic linear heat detection system and the video fire detection system had nuisance alarms over 17 months of trials. A statistical representation of the alarms from the linear system per alarm criteria and per location is presented in Table 15 and Figure 43. Based on the LASH FIRE investigations, these nuisance alarms from the linear heat detection system were generated by refrigerator trucks known as reefer units or reefers which were allowed to keep their engine running in an idle mode. As discussed in section 5.2, this is done in cases where there are too many reefer units on board such that the number of charging points is not sufficient. As such, the units with their engine running will keep producing exhaust fumes which are detected by the linear heat detection system once there is enough heat accumulation along the deckhead representing a localized hotspot.

Table 14: History of nuisance fire alarms from the new systems installed on Hollandia Seaways as part of LASH FIRE.

	Fibre-optic linear heat detection system (uppermost open deck)[1]	Triple-IR flame wavelength detector (uppermost open deck)	Video fire detection (main deck, closed)[2]
Feb 2022	0	0	-[3]
March	2	0	-[3]
April	1	0	-[3]
May	0	0	-[3]
June	1	0	-[3]
July	2	0	-[3]
Aug	1	0	-[3]
Sept	2	0	-[3]
Oct	0	0	-[3]
Nov	0	0	-[3]
Dec	0	0	-[3]
Jan 2023	2	0	-[3]
Feb	0	0	-[3]
March	0	0	4
April	0	0	1
May	0	0	1
June	1	0	1
July 2023	0	0	4

1 Based on the investigations, nuisance alarms were generated by refrigerator trucks (reefer units) which were allowed to keep their engine running in an idle mode.
2 Based on continuous monitoring, it is expected that all the alarms were associated with the routine washdowns performed by the crew (see text for explanations).
3 The history of alarms for the video analytics were overwritten every 6 months.

Table 15: Nuisance fire alarms from the fibre-optic linear heat detection system installed on Hollandia Seaways as part of LASH FIRE.

Configuration	Criteria	Quantity of nuisance alarms between Feb 2022 and July 2023
Single-ended DTS, 10 s measurement time, 1 confirmation cycle	Maximum Temperature 50°C	0
	Maximum Temperature 57°C	0
	Maximum Temperature 60°C	0
	Zone Avg. +15°C	0
	Rate of Rise (RoR) 8°C/120s	12
	RoR 10°C/120s	4
	RoR 14°C/120s	1
	RoR 20°C/240s	0
	RoR 26°C/360s	0
Dual-ended DTS, 20 s measurement time, 1 confirmation cycle	Max. Temp 50°C	0
	Max. Temp 57°C	0
	Max. Temp 60°C	0
	Zone Avg. +15°C	0
	RoR 8°C/120s	3
	RoR 10°C/120s	0
	RoR 14°C/120s	0
	RoR 20°C/240s	0
	RoR 26°C/360s	0

Measurement time	Criteria	Symbol
10s	8°C/120s	▲
10s	10°C/120s	▲
10s	14°C/120s	▲
20s	8°C/120s	▲

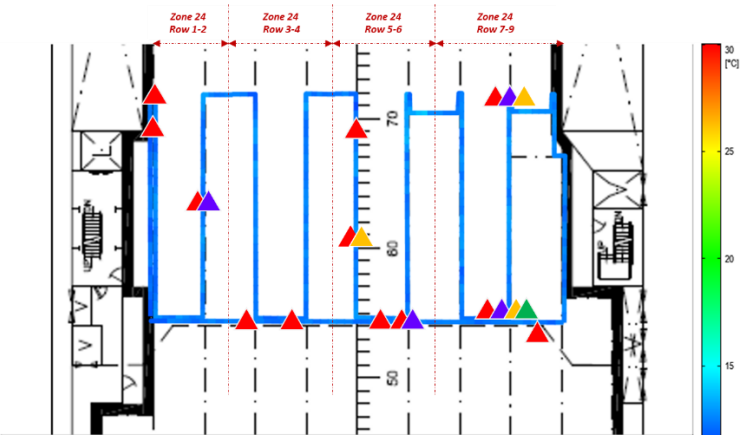

Figure 44: Locations of nuisance fire alarms from the fibre-optic linear heat detection cable installed on Hollandia Seaways as part of LASH FIRE. The data is shown for each alarm criterion and includes the period between Feb 2022 and May 2023 (Illustration provided by AP Sensing).

Figure 45: Nuisance alarm example from the video fire detection system during washdowns: the droplets landing and moving on the lens of the camera are misinterpreted as smoke (boundaries highlighted using grey and blue contours in mid-top and top right respectively).

Based on the nuisance fire alarm data shown in Table 15 and Figure 43 for the fibre-optic linear heat detection system, only some alarm criteria caused nuisance alarms in conjunction with the running reefer units, depending on the measurement configuration and the corresponding measurement time. The single-ended configuration with a 10-s measurement time detected more nuisance alarms in contrast to the dual-ended (loop) configuration with a 20-s measurement time. Moreover, the Rate of Rise (RoR) criterion of 8°C in 120 s was the most sensitive and hence, produced the greatest number of nuisance alarms as expected, while the RoR criterion of 14°C in 120 s produced the fewest number of nuisance alarms.

The video analytics algorithm tested for the closed ro-ro deck generated nuisance alarms only during the routine washdowns of the deck. This is because the water droplets landing and moving on the lens of the camera were interpreted as smoke movements, as shown in Figure 45. This type of nuisance alarm can be avoided either by switching off the detection system during the washdowns or by proactively muting the alarms during the washdown operation around the cameras used for video analytics. Another isolated incident of a nuisance alarm generated by the video fire detection system was from a crewmember on a scissors lift appearing in front of the camera. During the laboratory experiments, a similar observation was made where a person wearing a reflective jacket was misinterpreted as a fire source. However, this was not a regular problem during the onboard

evaluations because the detection zones where defined such that they avoided the lower heights where people and vehicles will be normally visible in the footage.

11.4 Fire experiments in open ro-ro space with side walls simulating trucks

11.4.1 Setup

Fire detection in the open ro-ro deck was investigated at the end of the operational trial using the propane burner shown in Figure 23 with the heat output shown in Figure 28 by placing it at three different locations below the fibre-optic linear heat detection system with one or two side panels as shown in Figure 46.

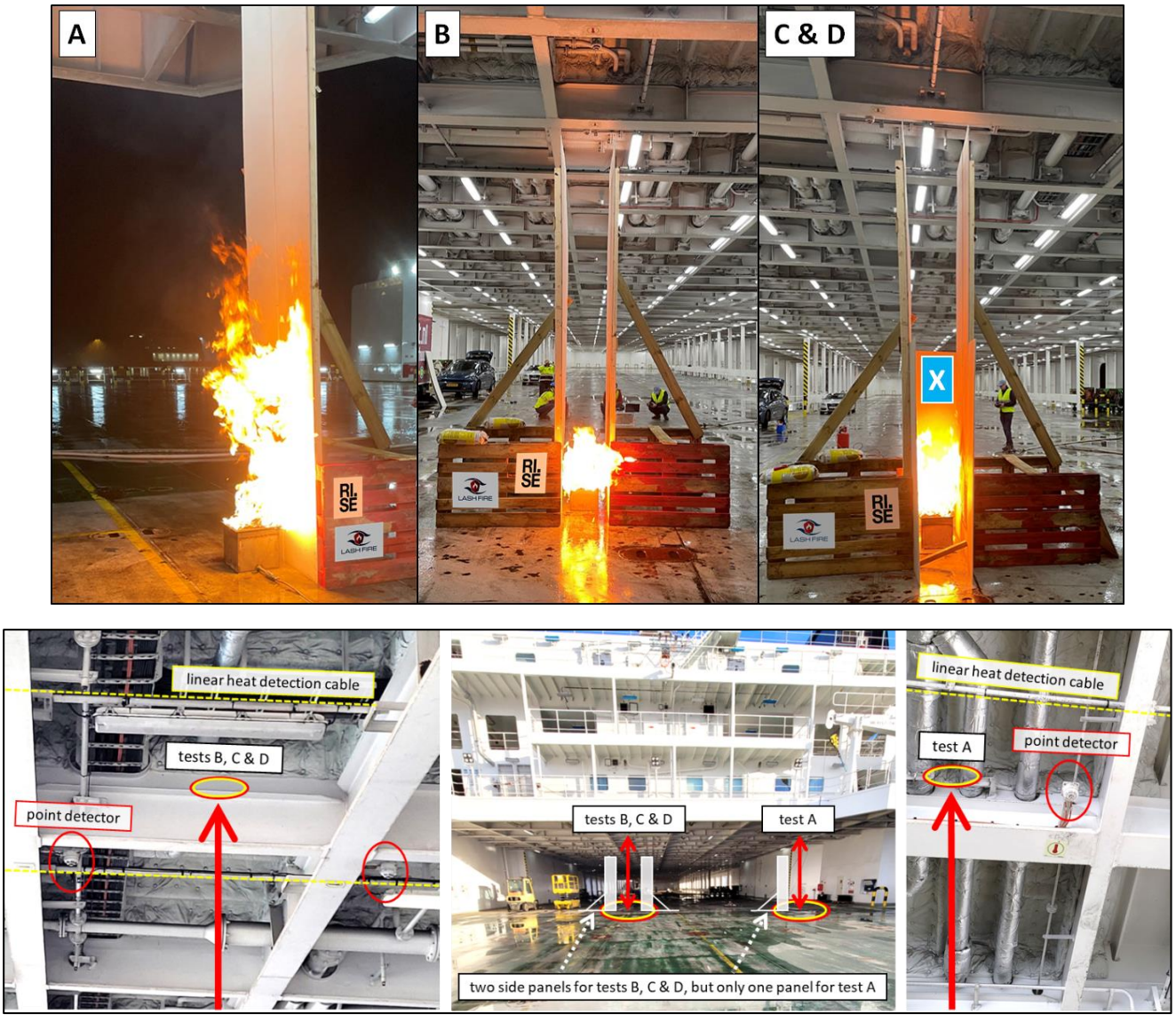

Figure 46: Setup of fire detection experiments on board Hollandia Seaways for the comparison of fibre-optic linear heat detection versus ceiling-mounted heat detectors on the open ro-ro deck in three scenarios: (A) a fire beside a truck-height panel near one side of the deck; (B) a fire between two truck-height panels in the middle of the deck and at the centre of a car lane; (C) a fire between two truck-height panels in the middle of the deck and on the sideline of a car lane; (D) similar to scenario 'C' but with a wind screen created using a car-height panel (marked with an X on the photo to the right).

After the panels had been installed, the burner was ignited using a gas torch. The burner was switched off after the linear system detected the fire, or after 10-15 minutes if there was no

detection. In case of detection, notes were made of the response time of the linear heat detection system and that of the ship's own heat detectors (EN54-22 point detector with alarm criterion of 54°C maximum temperature). The design of the setup was similar to that tested at the laboratory as described in section 10.2.2. A portable (handheld) thermal camera was used to measure the temperatures surrounding the setup. According to the ship's control room, there was crosswind blowing against the ship at the time of the tests with a velocity in the order of 13 m/s. Moreover, the ambient temperature was 10°C, and the relative humidity level was between 75 and 100% during the tests.

In test scenario B shown in Figure 46, the burner was placed at the centre of a car lane to be equally away (~1.5 m) from the linear heat detection cable and the ship's own point heat detector. In test scenario C, the burner was placed on the sideline of a car lane, i.e., in a position that is normally between two trucks. In test scenario D, a car-height panel was placed at the backside of the setup to reduce the effect of wind. This was done because the ro-ro space was empty at the time of the fire tests, and this created an unrealistically windy condition compared to a real scenario in which the deck is filled with trucks and trailers which are expected to provide significant resistance against wind at lower heights.

11.4.2 Results

In test scenario A shown in Figure 46, the fire was not detected by the ship's own heat detectors after approximately 10 minutes. In contrast, the fire was detected by the fibre-optic linear heat detection system (see Figures 47 and 48), namely, using the single-ended DTS configuration in 103 s with the RoR criterion of 8°C/120 s, in 163 s with the RoR criterion of 10°C/120 s, and in 173 s with the RoR criterion of 14°C/120 s. With the dual-ended DTS configuration, the detection times were 182 s using the RoR criterion of 8°C/120 s and 202 s using the RoR criterion of 10°C/120 s.

In test scenario B shown in Figure 46, the fire was neither detected by the ship's own heat detectors nor by the fibre-optic linear heat detection system after 15 minutes because there was too much unfavourable wind inside the deck along its longitudinal direction which titled the fire plume and blew the smoke away toward the weather deck. This was due to the ro-ro space being empty at the time of the fire tests. This created an unrealistically windy condition compared to a real scenario in which the deck is filled with trucks and trailers which are expected to provide significant resistance against wind at lower heights. According to the ship's control room, there was crosswind blowing against the ship at the time of the tests with a velocity in the order of 13 m/s. Based on local wind speed measurements using a weather probe placed in front of the test area, it is expected that the wind speed along the longitudinal direction of the deck was in the order of 3 m/s.

In test scenario C shown in Figure 46, the fire was neither detected by the ship's own heat detectors nor by the fibre-optic linear heat detection system after 15 minutes. This was again because of the strong unfavourable wind inside the deck along its longitudinal direction.

In test scenario D shown in Figure 46, the car-height panel placed at the backside of the setup was able to reduce the effect of wind, making it more like a scenario in which the deck is filled with trucks and trailers with less wind effects at lower heights. Moreover, the fire was directly below the linear heat detection cable, so the fire was detected by the linear system this time (see Figures 49 and 50), while the ship's own heat detectors still could not detect the fire after 15 minutes, despite a point detector being very close. In the case of the linear system, the fire was detected in 73 s with both the RoR criteria of 8°C/120 s and 10°C/120 s, in 83 s with the RoR criterion of 14°C/120 s, and in 263 s with the RoR criterion of 20°C/240 s. With the dual-ended DTS configuration, the detection time was 92 s using the RoR criteria of 8°C/120 s, 10°C/120 s, as well as 14°C/120 s. According to the handheld

thermal camera, the maximum temperature reached along the deckhead during test scenario D was nearly 49°C (see Figure 51), although this is expected to be an overestimation related to the surface emissivity assumptions. The linear heat detection system indicated a maximum temperature of only 36°C in the fibre-optic cable.

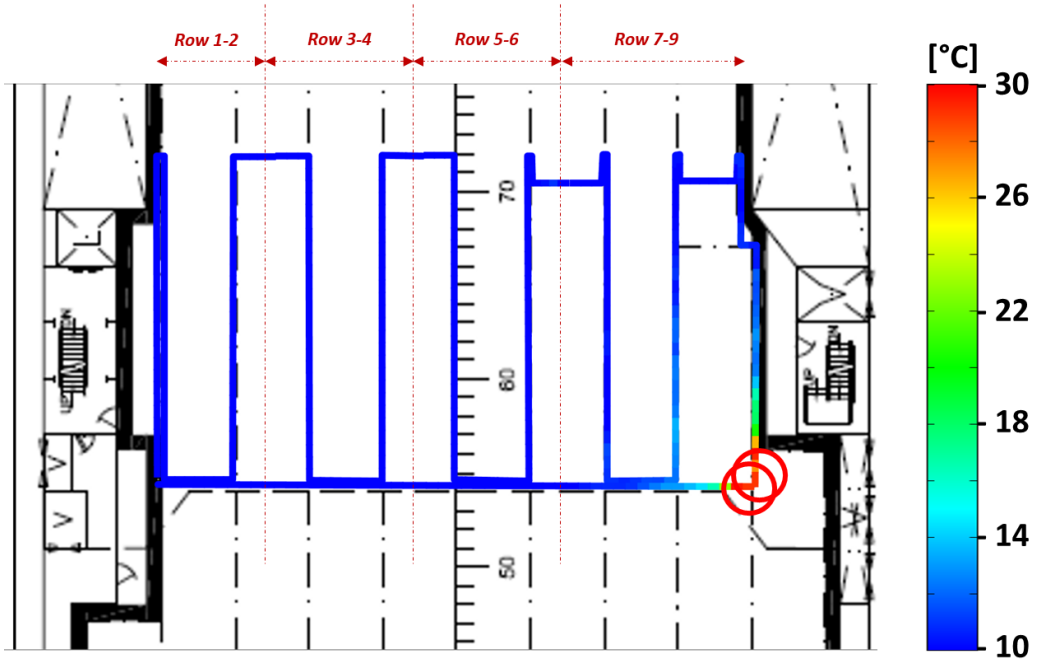

Figure 47: Thermal map showing the locations of fire detection using the fibre-optic linear heat detection cable during test scenario A with the setup shown in Figure 46 (Illustration provided by AP Sensing).

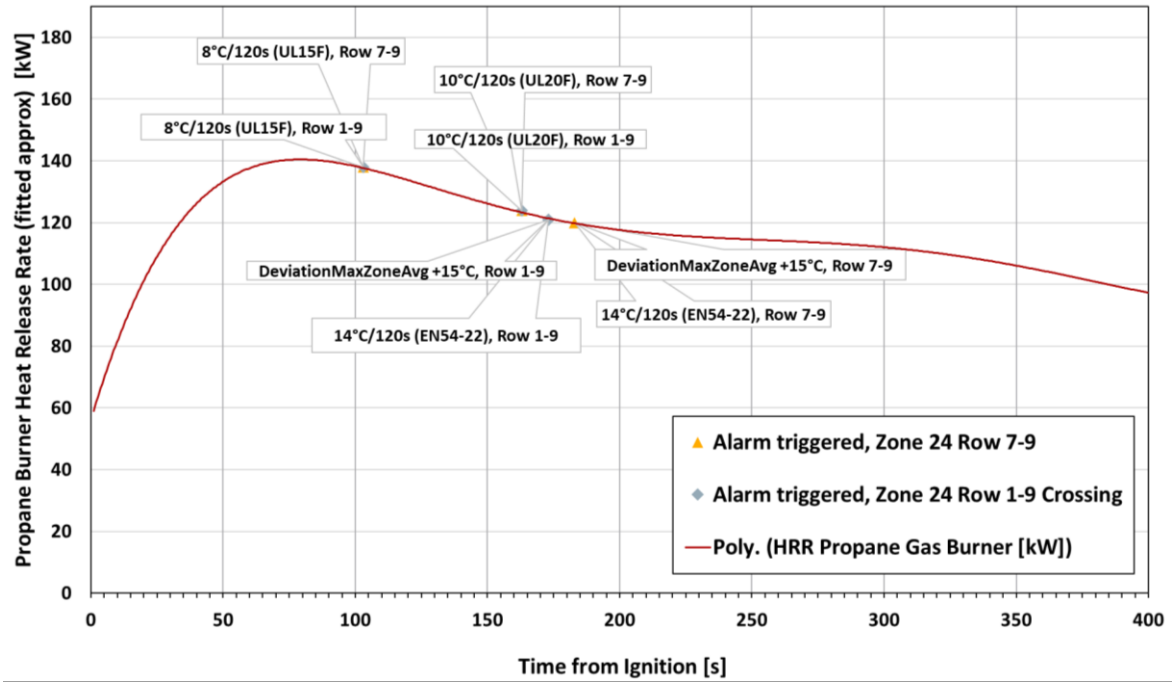

Figure 48: Heat release rate of propane burner annotated with the fire detection times obtained based on different alarm criteria using the fibre-optic linear heat detection cable during test scenario A with the setup shown in Figure 46 (Illustration provided by AP Sensing).

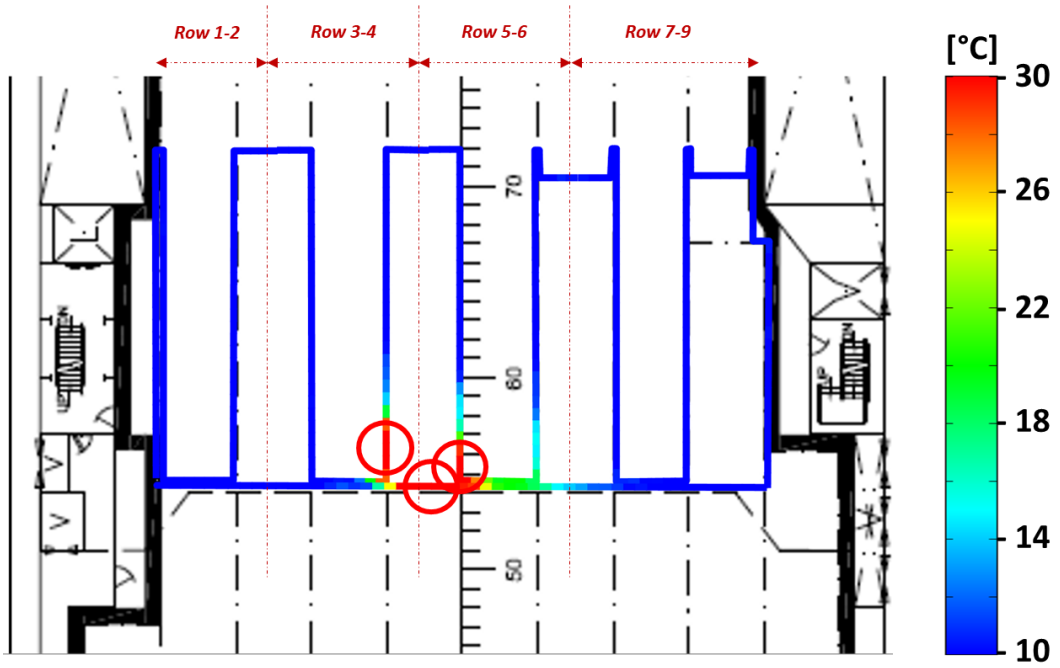

Figure 49: Thermal map showing the locations of fire detection using the fibre-optic linear heat detection cable during test scenario D with the setup shown in Figure 46 (Illustration provided by AP Sensing).

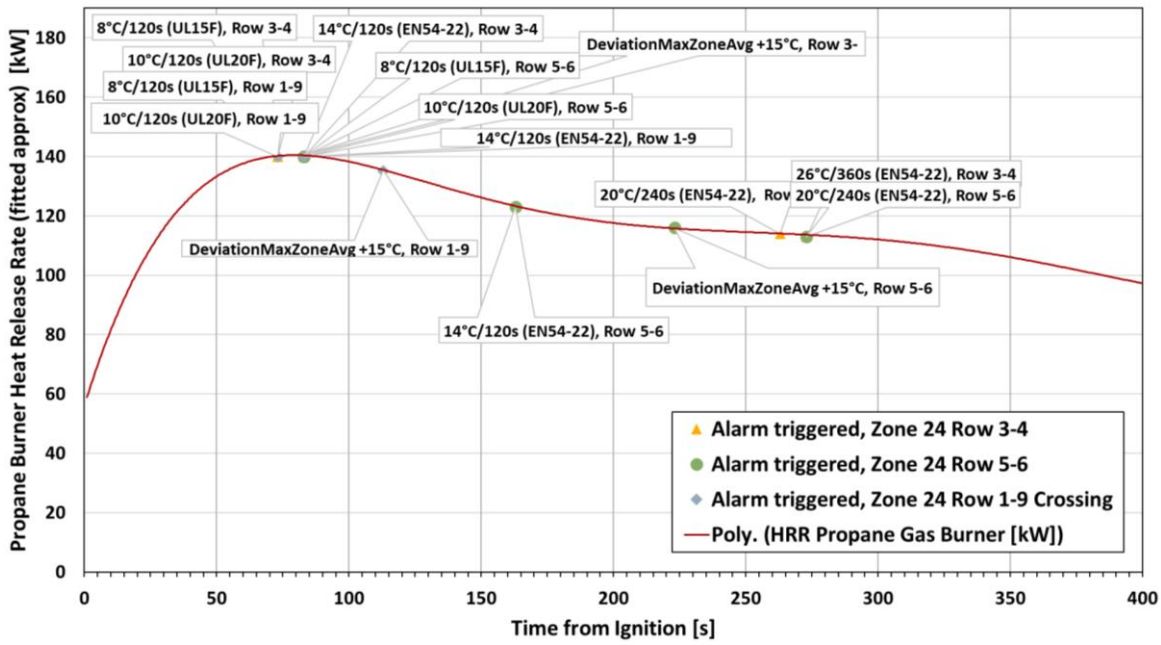

Figure 50: Heat release rate of propane burner annotated with the fire detection times obtained based on different alarm criteria using the fibre-optic linear heat detection cable during test scenario D with the setup shown in Figure 46 (Illustration provided by AP Sensing).

Figure 51: Handheld thermal camera showing temperatures along the deckhead during fire test scenario D shown in Figure 46.

11.5 Flame wavelength detection in open ro-ro space

During the experiments discussed in section 11.4, the triple-IR flame wavelength detector installed in the open ro-ro space detected the reflection of the flame within seconds in test scenarios B, C and D, but the flame in scenario A was not detected, perhaps due to the absence of a reflection. In these cases, the surface reflecting the flame was not visible in the footage of the detector's built-in video camera. However, the reflection surface is expected to have been either the surface of small puddles on the floor or the surfaces of two cars parked on the side of the deck.

11.6 Video fire detection experiments in closed ro-ro space

11.6.1 Setup

To test the video fire detection system installed in the closed ro-ro space, a fog machine was used to conduct smoke tests. The fog machine was operated as shown in Figure 52 and was switched off after the video fire detection system detected the smoke. The tests were performed in two positions: once 27 m from the video detection camera, and once 72 m from the camera. The video analytics settings were set to low sensitivity and a time delay of 5 s. The alarm was set to trigger when the smoke reached the ceiling.

Given that the detection zone for flames was defined at high heights (see Figure 43), flame experiments could not be performed in the closed deck on board due to safety concerns, so the flame detection capability of the video analytics system was not tested during the onboard experiments. However, it is expected the results of the laboratory experiments discussed in section 10 are representative of the performance expected on board.

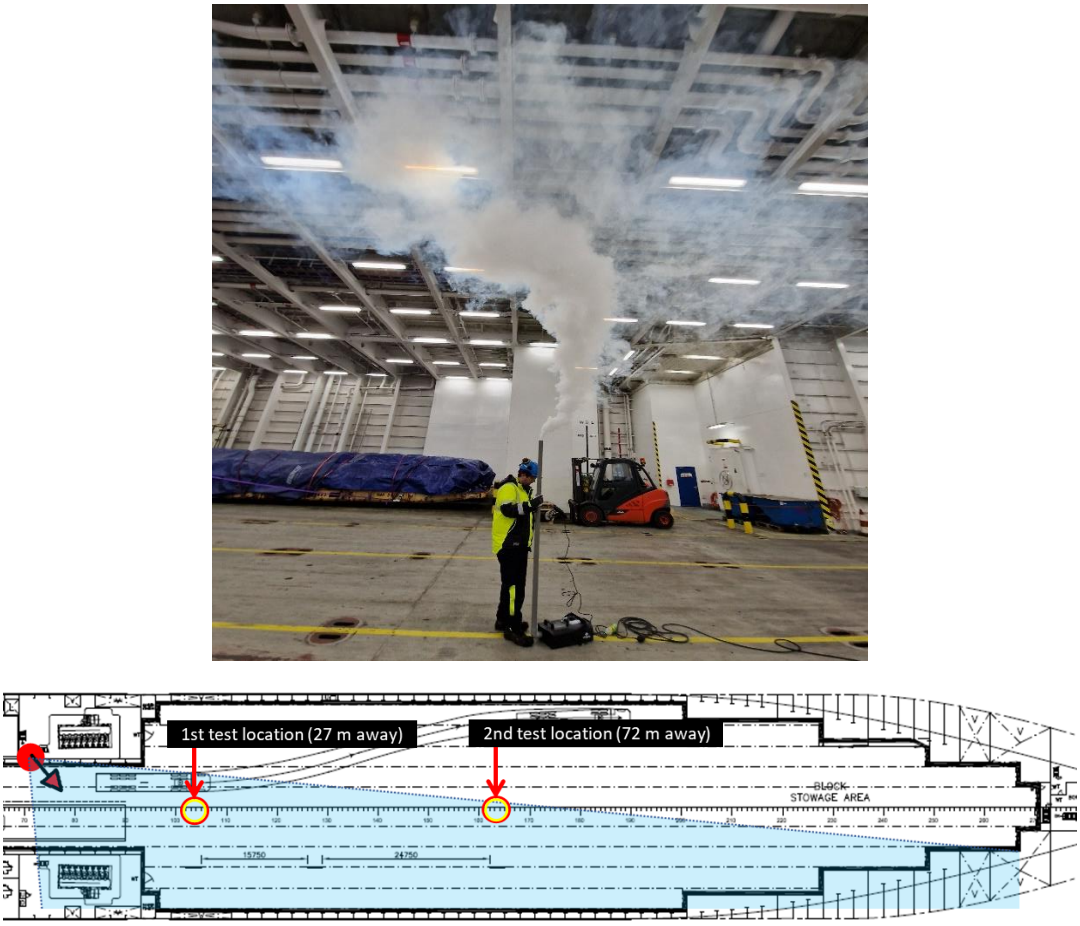

Figure 52: Smoke tests in two locations in the closed deck using a fog machine connected to a duct with a length of 2 m and a diameter of 50 mm. The fog machine essentially heated up a mixture of water and glycol to create artificial smoke.

11.6.2 Results

The video detection system detected the smoke in both the tests. When the smoke source was placed 27 m from the camera, the detection time was 30 s. When the smoke source was placed 72 m from the camera, the detection time was 114 s.

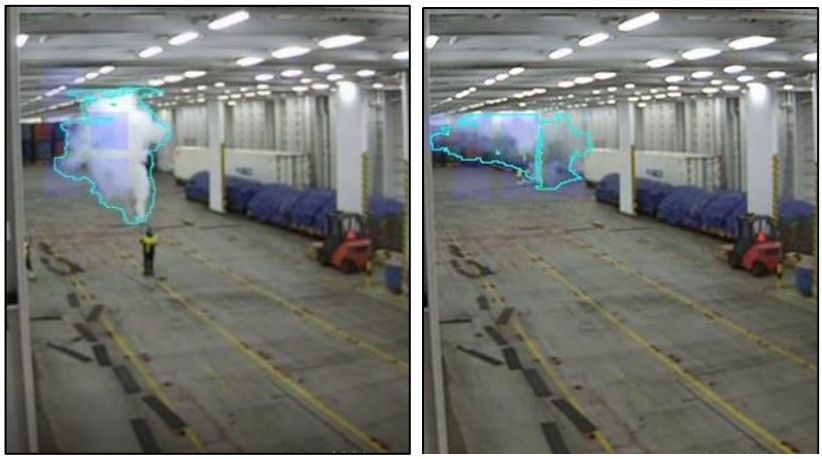

Figure 53: Smoke detected in the closed ro-ro space using video fire detection in 30 s when the smoke source was placed 27 m from the camera (left) and in 114 s when the smoke source was placed 72 m from the camera (right).

It must be noted that the ventilation system was off during the smoke tests, so the detection times may be somewhat longer in reality as the ventilation system is expected to delay the accumulation of smoke, namely by means of extraction through output vents placed at higher heights (exhaust flow in the order of 52000 m^3/hour). Nevertheless, if the smoke source is further away from the output vents, it is expected that the effect of the ventilation system on video smoke detection is not very significant. This is especially likely because the vents are normally placed at the two ends of the deck, whereas the possible fire area could be anywhere along the length of the deck, albeit the fire must generate visible smoke to be detected using the video fire detection system. During the conducted tests, the artificial smoke produced by the fog machine was highly visible and took approximately 5 minutes to fill up the area visible in the camera footage. By switching the fans on, the smoke was cleared within several minutes. Note also that the deck was empty during the tests. This caused the smoke to expand and scatter more easily than in a real fire situation in which the deck is expected to be fully loaded such that the presence of vehicles in the deck would help accumulate more substantial and thicker smoke, resulting potentially in a shorter detection time in a real situation than in the tests.

11.7 Main findings from onboard evaluations

Implementing different (adaptive) detection settings became unnecessary for the systems installed on board the ship because of the very low rate of nuisance alarms. The video fire detection system in the closed deck only produced nuisance alarms when the crew did a routine washdown of the deck. Similarly, the fibre-optic linear heat detection system in the open ro-ro space produced nearly one alarm per month which is considered a great improvement compared to the nuisance alarm rate of conventional detectors in the open ro-ro decks which habitually go off due to sea spray or heavy rain from the shipside. According to the ship's chief officer, it is expected or "normal" to get nuisance alarms from point detectors in bad weather conditions at sea. Moreover, the point detectors in the main deck generate nuisance alarms during cargo operations so the detectors in the main deck are normally deactivated using a timer until the cargo operation is completed. Based on the analysed alarm criteria of the linear heat detection system, it is possible to use more optimal settings to reduce the alarms even further under such operational conditions if desired.

The final fire experiments conducted on board indicated that the systems which spent over a year on board were still responsive to flame and smoke as well as they were during the laboratory experiments. The fibre-optic linear system was able to detect the propane fire in two scenarios where the point heat detectors did not activate after 10-15 minutes. Similarly, the video fire detection system was able to detect the smoke produced by a fog machine based simply on its visual characteristics, whereas the fog machine did not trigger the point smoke detectors because the fog was just a heated mixture of water and glycol, not real smoke from a fire.

All in all, linear heat detection systems are found to be very useful for fire detection in ro-ro spaces, especially for open decks where linear systems can perform better than conventional heat sensors. Moreover, video fire detection seems to be useful for closed ro-ro decks where light conditions are stable and just a few cameras can be used to cover a large distance for fire detection.

12 Recommendations

Main author of the chapter: Davood Zeinali, FRN

As part of Risk Control Option 11 (RCO11) of LASH FIRE, the following Risk Control Measures (RCMs) are considered for fire detection on open and closed ro-ro decks:

(1) Video fire detection: this RCM includes Video Flame Detection (VFD) and Video Smoke Detection (VSD), relying on the analysis of video footage for the recognition of flames and smoke, respectively.
(2) Linear heat detection: this RCM includes the different types of linear heat detection systems (fibre-optic, electric, etc.).
(3) Adaptive threshold settings for detection: this RCM includes the use of different settings at different times, either automatically or manually, to ensure optimal fire detection with fewer nuisance alarms by adapting to the ongoing operations and related conditions, especially for cargo loading and unloading operations which are normally done with disabled detection systems.

This chapter includes a summary of recommendations for the respective RCMs which are found appropriate for open and closed ro-ro decks.

12.1 Video fire detection

In the case of Video Flame Detection (VFD) systems, it is customary to certify Product Design Assessment (PDA) based on classification society approvals, including Det Norske Veritas (DNV) and American Bureau of Shipping (ABS), or by the German association of insurers (VdS) according to EN54-10 [18, pp. 54–10], or by Factory Mutual (FM) Global according to FM3260 [40]. However, these standards are not specifically designed to challenge VFD systems. To date, the most relevant existing standard that can be recommended specifically for the testing of VFD systems is FM 3232 [41], although other standards from Underwriters Laboratories (UL) and International Organization for Standardization (ISO) are under development.

According to the SOLAS Fire Safety Systems (FSS) Code [32], point detectors of flame shall be tested as per EN 54-10 [18, pp. 54–10]. This standard specifies that it only concerns detectors that operate using “radiation from a flame.” However, the term “radiation” is not clearly defined in the document and does not preclude the use of visible spectrum radiation to detect a flame based on visible colours, light levels, and light movements across pixels, which is what VFD systems do. The main test apparatus described in Annex A of EN 54-10 [18, pp. 54–10] includes a methane burner for its radiation source (which has a visible flame) as well as a radiometer for confirming the stability of source radiation but only in the wavelength range that the detector is to be certified. If no specific wavelength range is requested for certification, the standard requires the radiometer to monitor only radiation in the range 4 to 4.8 µm for IR detectors and 160 to 280 nm for UV detectors. As such, the standard does not mention specific testing configurations which will challenge video flame detectors with respect to real fire detection expectations.

Among the factors that are not considered by EN 54-10 [18, pp. 54–10] for video flame detection systems, the following items are recommended to be considered based on LASH FIRE evaluations for ro-ro ships:

- Any VFD system to be used in open ro-ro spaces must be tested for the effects of sunlight and its reflections from moving surfaces. Moreover, fixed and moving vehicle lights, deckhead lamps, portable halogen lights, and arc welding sources must be considered, both

for nuisance alarm immunity evaluations and for fire detection evaluations in the presence of such factors. The testing environment must correspond to the environment in which the VFD system will be used as similarly as practicable. It is also recommended to consult FM 3232 [41].

- If a VFD system has not been tested for outdoor conditions, the system is not recommended for open ro-ro spaces.
- Dazzling tests performed according to Annex D of EN 54-10 using regularly modulated light are not relevant for the evaluation of nuisance alarm immunity of VFD systems. It is expected that nuisance alarms of such systems in ro-ro deck environments are caused by non-modulated and random flickering of sunlight reflections or other light reflections on shiny surfaces such as those of vehicles. Immunity to such nuisance alarm sources is best verifiable in the given operational environment over some time with natural sunlight conditions. After the operational evaluation, fire testing must be performed to confirm the expected detection capability at desired distances and fire sizes with the sensitivity settings that allowed an acceptable rate of nuisance alarms.
- Background colour combinations with matching flame colours can challenge VFD systems relying on contrast and colour recognition of flames. Different background colours and flame shapes relevant to the operational environment must be tested for the desired VFD system to verify the system's responsiveness.
- Spontaneous visual saturation, i.e., instantaneously appearing large flames such as gas fires and spray flames that occupy a significant part of the field of view of the detector may challenge VFD systems [42]. The responsiveness of VFD systems in the case of spontaneous saturation must be verified.
- Gaseous jet flames and liquid spray fires do not exhibit typical flickering or pulsations like those of pool fires can be difficult to detect for certain video analytics algorithms, especially when the jet or spray is horizontally oriented. The detection of such fires must be tested for VFD systems to be installed in ro-ro decks given that some vehicles or goods in those decks can create such fires.
- The detection sensitivity of the detectors may be unacceptably lower in off-axis locations. To verify the desired sensitivity, different angles must be considered in the tests, including upward, downward, leftward, and rightward angles as shown in Figure 54.
- The flames of some fuels that burn invisibly, e.g., hydrogen and methanol, cannot be detected using visual analysis by VFD systems. Such flames may only be detected using IR or UV radiation signatures. However, secondary objects that catch fire due to the invisible flame are identifiable using VFD systems. Such flame spread events are likely to occur in ro-ro decks because the space is tightly packed with cargo. Therefore, it cannot be a general recommendation to exclude VFD for the detection of fires originating from such invisible flames in ro-ro decks.
- The system settings for the use of VFD in ro-ro spaces may consider a flame alarm zone for the area above the height of trucks because flames are not expected to be visible at lower heights while such heights may produce frequent nuisance alarms, e.g., due to moving vehicle lights. However, the settings may consider detection zones and pre-alarm (warning) zones for areas below the height of trucks to speed up the identification of potential flames.
- Existing CCTV cameras on the ship may be used with the VFD algorithm software if it is integrable in the ship's system, but the cameras must offer a minimum video quality of 25 frames per second and 0.4 megapixels per image.

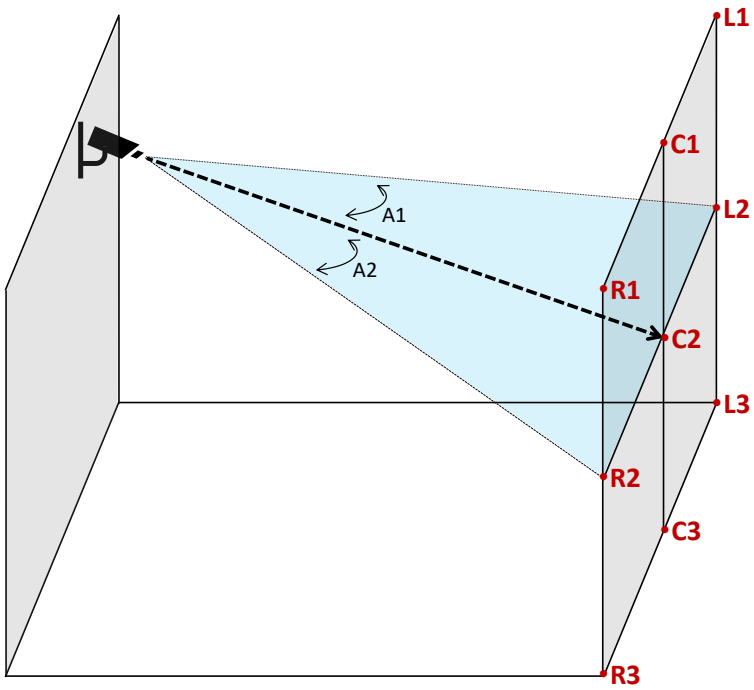

Figure 54: Test locations for detector performance evaluations on and off axis. Location C2 is on axis, i.e., the detector is directly aimed at this location. Indicated angles A1 and A2 are the degrees with which locations L2 and R2 are off axis, respectively. Accordingly, the evaluated horizontal field of view is as wide as A1+A2 degrees. The width of the evaluated vertical field of view can be quantified the same way by adding up the vertical angles tested off axis.

In the case of Video Smoke Detection (VSD) systems, the following factors are recommended to be considered:

- VSD systems are recommended to be used together with VFD or other flame detection systems because the generation of visible smoke to be detected may take a considerable amount of time in some gas fire scenarios.
- VSD systems are generally not recommendable for outdoor use. Therefore, if a VSD system has not been tested specifically for outdoor conditions, the system is not recommended for open ro-ro spaces.
- The testing environment for VSD systems must correspond to the environment in which the VSD system will be used as similarly as practicable. It is also recommended to consult FM 3232 [41].
- Regular washdowns of the ro-ro deck are observed to trigger nuisance alarms if water droplets land on the detector lens, and thus it may be desirable if VSD systems are tested against such nuisance alarm sources. Alternatively, the crew will have to switch off the VSD during the washdowns and clean the detector before switching it on.
- Background colour combinations with matching smoke colours can challenge VSD systems relying on contrast and colour recognition of smoke. Different background colours and smoke thickness relevant to the operational environment must be tested for the desired VSD system to verify the system's responsiveness.
- The sensitivity of detectors may be reduced when tested off-axis. To verify the desired sensitivity, different angles must be considered in the tests, including upward, downward, leftward, and rightward angles as shown in Figure 54.

- The system settings for the use of VSD in ro-ro spaces may consider a smoke alarm zone for areas along the deckhead because smoke is expected to rise and accumulate along the ceiling while lower heights may produce frequent nuisance alarms. However, the settings may consider detection zones and pre-alarm (warning) zones for areas at lower heights to speed up the identification of smoke sources.
- Existing CCTV cameras on the ship may be used with the VSD algorithm software if it is integrable in the ship's system, but the cameras must offer a minimum video quality of 25 frames per second and 0.4 megapixels per image.

12.2 Linear heat detection

Linear systems for heat detection in ro-ro spaces must be resettable and able to continuously measure and record temperatures at addressable locations along a sensing cable as described in EN 54-22 [20]. Moreover, fire detection system cables are classified as emergency service cables which are required to be operable under fire conditions [31]. Parts of the system that are self-monitoring, fail-safe or duplicated with runs as widely as is practicable may be exempted from stringent fire resistance requirements such as those of IEC 60331-23 [43] and IEC 60331-25 [21]. Nonetheless, some existing systems such as fibre-optic cable solutions can already pass IEC 60331-25, i.e., 2 hours testing with a minimum flame temperature equal to 750°C.

According to DNV Rules for Classification [31] all cables along the deckhead must be fixed at regular intervals (see Table 16). In addition, when cables are not laid on top of horizontal cable trays or supports, it is required to add metallic cable clips or saddles at regular distances (e.g., 1 m to 2 m). This is to retain the cable during a fire. In the case of hoistable decks, the sensor cable routes must be designed such that the cables do not interfere with the operation of the hoistable deck. Moreover, any cables that bend or move as part of the regular operation of the hoistable decks must be able to maintain long-term functionality with normal wear and tear.

Table 16 Spacing of fixing points for cables not carried in pipes according to DNV [31]

External diameter of cables		**Spacing of fixing points**	
Exceeding [mm]	**Not exceeding [mm]**	**Non-armoured or unbraided cables [mm]**	**Armoured or braided cables [mm]**
-	8	200	250
8	13	250	300
13	20	300	350
20	30	350	400
30	-	400	450

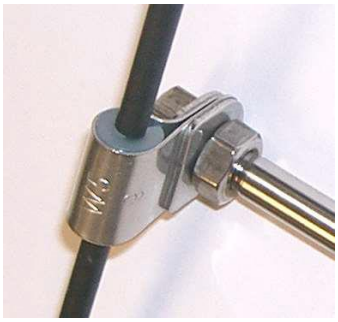

Figure 55: Example sensor cable installation with a steel clamp (DIN 3016) with a reduction sleeve for thermal insulation.

Sensor cables should not be in direct contact with any cool/hot surfaces, as these might have an additional cooling/heating effect on the sensor cable, interfere with the temperature readings and thus the detection. An example fixing which allows isolating the heat sensing cable is shown in Figure 55.

The sensor cables must go through all the deckhead compartments created by the longitudinal and transversal girders on the deckhead (see example illustrated in Figure 56). Such a configuration of sensor cables will minimize the time required for the hot gases to reach the sensors to be detected. The optimal routing of sensor cables through all the compartments should be evaluated based on the ship design and geometry on a case-by-case basis, making sure that all the cargo lanes are covered.

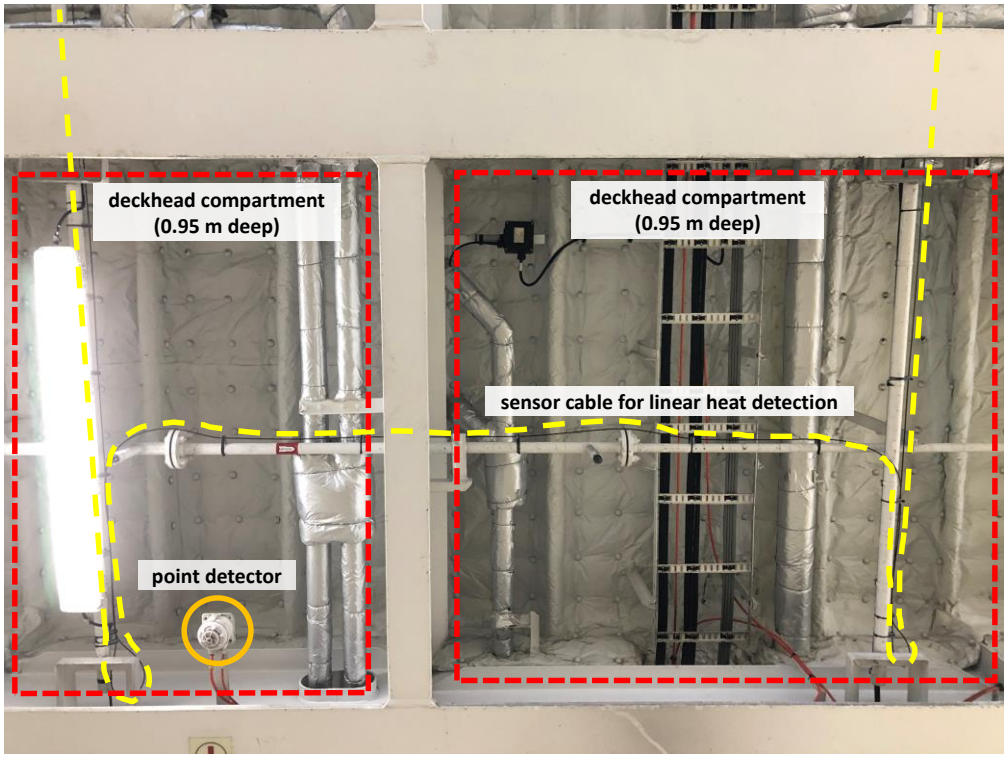

Figure 56: Fibre-optic linear heat detection cable (dashed yellow line) going through different deckhead compartments (dashed red squares) for optimal detection coverage. Note that the point detector (orange circle) covers a much smaller detection area.

Sensor cable redundancy should be considered in the design of the linear heat detection system, so that in the event of damage or complete breakage of the sensor cable, functionality is also ensured for areas behind the point of damage and thereby in each deckhead compartment. An error message must be generated by the system in such cases that locates the failure point along the cable. Without redundancy, damage or breakage of the sensor cable could mean loss of monitoring capability behind the break point.

The spatial resolution for temperature measurements along the cable must provide no fewer than 1 measurement sample per 1 meter to provide adequate coverage for cargo items as small as conventional passengers cars (see example in Figure 57). Electric systems that have individual sensors must consider this via the placement of sensors in the cables, while fibre-optic systems must consider this through an appropriate sampling interval. The consecutive parallel rows of cables must also be spaced shorter than or at least comparable to the width of the cargo lanes along the length of the ship, so that no cargo lane is disproportionately away from the sensor cables.

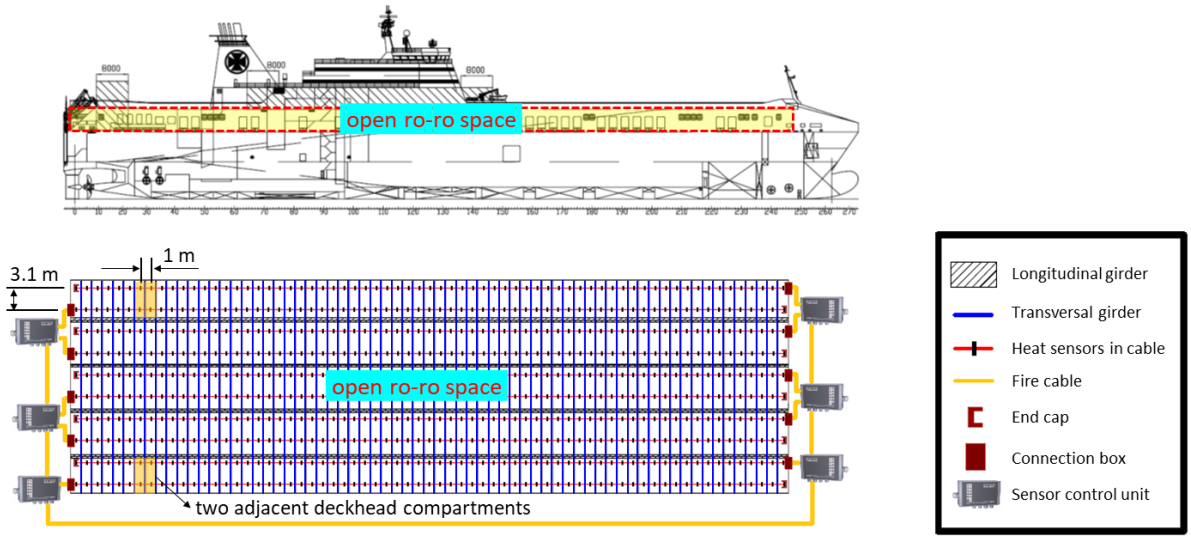

Figure 57: Example electric linear heat detection system solution with redundancy for an open ro-ro. Note that there are two branches of sensors in each deckhead compartment. The sensors in each branch are spaced at every 1 m, and there is 3.1 m distance between the adjacent branches in each deckhead compartment.

According to the onboard evaluations using a fibre-optic system on Hollandia Seaways, the dual-ended configuration with the detection criterion of 8°C/120 s Rate of Rise (RoR) is found to be optimal for open ro-ro spaces, balancing the detection speed and the frequency of nuisance alarms. The redundancy of such a design is also more advanced than the single-ended configuration (see redundancy design explanations in section 6.1.5). For closed ro-ro spaces, however, there could be a higher frequency of nuisance alarms because of the easier build-up of heat, so higher RoR criteria such as 10°C/120s or 14°C/120s may be used to lower the sensitivity slightly and thus lower the number of nuisance alarms. It is expected that the system can remain enabled l during loading/unloading operations.

12.3 Adaptive threshold settings

Implementing different (adaptive) threshold settings became unnecessary for the systems tested in the LASH FIRE project on board an operational ship for over a year. This was because of the very low rate of nuisance alarms. The video analytics algorithm in the closed deck only produced nuisance alarms when the crew did a routine washdown of the deck. Similarly, the fibre-optic system produced an average of less than one alarm per month, typically when trucks with reefer units were allowed to operate during the voyage. This was considered a great improvement compared to the nuisance alarm rate of conventional detectors in the open ro-ro decks which habitually go off due to sea spray or heavy rain from the shipside according to the ship's chief officer. Still, some detection settings allowed for fewer alarms, so it is still possible to use the best observed settings under different operational conditions if desired (refer to setting recommendations described in section 12.2). Operating the detection system with the highest possible sensitivity setting will allow the earliest detection of fire, while the number of nuisance alarms will increase. Implementing information of running reefer units or other activities that can trigger nuisance alarms in fire detection systems can be used to selectively reduce the sensitivity of the detection system at certain times or locations while maintaining a higher sensitivity when and where no known risk factors are present. The reduced sensitivity setting should also be sufficient to detect a fire within an acceptable time. An adaptive configuration like this would allow the detection system to operate at a higher sensitivity and detect fires earlier most of the time and in most locations.

13 Conclusion

Main author of the chapter: Davood Zeinali, FRN

LASH FIRE action 9B was aimed at providing quicker and more reliable fire detection, localization, and confirmation in all types of ro-ro spaces by evaluation of new and advancing technologies. This predominantly required addressing the shortcomings of conventional point detectors. Through RCO11, action 9B proposes to implement video analytics and linear heat detection systems as alternative means for fire detection in ro-ro spaces.

Video fire detection systems can use video analytics to identify fires from a long distance, without the need for the transport of smoke or heat toward their sensor, while linear heat detection systems can provide heat detection along the entire length of the deck using a sturdy sensor cable installed on the deckhead. Based on the findings of the conducted simulations, laboratory experiments, and onboard evaluations, these detection systems make it possible to reduce the time required for fire detection, while they also reduce the maintenance work requirements and can provide acceptable nuisance alarm rates.

A video analytics system was evaluated through laboratory experiments and was able to recognize open flames and smoke visible to the camera. However, nuisance alarms were generated easily several times when the ambient light conditions were changed, e.g., when the gate to the test hall was opened. Accordingly, the tested algorithm was found to be only reliable for closed ro-ro spaces where the ambient lighting conditions are stable, so onboard evaluations of this system were continued only on a closed deck (on board Hollandia Seaways). In the closed ro-ro space, the system performed very well. The flame and smoke detection zones adopted in the video analytics software made it possible to avoid vehicle lights and similar moving objects in the lower heights which would have otherwise triggered nuisance alarms. The system produced no false alarms other than those produced from regular washdowns of the deck. This type of nuisance alarm can be avoided either by switching off the detection system during the washdowns or by proactively muting the alarms during the washdown operation around the cameras used for video analytics.

Two linear heat detection systems (electric and fibre-optic) were evaluated through laboratory experiments, but the systems could not be compared directly against each other because of their different default sensitivity settings which were kept as such during the experiments. Nevertheless, the default settings allowed a higher number of fires to be detected by the fibre-optic system. Moreover, in cases where both the systems detected the fire, the detection time of the fibre-optic system was often shorter than that of the electric system. Based on these experiments and the limited resources available for further experiments on board, only the fibre-optic system was prioritized for onboard evaluations. The system was installed on Hollandia Seaways in the uppermost open ro-ro space. The system generated an average of nearly one alarm per month (caused by localized hotspots of reefer units), while it was found possible to use other settings to reduce the alarms under different operational conditions based on the analysed alarm criteria. This is considered a great improvement compared to the nuisance alarm rate of conventional detectors in the open ro-ro decks which habitually go off due to sea spray or heavy rain from the shipside according to the ship's chief officer.

The experiments conducted on board the ro-ro ship at the end of the operational trial using a propane burner and a fog machine indicated that the systems which spent over a year on board were still responsive to flame and smoke as well as they were during the laboratory experiments. Most remarkably, the conventional point heat detectors with a 54 °C alarm criterion did not activate after

15 minutes during any of the four propane fire experiments with up to 140 kW heat release in the open ro-ro space (possibly due to the unfavourable wind direction), whereas the fibre-optic linear heat detection system was able to detect the fire in two of the experiments within a few minutes with different rate of rise criteria. Similarly, video analytics was able to detect the smoke produced by the fog machine based simply on its visual characteristics.

All in all, linear heat detection systems are found to be very useful for fire detection in ro-ro spaces, especially for open decks where conventional point detectors seem to be less responsive in the presence of wind (as suggested by the laboratory wind experiments discussed in section 10.1.3.1 and the onboard experiments discussed in 11.4.2). Moreover, video analytics is found to be very useful for closed ro-ro decks where light conditions are stable and just a few cameras can be used to cover a large distance for fire detection.

Supplementary conclusions are communicated through LASH FIRE deliverables D04.8 [44] and D04.10 [45] as well as deliverables D05.6 [26], D05.7 [27], D05.8 [28], and D05.9 [29].

14 References

[1] D. Zeinali, R.Stølen, and L. Jiang, 'LASH FIRE D09.1 – Developed weather deck fire detection solutions and recommendations', LASH FIRE deliverable report D09.1, Aug. 2023. [Online]. Available: https://lashfire.eu/deliverables/

[2] IMO, *SOLAS Convention*, Consolidated Edition, as Amended. 2014.

[3] E. Wiberg and P. Bremer, 'Multifuel energy stations for cars, buses and trucks. Technical Support Document', RISE and Skåne Association of Local Authorities, Technical Support Document A2.2, Oct. 2018.

[4] C. Rivkin, R. Burgess, and W. Buttner, 'Regulations, Codes, and Standards (RCS) for Multi-Fuel Motor Vehicle Dispensing Stations', NREL, 2017. [Online]. Available: https://www.hysafe.info/wp-content/uploads/2017_papers/110.pdf

[5] D. Zeinali, K. Sarp Arsava, and C. Sanfeliu Melia, 'Recent developments in vehicle-to-grid (V2G) and smart ventilation technologies', RISE Research Institutes of Sweden, Fire and Safety, 2022.

[6] C. Lam, 'Full-Scale Fire Testing of Electric and Internal Combustion Engine Vehicles', in *Proceedings from 4th International Conference on Fires in Vehicles - FIVE 2016 October 5-6, 2016 Baltimore, USA*, Baltimore, USA: Fourth International Conference on Fire in Vehicles, Oktober 2016, pp. 95–106. [Online]. Available: https://ri.diva-portal.org/smash/get/diva2:1120218/FULLTEXT01.pdf

[7] N. Späth and A. Tosseviken, 'Fires on ro-ro decks', Jun. 2016. [Online]. Available: https://www.dnvgl.com/news/enhancing-fire-safety-on-ro-ro-decks-69059

[8] A. W. Brandt and K. Glansberg, 'Lading av elbil i parkeringsgarasje', RISE Fire Research, RISE rapport 2019:123, 2019. [Online]. Available: https://risefr.no/media/publikasjoner/upload/2019/rapport-2019-123-lading-av-elbil-i-parkeringsgarasje.pdf

[9] 'Kings Dock car park fire - Protection report', Merseyside Fire & Rescue Service, Apr. 2018. Accessed: May 07, 2019. [Online]. Available: https://www.bafsa.org.uk/wp-content/uploads/bsk-pdf-manager/2018/12/Merseyside-FRS-Car-Park-Report.pdf

[10] K. Storesund, C. Sesseng, R. F. Mikalsen, O. A. Holmvaag, and A. Steen-Hansen, 'Evaluation of fire in Stavanger airport car park 7 January 2020', RISE Fire Research, Trondheim, Norway, RISE-rapport 2020:91, Nov. 2020. doi: 10.13140/RG.2.2.24520.14080.

[11] H. Høyland and Ø. Ellingsen, 'Deler av parkeringshuset har rast sammen', *nrk.no*, Jan. 07, 2020. Accessed: Jan. 22, 2020. [Online]. Available: https://www.nrk.no/rogaland/biler-i-full-fyr-i-parkeringshuset-pa-stavanger-lufthavn-1.14850087

[12] 'Historic weather Sola Airport 2020-01-07 yr.no', Yr.no. Accessed: Feb. 28, 2020. [Online]. Available: https://www.yr.no/nb/historikk/tabell/1-15399/Norge/Rogaland/Sola/Stavanger%20lufthavn,%20Sola?q=2020-01-07

[13] R. Larsen, 'Parkeringshus kollapset under brann', *Brannmannen*, vol. Årgang 75, no. 1/2020, pp. 4–5, 2020.

[14] E. Frafjord, 'Her er parkeringen mye smalere enn der storbrannen startet', NRK. Accessed: Feb. 27, 2020. [Online]. Available: https://www.nrk.no/rogaland/her-er-parkeringen-mye-smalere-enn-der-storbrannen-startet-1.14882389

[15] Building Research Establishment, 'Fire spread in car parks', Building Research Establishment, London, England, BD2552, Dec. 2010.

[16] 'Marine Accident Report - URD Fire on 4 March 2014', The Danish Maritime Accident Investigation Board, Marine accident report Case no.: 2014006771, Jun. 2014.

[17] AP Sensing, 'Fiber optic linear heat detection for special hazard applications'. Accessed: Aug. 16, 2023. [Online]. Available: https://apsensing.com/application/fire-detection

[18] EN 54-10, 'Fire detection and fire alarm systems – Part 10: Flame detectors – Point detectors'. European Committee for Standardization, CEN-CENELEC, Brussels, Feb. 08, 2002.

[19] W. Grosshandler and E. Braun, 'Early Detection of Room Fires Through Acoustic Emission', NIST, 1994.
[20] EN 54-22, 'Fire detection and fire alarm systems – Part 22: Resettable line-type heat detectors'. CEN, European Committee for Standardization, 2020.
[21] 'IEC 60331-25:1999 Tests for electric cables under fire conditions - Circuit integrity - Part 25: Procedures and requirements - Optical fibre cables'. The International Electrotechnical Commission (IEC), 1999.
[22] P. Mindykowski *et al.*, 'FIRESAFE II Detection systems in open ro-ro and weather decks', Dec. 2018.
[23] R. Chagger, 'The development of test methods to assess video flame and video smoke detectors', p. 24, May 2019, Accessed: Oct. 24, 2019. [Online]. Available: https://files.bregroup.com/research/Video-Fire-Detection_2019-May.pdf
[24] M. Damschen, 'LASH FIRE D07.7 – Development and onboard assessment of drone for assistance in firefighting resource management and rescue operations', LASH FIRE deliverable report D07.7, Dec. 2021. Accessed: May 30, 2023. [Online]. Available: https://lashfire.eu/media/2023/03/LASH-FIRE_D07.7_Development-and-onboard-assessment-of-drone-for-assistance-in-firefighting-resource-management-and-rescue-operations_V03.pdf
[25] M. Torstensson, R. Rylander, and L. Sütfeld, 'LASH FIRE D08.10 – Demonstration of prototype for detection of potential ignition sources', LASH FIRE deliverable report D08.10, Mar. 2023. Accessed: Jul. 23, 2023. [Online]. Available: https://lashfire.eu/deliverables/
[26] V. Radolovic, 'LASH FIRE D05.6 – Ship integration requirements', LASH FIRE deliverable report D05.6, Aug. 2022. Accessed: Jul. 06, 2023. [Online]. Available: https://lashfire.eu/media/2022/10/LASH-FIRE_D05.6_Ship-integration-requirements-V02.pdf
[27] V. Radolovic and O. Kuzmanovic, 'LASH FIRE D05.7 – Ship integration evaluation', LASH FIRE deliverable report D05.7, Feb. 2023. Accessed: Jul. 06, 2023. [Online]. Available: https://lashfire.eu/media/2023/03/LASH-FIRE_D05.7_Ship-integration-evaluation-Version2.pdf
[28] V. Radolovic, O. Kuzmanovic, and I. Vidic, 'LASH FIRE D05.8 – Ship integration cost and environmental assessment', LASH FIRE deliverable report D05.8, Feb. 2023. Accessed: Jul. 06, 2023. [Online]. Available: https://lashfire.eu/media/2023/04/LASH-FIRE_D05.8_Ship-integration-cost-and-environmental-assessment-V3.pdf
[29] V. Radolovic and O. Kuzmanovic, 'LASH FIRE D05.9 – Performance, feasibility and integration assessment', LASH FIRE deliverable report D05.8, Jun. 2023. Accessed: Jul. 06, 2023. [Online]. Available: https://lashfire.eu/deliverables/
[30] V. Radolovic and O. Kuzmanovic, 'LASH Fire D5.7 - Ship integration evaluation', Feb. 2023.
[31] DNV AS, 'DNV Rules for Classifications: Ships – Part 4, Systems and components, Chapter 8, Electrical installations', Jul. 2022.
[32] 'IMO Res. MSC.98(73) International Code for Fire Safety Systems (FSS Code)'. International Maritime Organization, 2016.
[33] K. McGrattan, S. Hostikka, R. McDermott, J. Floyd, C. Weinschenk, and K. Overholt, 'Fire Dynamics Simulator, Technical Reference Guide, Volume 1: Mathematical Model', National Institute of Standards and Technology, Gaithersburg, Maryland, NIST Special Publication 1018-1, 2023.
[34] K. McGrattan, S. Hostikka, R. McDermott, J. Floyd, C. Weinschenk, and K. Overholt, 'Fire Dynamics Simulator, Technical Reference Guide, Volume 3: Validation', National Institute of Standards and Technology, Gaithersburg, Maryland, NIST Special Publication 1018-3, 2023.
[35] M. K. Cheong, M. J. Spearpoint, and C. M. Fleischmann, 'Calibrating an FDS Simulation of Goods-vehicle Fire Growth in a Tunnel Using the Runehamar Experiment', *Journal of Fire Protection Engineering*, vol. 19, no. 3, pp. 177–196, 2009, doi: 10.1177/1042391508101981.
[36] M. K. Cheong, M. J. Spearpoint, and C. M. Fleischmann, 'Design fires for vehicles in road tunnels', in *Proc. 7th International Conference on Performance-Based Codes and Fire Safety Design Methods*, Auckland, New Zealand, 2008, pp. 229–240.

[37] N. Iqbal and M. H. Salley, *Fire Dynamics Tools (FDTs): Quantitative Fire Hazard Analysis Methods for the U.S. Nuclear Regulatory Commission Fire Protection Inspection Program : Final Report*. United States Nuclear Regulatory Commission, Office of Nuclear Regulatory Research, 2004. [Online]. Available: https://books.google.no/books?id=8a_stAEACAAJ

[38] B. Karlsson and J. G. Quintiere, *Enclosure fire dynamics*. 1999.

[39] EN 54-29, 'Fire detection and fire alarm systems - Part 29: Multi-sensor fire detectors - Point detectors using a combination of smoke and heat sensors'. CEN, European Committee for Standardization, Apr. 2015.

[40] FM 3260, 'Radiant energy-sensing fire detectors for automatic fire alarm signaling'. 2021. Accessed: Jun. 14, 2023. [Online]. Available: https://www.techstreet.com/standards/fm-approvals-3260-2021?product_id=2252594

[41] FM 3232, 'Video image fire detectors for automatic fire alarm signalling'. 2023. Accessed: Jun. 14, 2023. [Online]. Available: https://www.techstreet.com/standards/fm-approvals-3232?product_id=2562667#jumps

[42] D. T. Gottuk and J. B. Dinaburg, 'Video Image Detection and Optical Flame Detection for Industrial Applications', *Fire Technology*, vol. 49, no. 2, pp. 213–251, Apr. 2013, doi: 10.1007/s10694-012-0254-0.

[43] 'IEC 60331-23:1999 Tests for electric cables under fire conditions - Circuit integrity - Part 23: Procedures and requirements - Electric data cables'. The International Electrotechnical Commission (IEC), 1999.

[44] E. D. Carvalho and B. Vicard, 'LASH FIRE D04.8 – Impact on regulations by new solutions and consolidation of new proposals for regulations', LASH FIRE deliverable report D04.8, Aug. 2023. [Online]. Available: https://lashfire.eu/deliverables/

[45] E. D. Carvalho, S. Andersson, and R. Pramanik, 'LASH FIRE D04.10 – Consolidation of performance assessments and solutions' impact on safety', LASH FIRE deliverable report D04.10, Aug. 2023. [Online]. Available: https://lashfire.eu/deliverables/

15 Indexes

15.1 Index of tables

15.2 Index of figures

16 ANNEXES

Annex A. Early detection of thermal runaway in lithium-ion batteries

Main author of the chapter: Stina Andersson, RISE

Battery electric vehicles constitute a growing category of cargo transported using ro-ro ships, and the most popular chemistry used for the battery of electric vehicles is lithium-ion. However, the possibility of a thermal runaway in lithium-ion batteries is a fire risk which needs to be managed. Accordingly, the early detection of a thermal runaway event is important for managing its fire risks. An overview of relevant literature that discusses early detection of thermal runaway in lithium-ion batteries has been made and is presented in this annex.

A.1 Introduction

Cargo inside ro-ro spaces constitutes a well-known fire risk and has been the cause of several severe fires on board ro-ro ships [1-3]. Other work in work package 09 (WP09) has focused on developing methods for improved detection of fires in different types of ro-ro spaces. For example, flame wavelength detectors and thermal imaging cameras have been evaluated for weather decks, and linear heat detection has been suggested as an improved detection method for closed and open ro-ro spaces (see LASH FIRE deliverable D04.6).

Electrification of the transport sector is ongoing [4], and with it, the proportion of battery electric vehicles (BEVs) carried on board ro-ro ships is expected to increase. The possibility of a thermal runaway (TR) event in BEV constitutes a new fire risk on board which needs to be properly addressed. One important step in addressing this new fire risk is to provide ro-ro ships with the ability to detect a thermal runaway at an early stage.

There are several factors that make the detection of a thermal runaway event challenging. Battery cells are structured in modules, which in turn are enclosed inside a battery pack. Furthermore, the battery pack is often installed inside stiffened and reinforced compartments or so-called "safe zones", where the battery is more protected from crashes. For passenger cars, the battery is usually located underneath the vehicle [5]. Due to this packaging and installation, a thermal runaway which starts in a battery cell is quite hidden from view, which makes the signatures of a thermal runaway event obscure and challenging to detect.

Damage and contamination of the smoke chamber of detectors is a cause of detector failure inside ro-ro spaces [6]. This also constitutes a challenge for any technology aimed at early detection of TR in a ro-ro space.

To address the challenge to detect a thermal runaway early, a literature review has been carried out. This focuses on articles and reports that address the early detection of thermal runaway events in lithium-ion batteries and includes a review of two alternative detection technologies.

A.2 Literature Screening and Selection

The following search words were used for a literature search in the database Scopus: "lithium-ion" AND "thermal runaway" AND "detection". The following limitations were applied to the search results: only articles published during 2018-2022, only articles with publication state *final*, and only articles written in English. The search gave 109 document results (search made at the beginning of November 2022).

In addition to the limitations, the following two selection criteria were used to identify relevant articles:

1. Relevance: Literature is included if the literature was deemed likely to contain accounts of methods for detecting a thermal runaway in a lithium-ion battery at an early stage.
2. Quality: Publications were included if they were deemed to be easy to understand and credible in their account of results.

Five articles from the search result that met the selection criteria were identified. These five articles are listed in Table 17.

Table 17. List of identified and reviewed articles from Scopus database.

Year	Authors	Name of article	Summary	Detection level
2018	Koch, Birke & Kuhn [11]	Fast Thermal Runaway Detection for Lithium-Ion Cells in Large Scale Traction Batteries	In this study, different sensors' abilities to quickly detect a thermal runaway within a battery were tested. Seven types of sensors and detectors were tested: voltage, gas, smoke, creep distance, temperature, pressure and force. The result shows that all the tested sensors were able to detect a thermal runaway, independent of cell capacity, energy density and battery system size. No single type of sensor or detector is promoted.	Inside battery pack
2019	Liao, Zhang, Li, Zhang & Habetler [8]	A survey of methods for monitoring and detecting thermal runaway of lithium-ion batteries.	The article summarises existing literature about methods for monitoring and detecting thermal runaway events in lithium-ion batteries. Terminal voltage, surface/inner temperature, and vented gas are the three main listed characteristic fault signals to be monitored. It is concluded that gas sensors are more effective than voltage or temperature sensors.	Inside battery pack
2019	Raijmakers, Danilov, Eichel, & Notten [7]	A review on various temperature-indication methods for Li-ion batteries.	Different methods for monitoring the temperature of a lithium-ion battery are reviewed and compared. It is concluded that the most appropriate method is dependent on a number of aspects, such as measurement range, accuracy and cost.	Inside battery pack
2021	Cai, Valecha, Tran, Engle, Stefanopoulou & Siegel [10]	Detection of Li-ion battery failure and venting with Carbon Dioxide sensors	The study performs a literature summary regarding the composition of vent gas during a thermal runaway event. The authors proposed CO_2 as the most appropriate vent gas to detect. The study suggests the Non-Dispersive Infrared (NDIR) CO_2 sensor. An overcharging experiment for cell	Inside battery pack

			validation of NDIR showed that CO_2 detection is effective for gas venting in a single-cell case. It is stated that CO_2 detection is effective in a large battery pack.	
2021	Essl, Seifert, Rabe & Fuchs [9]	Early Detection of Failing Automotive Batteries Using Gas Sensors	The article investigates gases that are produced before and during a thermal runaway as well as results from testing of different commercially available gas sensors. It is argued that state-of-the-art monitoring equipment, such as cell voltage measurement and temperature sensors that are installed inside the battery pack do not provide sufficiently early detection of a thermal runaway. It is proposed that the current state-of-the-art monitoring should be combined with additional gas sensors to provide sufficiently early detection.	Inside battery pack

In addition to these articles, one report has been identified as relevant for review. The report is listed in Table 18.

Table 18. List of identified reports for review.

Year	Authors	Name of report	Summary	Detection level
2021	Barowy, Klieger, Regan, & McKinnon [13]	UL 9540A Installation Level Tests with Outdoor Lithium-ion Energy Storage System Mockups	Reporting of three fire tests with batteries inside a container. Among other things, different types of detectors' abilities to detect a thermal runaway event were evaluated. Commonly available combustible gas detectors were highlighted as effective in giving an alarm, but only after a thermal runaway event had happened.	Outside battery pack

A.3 Findings

A.3.1 Fast detection of thermal runaway

Thermal runaway can be described as a three-stage process consisting of onset, acceleration and runaway. When the onset temperature is reached there is a self-heating of the lithium-ion battery, meaning that there is a heat rate (temperature increase over time) within the battery without any external heat being added. During the acceleration stage the heat rate increases and there can be a release of smoke or gas-venting [7]. At a certain point, a thermal runaway occurs, during which the temperature increases extremely fast. Internal short-circuit fault is the main cause of a thermal runaway event [8]. Mechanical abuse, electrical abuse and thermal abuse may all cause damage to the separator, leading to an internal short-circuit. The internal short-circuit will generate heat, which

in turn will intensify the internal exothermic chain reactions and may release flammable gas. The release of gases will increase the pressure inside the battery, which may cause the outer case of the lithium-ion battery to expand [8]. If thermal runaway occurs in one cell, the heat can transfer to other cells (through conduction and convection), creating a domino effect ending with thermal runaway occurring in all cells within the battery pack [8].

Some regulations require the battery pack or system to provide a warning to passengers in a BEV five minutes prior to danger due to a thermal runaway event (GB 38031-2020). The battery management system (BMS) monitors several parameters in a battery, including voltage, temperature and current. However, current state-of-the-art monitoring equipment, such as cell voltage measurement and temperature sensors that are installed inside the battery pack do not provide sufficiently early detection of a thermal runaway [9]. This makes new and improved ways to quickly detect a thermal runaway event an important issue to resolve. As stated above, a thermal runaway may be preceded by both an increase in temperature and by release of smoke. This makes temperature and gas two interesting characteristic signals of a thermal runaway event to investigate further.

A.3.1.1 Gas

Liao et al. [8] suggest voltage/current, temperature and gas components as characteristic signals of a thermal runaway event which can be monitored to effectively improve lithium-ion battery safety. They also investigated three types of real-time TR monitoring and detection approaches, which can be summarised as follows [8]:

- Detection of cell/module terminal voltage and surface temperature,
- Monitoring and estimation of internal temperature and the strain of lithium-ion batteries,
- Monitoring and analysing the characteristic vent gas components during a TR.

According to Liao et al., a benefit of using a voltage sensor-based approach is that the faulty battery cell can be located inside the battery pack. When using a temperature or gas-based approach, it is difficult to locate the faulty cell. However, the approach of monitoring voltage and surface temperature showed a low accuracy of TR prediction as well as a high cost. High accuracy of thermal runaway predictions was seen for internal temperature monitoring as well as monitoring of vent gas components [8]. Through a summary of existing literature and a comparative study, the article shows that gas sensors are more effective than voltage sensors or temperature sensors, meaning that monitoring the gas signal results in the earliest detection of a thermal runaway.

In an article from 2021, Essl et al. [9] present an investigation of gases that are produced before and during a thermal runaway. It is shown that hydrogen (H_2) and Volatile Organic Compound (VOC) gases are produced before a thermal runaway event occurs. The article also presents test results from testing of different commercially available gas sensors. Sixteen sensors were included in the experiments, with the following sensory principles represented:

- Metal oxide semiconductor (sensor)
- NDIR
- Electrochemical sensors
- Thermometer
- Hygrometer

The sensors are meant to be installed inside the battery pack [9]. The sensors were tested in four different failure cases: unwanted electrolysis of voltage carrying part, electrolyte vapour, first venting of the cell and thermal runaway [9]. The three first listed failure cases occur before the thermal runaway event [9]. The results show that gas sensor-based detection is dependent on the failure case

but that all tested failure cases can be detected through a multi-sensor reactive detection method where temperature, pressure voltage and gas sensors are combined. The authors propose that the current state-of-the-art monitoring is combined with additional gas sensors to provide sufficiently early detection. The proposed gas sensors are to be installed in the existing monitoring system inside the battery pack. Metal oxide semiconductor (MOx) sensors are highlighted as the most promising type of gas sensors for detecting battery failures before a thermal runaway event occurs.

Cai et al. [10] also conclude that a gas detection method should be proposed. In their study, Cai et al. [10] go through the composition of vent gas during single-cell abuse experiments. In their review, CO_2, CO, H_2 and VOCs are highlighted as the main present gas components among the reviewed single-cell abuse experiments. Similar to Essl et al. [9], Cai et al. [10] found that the composition of vent gas is affected by, among other things, how the thermal event is initiated. Different amounts of the four gas components were detectable depending on the abuse case of the cell. By comparing these four gas components in terms of consistency, early presence and leakage detection, the authors proposed CO_2 as the most appropriate vent gas to detect. The study evaluated different sensors and suggested the Non-Dispersive Infrared (NDIR) CO_2 sensor. This can be compared to the suggestions found in the article by Essl et al. [9], where MOx sensors were preferred over NDIR sensors. Cai et al. [10] performed an overcharging experiment for cell validation of NDIR, which showed that CO_2 detection is effective for gas venting in a single cell case. In addition to this, the article states that CO_2 detection is effective in a large battery pack as well.

Although the three above reviewed articles [8-10] promote gas as a signature that should be monitored and detected to detect a thermal runaway event at an early stage, there are studies that do not support the preference of monitoring gas. In their 2018 article, Koch et al. [11] present a study where different sensors' abilities to quickly detect a thermal runaway within a battery were tested. In the study, seven types of sensors and detectors were tested: voltage, gas, smoke, creep distance, temperature, pressure, and force. The result shows that all the tested sensors were able to detect a thermal runaway. This was independent of cell capacity, energy density and battery system size. Contrary to the two previous articles, this article does not promote a single type of sensor or detector.

A.3.1.2 Temperature

An increase in temperature is usually an early sign of a thermal runaway event. By monitoring the internal temperature, these early signals can be detected by the battery management system (BMS). However, as detailed by Raijmakers et al. in their article from 2019, there are several challenges for measuring the temperature inside a lithium-ion battery. Firstly, the process of charging and discharging generates some heat. This heat generation during normal operations complicates temperature measurements at the battery surface. Raihmakers et al. [7] reviewed different temperature measurement methods and concluded that local surface or internal temperature measures can be made with a thermistor, Resistance Temperature Detectors (RTD), or thermocouple, which are all considered to be traditional measurement methods. However, it is not certain that these traditional methods are suitable for internal measurement. If temperature measurement inside the battery is to be made, it needs to be made with appropriate temperature measurement methods. Measurement range, accuracy, resolution, and cost all influence which method is best suited.

The efficiency of additional sensors in a battery pack would likely depend on the placement and number of sensors. This is deemed to be especially relevant for temperature sensors.

The above articles have addressed sensors inside a battery pack. Cooperative Intelligent Transport Systems (C-ITS) and how vehicle sensor communication could improve early detection of fires in vehicles (not just BEVs) are described in LASH FIRE IR09.2 [12]. Currently, BEV manufacturers do not support data transfer between the vehicle and the ship. This means that ship owners currently must rely on detection methods outside the battery pack.

A.3.1.3 Indicators outside of the battery pack

In 2021, UL released a 9540A test report [13] which presents the outcome of three fire tests with batteries inside a container. Contrary to the reviewed articles which focused on detection inside the battery pack, the UL report addresses detection outside the battery pack. Different types of detectors inside the container were evaluated in three tests, namely smoke detector, CO detector, combustible gas detector and hydrogen detector. Table 3 summarises the detection times, given as seconds after the thermal runaway event, for the different detector types. The hydrogen detector results are not included due to unclarities in the alarm time for this detector.

Table 19. Compiled data from UL 9540A test report [13] showing alarm time for different detectors. Data is time [s] after the thermal runaway event. Data is for 1 CO detector, 3 combustible gas detectors and 2 smoke detectors.

	Carbon Monoxide Detector [s]	Combustible Gas Detectors [s]	Smoke Detectors [s]
Test 1	20	27, 26, 20	46, 47
Test 2	23	30, 28, 21	53, 55
Test 3	10	29, 27, 4	50, 60

All combustible gas detectors gave alarm within 30 seconds after the thermal runaway event in all three tests. Smoke detectors gave alarm around 50 s after the TR event. The alarm time for both combustible gas detectors and smoke detectors depended on the proximity to the initiating unit. The detector closest to the initiating unit always gave alarm first. The report from UL shows that hydrogen is present after a TR event and that it is detectable, but there were issues with the instrumentation, which makes it difficult to evaluate the efficiency of hydrogen detectors. According to the UL report, commonly available hydrogen detectors outside the battery pack effectively indicated that a TR event had occurred.

The ALBERO project performed tests on lithium-ion batteries [14]. The release of H_2 and a slight increase of the surface temperature were reported during the thermal runaway of the batteries. Based on this, a detection method using a combination of temperature and H_2 monitoring was developed and tested onboard a ro-ro ship. The ALBERO project suggested a combination of H_2 and surface temperature increase monitoring as a method which can be used outside the battery pack to detect a thermal runaway event early [14].

Hydrogen diffuses quickly in air [15]. This means that a release of hydrogen will be quick to mix with the air and spread in a space. Ro-ro spaces use ventilation to maintain a good air quality and are usually well-ventilated. This makes monitoring of hydrogen challenging in ro-ro spaces. For example, it is likely that a reliable monitoring of H_2 requires no or very little airflow in the space. If there is an airflow in the space, the hydrogen will quickly mix with the air and become impractical to monitor. This was seen in the ALBERO project [14], where onboard testing showed that hydrogen sensors would need to be placed very close to the vehicle, and downstream the airflow, for detection to be possible.

A.3.2 Alternative detection methods

In this section, alternative methods for detection of a thermal runaway event are discussed.

A.3.2.1 Light detection and ranging

Light detection and ranging (LIDAR) is a technology where laser pulses are sent in the form of a laser beam. When the beam hits a target, such as a solid object or a gas, part of the light scatters back to the sensor. LIDAR technology is used in different fields such as autonomous vehicles [16] and forest inventories [17, 18]. The use of LIDAR technology to detect forest fires has been proposed in articles and conference papers [19, 20]. According to Utkin et al. [21], the signature of a smoke plume can be identified by measuring the intensity of the backscattered incident radiation as a function of time and analysing the signal with the help of artificial intelligence.

LIDAR uses a reference picture to detect changes and could potentially be used to map a ro-ro space and observe changes over time. Smoke would "muffle" the signal back to the sensor, which could be interpreted as a disruption. The potential in LIDAR within fire detection lies in the sensor's ability to detect gases as a form of disruption in the reference image. It is not established if LIDAR sensors can give an alarm if there is gas generation around a lithium-ion battery. The possibility for lidar sensors to detect gases from a lithium-ion battery could be further investigated in fire tests.

A.3.2.2 Optical Gas Imaging

Optical Gas Imaging (OGI) is a potential technology for detection of thermal runaway events since it can be used to detect gas. OGI works by detecting a gas plume's absorption of infrared light. The source of radiance is the background radiation, and there needs to be a temperature difference between the background and the gas to allow an OGI camera to provide an image of the gas [22]. An example of its current usage is leakage detection within the oil and gas industry [23]. To detect a gas, the absorption band of the camera must overlap with the infrared absorption spectrum of the gas [22]. OGI technology is commonly used to detect leakage of hydrocarbons. OGI camera can monitor large areas, and it would be interesting to investigate if it could be used in a ro-ro space to detect gases emitted from a battery pack during a TR event. The usability relies on whether OGI cameras can be calibrated to allow detection of gases specific to the initial stages of a TR event. The possibility for OGI technology to detect gases from a lithium-ion battery could be further investigated in fire tests.

A.4 Conclusion

There are different characterising signatures of a thermal runaway event that detection technology may focus upon. The two most prominent signals from the literature are temperature and gases which are monitored through sensors installed inside the battery pack. Increase in temperature and release of gases first occur on a cell level, and having a combination of different sensors directly inside the battery pack seems to make detection of early signals of a thermal runaway event possible. The gas components are affected by the abuse case, and there is no consensus found regarding a specific gas component which should be monitored. Nor is there a consensus found regarding which type of gas sensor is best suited for early detection of a thermal runaway event.

In a maritime context, there is currently no way for a ship operator to access data from sensors inside the battery pack. Communication between vehicle and ship which permits ships to use data from sensors to detect a failure has been suggested as a way of improving fire detection possibilities onboard. When considering detection outside the battery pack, common industrial carbon monoxide and combustible gas detectors seem to provide earlier alarms compared to conventional smoke detectors. Hydrogen is highlighted as a promising gas to monitor outside a battery pack to detect a TR event early. However, the ventilation conditions likely make hydrogen impractical to monitor in a

ro-ro space. The time to alarm is affected by the placement of the detector in relation to the TR event. The placement of detectors is an important factor for the response time until alarm. Further work is recommended to compare the effect of placement of conventional detection systems, such as smoke detection, and the effect of new gas detectors.

A TR event can evolve into a severe fire scenario in a short period of time. Even if signals of a TR can be detected in an early stage of the process, it is not certain that there will be time to take mitigating actions.

The following areas were identified as interesting for further investigation:

- The possibility for ship operators to receive information from the sensors inside the battery pack of BEVs onboard.
- Testing of the ability of alternative detection methods such as gas detectors, LIDAR sensors and OGI cameras to detect a thermal runaway event.

A.5 References

[1] Japan Transport Safety Board. (2011). Marine Accident Investigateion Report MA2011-10. Japan Transport Safety Board.

[2] National Transportation Safety Board. (2017). Marine Accident Brief- Fire aboard Vehilce carrier Courage.

[3] The Bahamas Maritime Authority. (2017). Report of the marine safety investigation into a fire on the vehicle deck in the outer approaches to Gdynia, Poland on 31 August 2016. London: Bahamas Maritime Authority.

[4] IEA. (2022). Global EV Outlook 2022, IEA, Paris. Paris, https://www.iea.org/reports/global-ev-outlook-2022, License: CC BY 4.0: IEA.

[5] Bisschop, R., Willstrand, O., & Rosengren, O. (2020). Handling Lithium-Ion Batteries in Electric Vehicles: Preventing and Recovering from Hazardous Events. Fire Technology, 56, 2671-2694.

[6] Leroux, J. (2018). FIRESAFE II Detection and Decision, Final Report, Version 1.1. 2017/EMSA/OP/17/2017, EMSA.

[7] Raijmakers, L. H., Danilov, D., Eichel, R.-A., & Notten, P. (2019). A review on various temperature-indication methods for Li-ion batteries. Applied Energy, 918-945.

[8] Liao, Z., Zhang, S., Li, K., Zhang, G., & Habetler, T. G. (2019). A survey of methods for monitoring and detecting thermal runaway of lithium-ion batteries. Journal of Power Sources, 436. https://doi.org/10.1016/j.jpowsour.2019.226879.

[9] Essl, C., Seifert , L., Rabe, M., & Fuchs , A. (2021). Early detection of Failing Automotive batteries Using Gas Sensors. Batteries, 7(25), https://doi.org/10.3390/batteries7020025.

[10] Cai, T., Valecha, P., Tran, V., Engle, B., Stefanopoulou, A., & Siegel, J. (2021). Detection of Li-ion battery failure and venting with Carbon Dioxide sensors. eTransportation, 7.

[11] Koch, S., Birke, K., & Kuhn, R. (2018). Fast Thermal Runaway Detection for Lithium-Ion Cells in Large Scale Traction Batteries. Batteries, 4(16).

[12] Stølen, R. (2020). IR09.2 Definition of conditions for detection in closed and open ro-ro spaces. LASH FIRE.

[13] Barowy, A., Klieger, A., Regan, J., & McKinnon, M. (2021). UL 9540A Installation Level Tests with Outdoor Lithium-ion Energy Storage System Mockups.

[14] ALBERO Project Work Package 4. (2020). 4.4 „Adaption of fire detection technology“ . ALBERO. Acessed trough https://alberoprojekt.de/#xl_xr_page_ergebnisse-eng.

[15] ISO. (2015). ISO/TR 15916:2015(E) Basic considerations for the safety of hydrogen systems, second edition. ISO.

[16] Patole, S. M., Torlak, M., Wang, D., & Ali, M. (2017). Automotive Radars: A review of signal processing techniques. IEEE Signal Processing Magazine, 34(2), 22-35.

[17] Dassot, M., Constant, T., & Fournier, M. (2011). The use of terrestrial LiDAR technology in forest science: application fields, benefits and challenges. Annals of Forest Science, 959-974.

[18] Disney, M. (2019). Terrestrial LiDAR: a three-dimensionalrevolution in how we look at trees. New Phytologist, 222(4), 1736–1741, doi: 10.1111/nph.15517.

[19] Utkin, A. B., Lavrov, A., & Vilar, R. (2002). Detection of small forest fires by lidar. Applied Physics B.

[20] Utkin, A. B., Piedade, F., Bexiga, V., & Lousa, P. (2014). Scalable lidar technique for fire detection. Proceedings of SPIE- The International Society for Optical Engineering.

[21] Utkin, A. B., Lavrov, A., & Vilar, R. (2011). Fire Surveillance and Evaluation by Means of Lidar Technique. In R. P. Bennett, Fire Detection (pp. 41-78). New York: Nova Science Publishers.

[22] Concawe Air Quality OGI Ad-Hoc Group. (2017). Report no 2/17: An evaluation of an optical gas imaging system for the quantification of fugitive hydrocarbon emissions. Brussels: Concawe.

[23] IRCameras. (2015). Optical Gas Imaging in the Oil and Gas Industry (White Paper). Santa Barbara: IRCameras.

Annex B. CFD simulations of fire detection in closed and open ro-ro spaces and recommendation for system verification

Main authors: Tuula Hakkarainen, Alexandra Tissari, and Nikhil Verma, VTT

This annex presents the design and results of CFD simulations conducted using the software Fire Dynamics Simulator (FDS) for the evaluation of smoke and heat detection using different technologies and during different ventilation conditions. Detectors were located in ro-ro spaces and ventilation ducts of closed ro-ro spaces. In addition to computational detection technology evaluation, recommendations for relevant scenarios for large scale system testing and validation are given.

Fires with different properties have been simulated in the ro-ro spaces in various locations, and the time to detection has been assessed for different detection technologies. For some new and advancing technologies, the detection time has been assessed qualitatively.

B.1 Introduction

Main authors of the chapter: Tuula Hakkarainen and Alexandra Tissari, VTT

B.1.1 Task definition and role in the project

The main goal of Action 9-B is to develop, demonstrate and evaluate in full-scale alternative and complementing means for quick and reliable detection on closed and open ro-ro spaces. This report, linked with Task T09.9, presents the conduction and results of CFD simulations of smoke and heat movement to determine the time until detection with different detection technologies and during different ventilation conditions in open and closed ro-ro spaces. In addition to computational detection technology evaluation, recommendations for relevant scenarios for large scale system testing and validation are given.

IR09.4 has received input from IR09.2 (Definition of conditions for detection in closed and open ro-ro spaces) where available fire detection technologies and their suitability for use in open and closed ro-ro spaces are evaluated.

IR09.4 provides input to Task T09.10 (Large scale validation of selected fire detection solutions for closed and open ro-ro spaces). The results of the CFD simulations will be utilized to give recommendations for relevant scenarios for large scale system testing and validation in T09.10.

B.1.2 Background

Efficient fire detection solutions allow fire suppression to start early, which is critical for minimizing the damage caused by fires. Quick and reliable solutions are required. Currently, smoke detectors are often found in closed and open ro-ro spaces, but due to the harsh environment and ventilation, there is a need for other detection systems to either replace or complement the existing systems. In order to meet the need, various conventional detectors like point and linear heat detectors, CO sensors (including smoke sensors) and non-conventional detectors like IR flame wavelength detectors and video-based smoke and flame detectors are addressed in this work. Their performance has been checked in various scenarios, and promptness in activation with respect to different environment and fire conditions have been outlined.

B.2 Methodology

Main authors of the chapter: Nikhil Verma and Alexandra Tissari, VTT

This task aims to computationally check the response of various detectors during a fire in open and closed ro-ro spaces in the generic ship model of Stena Flavia. The spaces having fire are simulated (along with the whole ship model for Stena Flavia), and various detectors are positioned in the space to check their responses. The simulations are based on Computational Fluid Dynamics (CFD), and the effects of wind are also included (for open ro-ro space). Results of the response time of various conventional detectors allowed by the CFD based simulation software are presented. Non-conventional detectors are not simulated because of the lack of advanced detection models in the software. Instead, field conditions in the vicinity of fire are checked to qualitatively assess the response of non-conventional detectors based on their activation mechanism.

B.2.1 Numerical approach

The CFD code Fire Dynamics Simulator (FDS) is used for making the simulations. FDS is a LES code meant primarily for studying low Mach thermally-driven flows [1]. The theoretical approach and numerical implementation of FDS have been documented in detail in the software's technical reference guide [1]. FDS has been validated for simulating both smoke and heat transfer in enclosure fires, but also its capability for producing correct wind profile has been assessed [2].

B.2.2 Considered detection technologies

Various detection technologies considered in the simulation are limited by the detection models inbuilt in the software. Primarily, the software includes the models for conventional detectors like Heat Detectors (point) and Smoke Detectors (point). It also provides an option to position devices in a computational domain to measure Carbon Monoxide concentration and temperature at various points. Such temperature measuring devices have been used to replicate the functionality of linear heat detectors. The working principles of such detectors are discussed in Section B.3.4. The section also outlines the thresholds for detection for detectors and devices. Moreover, to cater for the need of non-conventional detectors like Video Flame Detector, Video Smoke Detector, Flame Detector and Thermal Imaging Camera, certain outputs as shown in Table 5 are chosen. Such outputs are assessed to qualitatively evaluate the response of such non-conventional detection technologies. The chosen indicators for detection with the non-conventional detection technologies are presented in Table 20.

Table 20. FDS outputs provided for qualitative evaluation of response of non-conventional detection technologies.

Detection technologies	**FDS output**
Video Flame	Heat release rate per unit volume for flame height (HRRPUV) (kWm^{-3})
Video Smoke	Optical density (m^{-1})
Flame Detector	Radiant heat flux (kWm^{-2})
Thermal Imaging Camera	Gas temperature and surface temperature (°C)

B.2.3 Design fires

The FIRESAFE I study [3] collected statistical data on fires in vehicle decks in ro-ro ships from several different studies. Based on the findings, ship cargo is most likely the origin of the fire in the vehicle decks. Furthermore, of ship cargo, the vehicles are more likely to ignite than cargo units, such as reefers. [3] Thus, a heavy goods vehicle (HGV) fire is considered as the design fire in the simulations. Generally, such vehicles carry goods made of wood cellulose (wooden pallets, furniture, paper cartons etc.) and plastics (PE pallets, plastic toys, polystyrene cups etc.) [4] Moreover, based on Swedish statistics and professional goods transport agents, an 80% cellulose and 20% plastic fuel load

is a reasonable division to allocate goods transport on the road [5]. Thus, to represent the fire of wood and plastics, based on data provided in [6] (table B.1-2) T-squared fast fire curve is used in the simulation. Table 3.6 of [7] also presents the fast growth rate for various stuff made of wood and plastics. The fast fire curve has a growth constant of 0.047 kW/m^2, and it is shown in Figure 5. Figure 5 also includes the T-squared slow fire curve (growth constant of 0.003 kW/m^2), which have been used for the sensitivity study with the T-squared fast fire curve. The modelling of the fire in the simulations is described in Section B.3.3.2.

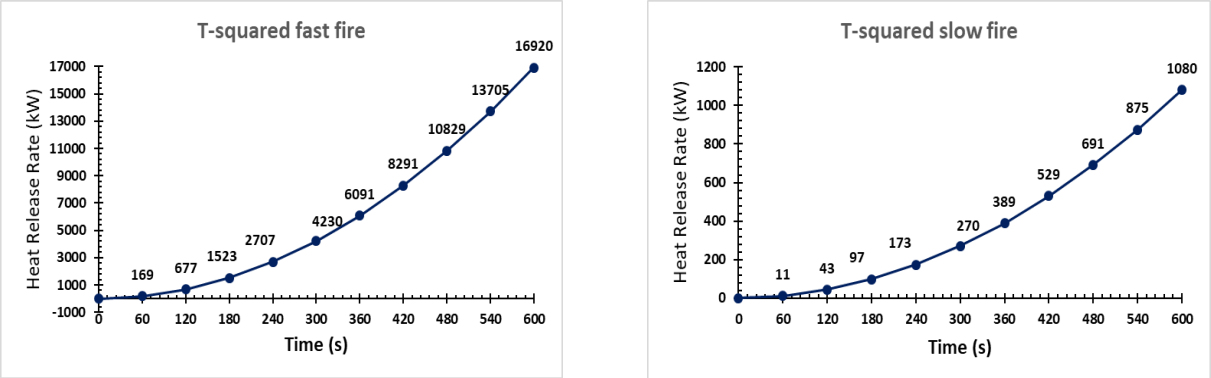

Figure 58. T-squared fast fire curve and T-squared slow fire

B.2.4 Simulation scenarios

Scenarios for simulations are shown in Table 7 and

Table 8. Fire locations and wind variables (for open ro-ro space) are chosen such that the conditions for easy, intermediate, and difficult detection are studied in different simulations. Moreover, Carbon Monoxide (CO) yield and Soot yield are also varied from low to high values such that a range of products composed of wood and plastics are covered. Low CO yield (0.012 g/g) and Soot yield (0.068 g/g) represents products composed of 75% wood and 25% polyurethane foam. High CO yield (0.025 g/g) and Soot yield (0.174 g/g) represents products composed of 25% wood and 75% polyurethane foam. Such values are based on estimation and interpolation of values of wood (red oak) and Polyurethane (flexible) foams (GM23) as mentioned in Table A.39 of [8]. Fire locations in the open ro-ro space simulations are shown in Figure 6, and respectively locations in the closed ro-ro space simulations in Figure 7.

Table 21. Open ro-ro space simulation scenarios.

ID	Fire growth rate	Fire location	Wind	CO & soot yield
S1	Fast	Starboard side opening	3.75 m/s starboard side wind	Low
S2	Fast	Starboard side opening	7.5 m/s starboard side wind	Low
S3	Fast	Centreline	7.5 m/s headwind	Low
S4	Fast	Centreline	7.5 m/s tailwind	Low
S5	Fast	Portside opening	7.5 m/s starboard side wind	Low
S6	Fast	Portside opening	3.75 m/s starboard side wind	High
S7	Fast	Starboard side opening	7.5 m/s starboard side wind	High
S8	Fast	Centreline	7.5 m/s headwind	High
S9	Fast	Centreline	7.5 m/s tailwind	High
S10	Fast	Portside opening	7.5 m/s starboard side wind	High

Table 22. Closed ro-ro space simulation scenarios.

ID	Fire growth rate	Fire location	CO & soot yield	Note
S11	Fast	Centreline	Low	
S12	Fast	Ventilation exhaust point	Low	
S13	Fast	Ventilation supply point	Low	
S14	Fast	Centreline	Low	Fire moved ½ beam span
S15	Fast	Centreline	Low	No openings in girders
S16	Slow	Centreline	Low	
S17	Slow	Ventilation exhaust point	Low	
S18	Slow	Ventilation supply point	Low	
S19	Fast	Centreline	High	
S20	Fast	Ventilation exhaust point	High	
S21	Fast	Ventilation supply point	High	

B.3 Simulation setup

Main authors of the chapter: Nikhil Verma and Alexandra Tissari, VTT

B.3.1 Geometries

B.3.1.1 Open ro-ro space

The deck 4 of Stena Flavia is an open ro-ro space. To include the effect of wind, the whole ship model above the waterline is considered in the simulation. The geometry of the Stena Flavia simulation model is shown in Figure 59. Girders and openings are taken into account in the model in order to study the effect of wind on the smoke movement and heat transportation and, thus on the detection. The height of the ro-ro space is 5.4 metres, and the girders have a height of 0.6 metres. The tops of the trucks have a height of 4.4 metres from the deck, which results in a distance of 0.4 metres between the tops of trucks and girder flanges. The distance between the top of the trucks and the deckhead is 1 metre.

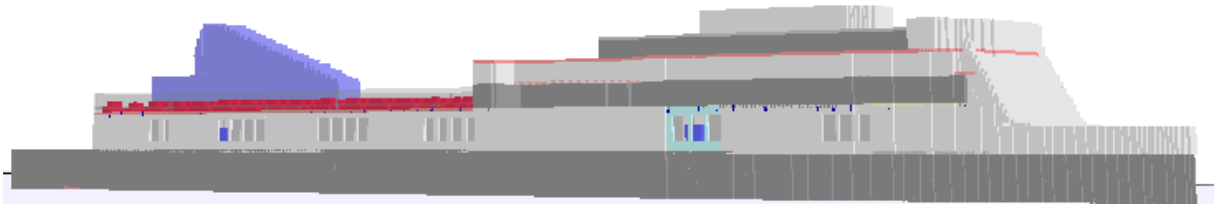

Figure 59. Stena Flavia simulation model.

Figure 6 shows the arrangement of trucks and fire locations on Deck 4 (top view). Trucks are placed close to each other to maximise the usage of available space. Fires are located at three different locations in different simulations. The first location is near the openings at the starboard side. The second location is at the centreline of the deck. The third location is near the openings at the portside. All the fire locations are at the deck level, surrounded by the truck body as per geometry.

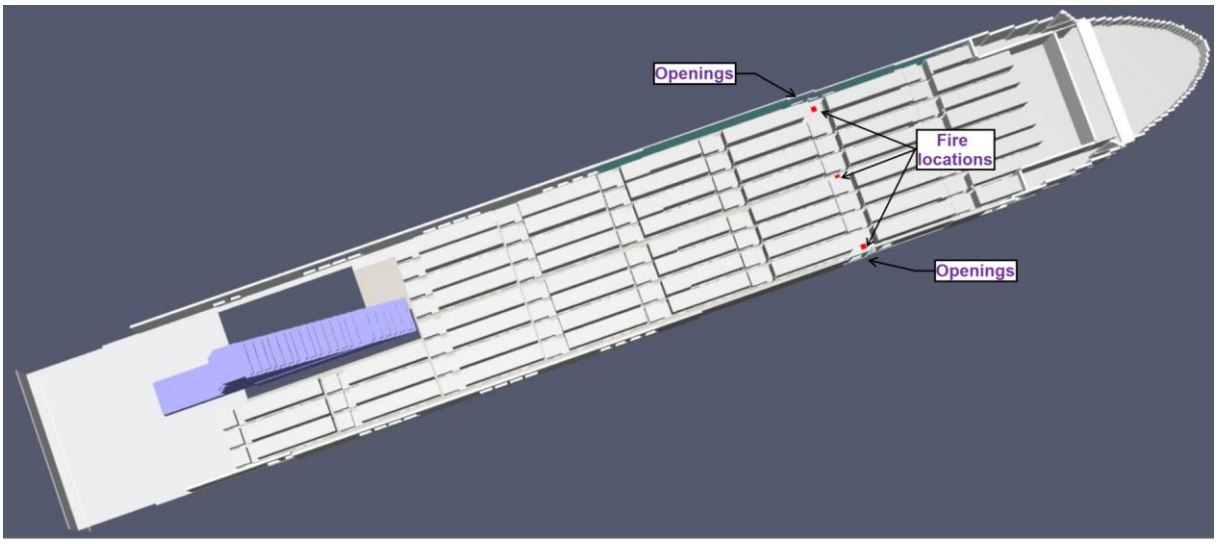

Figure 60. Trucks and fire locations on Deck 4 in Stena Flavia simulation model.

Figure 61 shows the girders and the locations of point detectors (top view). The locations of the point detectors are as per the detector arrangement of Stena Flavia. The detectors are at a height of 40 cm above the lower edge of the girder flange (20 cm below the ceiling).

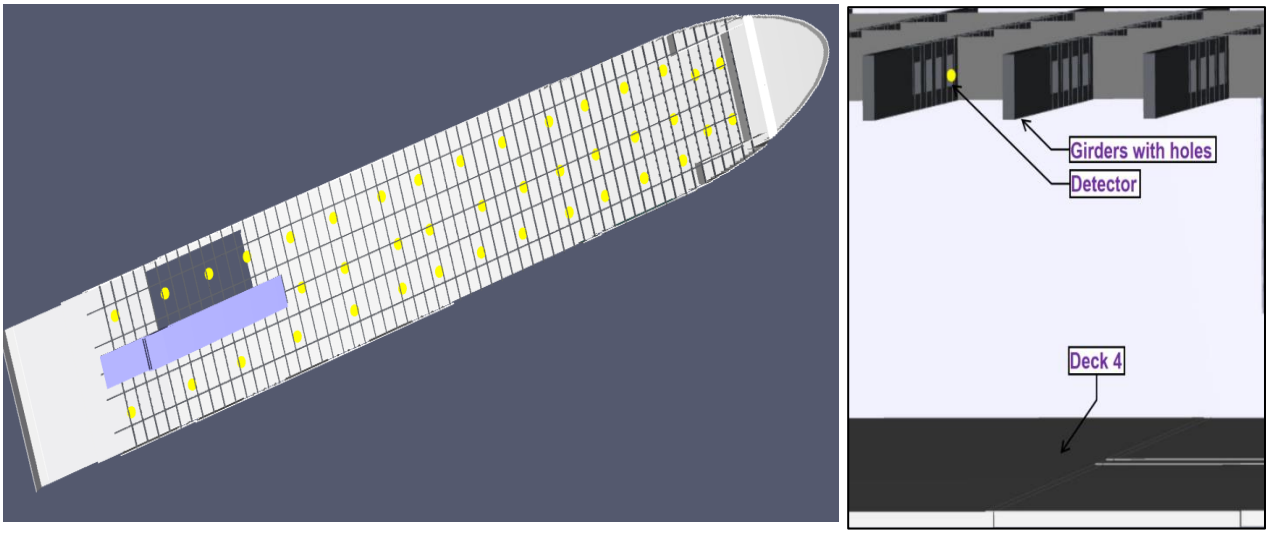

Figure 61. Girders and detectors on Deck 4 in Stena Flavia simulation model. The locations of the point detectors have been shown with yellow dots. (Trucks are not included in the figure)

B.3.1.2 Closed ro-ro space

The deck 3 of Stena Flavia is a closed ro-ro space. The modelled geometry of the space is shown in Figure 62. Girders and mechanical ventilation are taken into account in the model to study their effect on the smoke movement and heat transportation and thus, on the detection. The height of the ro-ro space is 5.8 metres, and the girders have a height of 0.8 metres. The tops of the trucks have a height of 4.0 metres from the deck, which results in a distance of 1.0 metres between the topcs of trucks and girder flanges. The distance between the top of the trucks and the deckhead is 1.8 metres.

A view of the model from below is shown in Figure 7. The girders on the deckhead can be seen in the figure. The locations of the point detectors have been marked with black dots in the figure, and

locations of the fires with orange rectangles. A fire located near a ventilation supply point is located in the forward part of the ship, and a fire located near a ventilation exhaust point is located in the aft part of the ship.

Points detectors were modelled as per the detector arrangement of Stena Flavia. Point detectors were modelled at two different heights to study their effect on the activation times. The lower detector is approximately at the same height as the girder flange next to it, which is a normal installation height, and the upper detector is located 40 cm above. The modelling of detector locations is visualized in Figure 64.

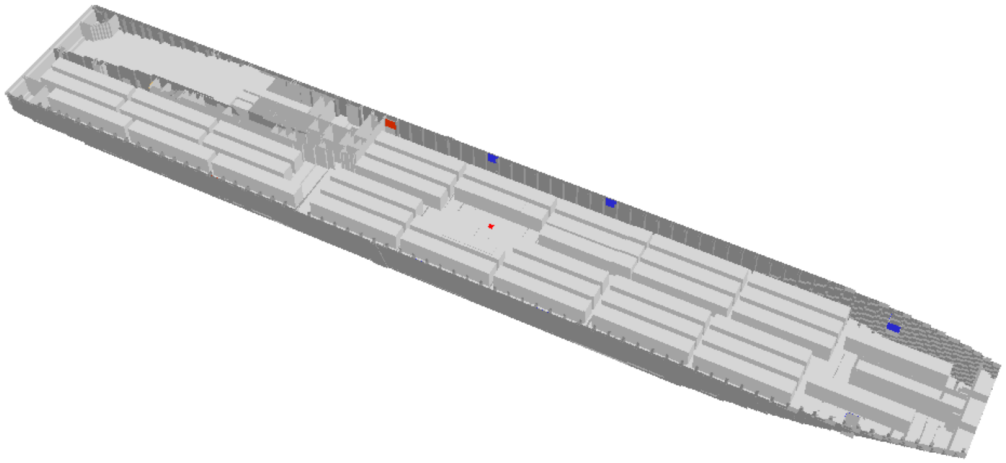

Figure 62. Deck 3 of Stena Flavia in the simulation model.

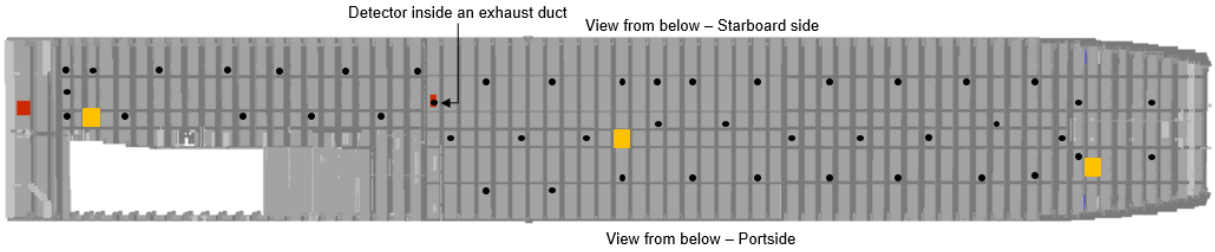

Figure 63. A view of the model from below. The girders on the deckhead can be seen. The locations of the point detectors have been marked with black dots, and locations of the fires with orange rectangles. A fire located near a ventilation supply point is located in the forward part of the ship, and a fire located near a ventilation exhaust point is located in the aft part of the ship.

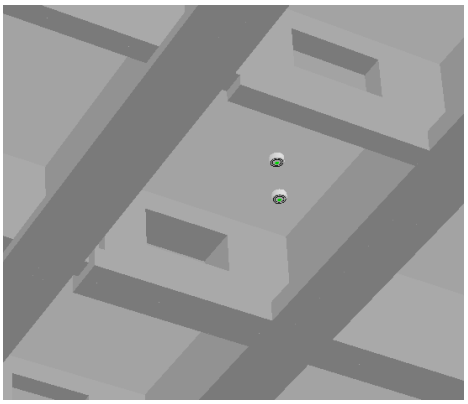

Figure 64. Point detectors at two different heights. The lower detector is approximately at the same height as the girder flange next to it, and the upper detector is located 40 cm above.

B.3.2 Domain and discretization

The simulation geometries shall conform to the rectilinear numerical grid of the FDS software. This limits the accuracy of geometrical descriptions, as simplifications are required. For open RO-RO space, the wind is included in the simulation. To achieve undisturbed wind flow over the ship, the computational domain has been large enough, especially along the wind direction for open RO-RO space. This has resulted in splitting the large computational domain using multiple meshes restricted by the available computational resources and constraints. A cell size of 20 cm has been used in the vicinity of the fire. A t^2 fire with a fast growth rate has a heat release rate of approximately 170 kW at 60 seconds and 16 MW at 600 seconds. Respectively, the chosen cell size corresponds to the characteristic fire size divided by 2.5 at 60 seconds and by 15 at 600 seconds [2]. As the cell size is limited by the computational resources and constraints, initially, the fire plume is not captured very accurately. The cell size is gradually increased when going further away from the fire, with the largest cell size being 3.2 m in the simulations.

For closed RO-RO space, a cell size of 10 cm was used in the vicinity of the fire. A t^2 fire with a fast growth rate has a heat release rate of approximately 170 kW at 60 seconds and 16 MW at 600 seconds. Respectively, the chosen cell size corresponds to the characteristic fire size divided by 5 at 60 seconds and by 29 at 600 seconds [2]. Initially, the fire plume is not captured very accurately, but the cell size is limited by the practical computational times.

The fire development was simulated for 600 seconds. The wind field was allowed to stabilize for at least 200 seconds in the simulation before the fire was included. Time step size is automatically controlled by the software. For each time step, the von Neumann and Courant-Friedrichs-Lewy stability constraints are checked [9].

B.3.3 Boundary conditions

B.3.3.1 Surfaces

All ship surfaces are assumed to be steel. It is assumed that steel surfaces are 10 mm thick. This estimate was made based on Stena Flavia's structural drawings, which were available. The surfaces are defined to be exposed to gas temperature on both sides of the surface.

Steel properties from Eurocode 3 [10] have been used. The material properties are presented in Table 23. Specific heat and conductivity depend on the solid temperature T_s, which is in Celsius degrees.

Table 23. Steel material properties [10]. T_s is the solid temperature in Celsius degrees.

Material property	Value
Emissivity (-)	0.4
Density (kg/m^3)	7850
Specific heat (J/kgK)	$450 + 0.28 \cdot T_s - 2.91 \cdot 10^{-4} \cdot T_s^2 + 1.34 \cdot 10^{-7} \cdot T_s^3$
Conductivity (W/mK)	$14.6 + 1.27 \cdot 10^{-2} \cdot T_s$

B.3.3.2 Fuel mass flux

To simulate a fire, a fuel mass flux boundary is defined. The amount of required mass flux is calculated based on the design fire curve shown in Section B.2.3. Combusting gas is assumed to be heptane, and its default value for the heat of combustion precompiled by FDS has been used. Fuel mass flux boundary condition is applied on the area of 0.8 m x 0.8 m such that at around 146 s, fire reaches the value of 1000 kW following T-squared fast fire curve. For slow fire, it takes around 584 s to reach the value of 1000 kW. In modelling the fire, it was attempted to mimic the full-scale experiments, and the fire was modelled to be similar to a burner located on the deck. An example of the modelling is shown in Figure 62.

B.3.3.3 Exterior boundaries

Velocity inlet boundary condition

A velocity inlet boundary condition is applied on the upwind side boundary in the open ro-ro space simulations. Spatially dependent wind velocity profile with the following definition is used:

$$u = u_0 \left(\frac{z}{z_0}\right)^p \quad (1)$$

where u is the wind velocity at height z, u_0 is the reference wind speed, z_0 is the reference wind height, and p is a model constant. The reference wind height z_0 is set to 10 m above sea level. A reference wind speed of 7.5 m/s is assumed, which corresponds to both the 50-year average of the southern Baltic Sea [11] and the 10-year average of the central Baltic Sea [12]. The exponent p is taken as 0.13, which is the same value as used, for example, by Rahimpour and Oshkai [13].

Upwind boundary condition

An upwind boundary condition, known as an "open boundary" using the software specific terminology, is applied on those domain sides that are parallel with the ship in the open ro-ro space simulation. In those simulations, it is also applied on the downwind domain side that is directly opposite to the velocity inlet. In the open ro-ro space simulations without wind, an open boundary condition is applied to all sides of the domain. With the upwind boundary condition, the pressure along flow streamlines remains constant and tangential velocity component gradients are set to zero.

Free-slip boundary condition

A free-slip boundary condition is applied on top of the domain in the open ro-ro space simulations. This boundary condition is required to obtain a correct velocity profile for the wind with the software.

Inert boundary condition

An inert boundary condition is applied on the bottom of the domain, i.e., the sea, in the open ro-ro space simulations. An inert boundary remains at the ambient temperature, which is set to 10 °C in

the open ro-ro space simulations. This value corresponds to an approximate annual mean value for both sea surface and air temperature in the central and southern Baltic Sea [14–16].

B.3.3.4 Ventilation

In the closed ro-ro space simulations, the ventilation outlets and inlets were modelled as per the Stena Flavia's existing arrangement as far as possible. The ventilation rate was modelled as constant, but localized leakage was applied on the doors leading to the ro-ro space so that there would not be an unphysical rise in pressure in the space.

B.3.4 Detector modelling

The following sections explain various detectors used in the simulation, along with their activation threshold. All the devices, excluding Linear Heat Detectors, are plotted as per the detectors layout provided for Stena Flavia drawing for Deck 3 and Deck 4. Locations of the points detectors in the simulation models are discussed in more detail in Sections B.3.1.1 and B.3.1.2, respectively.

B.3.4.1 Point Heat Detector

When the temperature of the sensing element of a point heat detector, referred to just as a heat detector throughout this document, exceeds the predetermined threshold value, then an activation signal is sent to the alarm panel. In FDS, the temperature of the sensing element estimated from the differential equation put forth by Heskestad and Bill [17] as

$$\frac{dT_l}{dt} = \frac{\sqrt{|u|}}{RTI}\,(T_g - T_l) \tag{2}$$

where t is the time, T_l is the temperature of the element, u is the gas velocity, T_g is the gas temperature, and RTI is the Response Time Index for the detector. RTI characterises the sensitivity of the sensing element. Low RTI values will lead to fast activation and vice versa. Furthermore, the model does not account for thermal radiation.

It can be noted that the activation of heat detectors in simulation uses a simplified model without incorporating any complexity as used in modern detection technologies. As the activation temperature used in various modern detection technologies are unknown and may differ from one to another, to capture a range of activation temperature, upper and lower limits have been chosen as 54 °C and 78 °C [18], respectively, for heat detectors in the simulations.

B.3.4.2 Point Smoke Detectors

It is very challenging to model point smoke detectors, which are referred to just as smoke detectors throughout in this document. The difficulty arises from a number of issues: (1) the production and transport of smoke in the early stage of a fire are not well-understood, (2) detectors often use complex response algorithms rather than a simple threshold or rate-of-change criteria, (3) detectors can be sensitive to smoke particle number density, size distribution, refractive index, composition, etc., and (4) most computer models, including FDS, do not provide detailed descriptions of the smoke besides its bulk transport. At best, FDS, in its present form, can only calculate the velocity and smoke concentration of the ceiling jet flowing past the detector. Regardless of the detailed mechanism within the device, any activation model included within FDS can only account for the entry resistance of the smoke due to the geometry of the detector. Issues related to the effectiveness of ionization or photoelectric detectors cannot be addressed by FDS. Nonetheless, FDS allows to take into consideration the characteristic filling time of the entire volume enclosed by the external housing and sensing chamber of a detector as smoke passing into the sensing chamber must first pass through the exterior housing, then it must pass through a series of baffles before arriving at the sensing chamber [2].

In this work, four Cleary smoke detection models (relevant to FDS software) have been used to simulate smoke detectors in various fire scenarios. Each model differs from each other based on the constants α_e, β_e, α_c, β_c that dictate the calculation of characteristic filling time and hence the detection time [1]. The values of these constants are shown in Table 24.

Table 24. Values of various constants for Cleary smoke detector model [1].

Detector	α_e	β_e	α_c	β_c
Cleary Ionization I1	2.5	-0.7	0.8	-0.9
Cleary Ionization I2	1.8	-1.1	1.0	-0.8
Cleary Photoelectric P1	1.8	-1.0	1.0	-0.8
Cleary Photoelectric P2	1.8	-0.8	0.8	-0.8

All these models use obscuration percentage value (obscuration caused by smoke particles) for activation. The default value is 3.24% (1/m) in FDS. To capture a range of obscuration, lower and upper limits have been chosen as 2% (1/m) and 12.5% (1/m) [18], respectively, for various smoke detectors in the simulations.

B.3.4.3 Linear heat detectors

FDS provides an option to measure temperature at a point using point devices. Such devices are plotted as arrays over the area having a fire with fixed intra-distance (2 m) in simulations. The arrangement of devices is discrete in nature but nearly provides continuous temperature monitoring as Linear Heat Detectors in the area of interest.

As Linear Heat Detectors can send alarm signals based on the attainment of a fixed temperature or at a fixed rate of rise of temperature, two values for each model have been chosen. These include fixed values of 57 °C [19] and 60 °C [20], and a fixed rates of rise 8 °C/120 s [19] and 14 °C/120 s [20]. Temperature lag between the cable material and the surrounding gas temperature due to the material's thermal inertia is considered[1].

Such limits are expected to cover a wide range of activation thresholds of Linear Heat Detectors commercially available.

B.3.4.4 Carbon Monoxide

FDS also provides an option to measure the concentration of Carbon Monoxide at a point using point devices. Such devices provide the value of Carbon Monoxide concentration as volume fraction, which can be converted to parts per million (ppm). To capture a range of concentration values in ppm, lower and upper limits have been chosen as 40 ppm and 400 ppm for simulations. For example, World Health Organisation recommendation is that exposure to CO level of 26 ppm is less than one hour, exposure to 52 ppm less than 30 minutes, and to 87 ppm less than 15 minutes. The health effects caused by such CO doses are considered acceptable by WHO. [21] The US Occupational Safety and Health Administration considers that the permissible exposure limit during an 8-hour time period is 50 ppm in maritime operations, but during cargo unloading and loading in ro-ro spaces, a peak CO value of 200 ppm is allowed. In other ship spaces, a maximum peak value of 100 ppm is allowed. [22]

B.3.4.5 Other non-conventional detection technologies

Activation times were estimated for the other non-conventional detection technologies based on the simulation results. It was assumed that the video flame detector would activate when there are

[1] The temperature lag was assessed based on confidential information received from a detector manufacturer. Information was received on two different linear heat detectors.

visible flames above the trucks, and the video smoke detector will activate when there is visible smoke above the trucks (optical density value of 0.1 1/m). The flame detector was assumed to activate when it was receiving more than 0.5 kW/m^2 radiation, which is estimated to correspond to a detector activating in 3–5 seconds at 10 meters from a 0.1 m^2 heptane fire. These values are supposed to represent a robust detector device, which has a relatively low sensitivity to prevent false alarms. The thermal imaging camera was assumed to activate when the temperature, either gas or surface, in the field of sight was above 200 °C.

B.3.4.6 Validation of the results

The results obtained in this work are highly qualitative in nature and have not been validated against any experimental results. The results are meant to give insight into what conditions the studied detection technologies could operate efficiently and in what conditions they might not. The activation times presented in this report are dependent on the chosen alarm sensitivities, detector types, fire locations, fuel types, environmental conditions, and many other factors.

FDS validation guide [2] has been referenced to check the validation of simulation results of detectors from the tests conducted in the past. Two fire tests from a series performed in a two-story residence were simulated, and smoke detector activation times were predicted using three different methods. The methods consisted of either a temperature correlation, a time-lagged function of the optical density, or a thermal device much like a heat detector. The purpose was to identify ways to reliably predict smoke detector activation using typical model output like temperature and smoke concentration. Another study provided a comparison between FDS computed gas velocity, temperature and concentrations at various detector locations. Few others were performed in corridors and full-scale compartments.

Some of such tests concluded that multi-room fire simulations with the FDS model can accurately predict the conditions that a sensor might experience during a real fire event. Although, a few others also reported that the smoke concentration predicted by FDS were two to five times greater than measured smoke concentrations.

As stated in the FDS Validation Guide [2], given the value (M) predicted by FDS, the true value is assumed to be normally distributed around the adjusted value $(\frac{M}{\delta})$ with the variance $(\widetilde{\sigma_M}\frac{M}{\delta})^2$, where ($\delta$) is the bias factor for a quantity, and $(\widetilde{\sigma_M})$ is the standard deviation of a predicted value. The Bias factor simply expresses the tendency for the model to overpredict or underpredict the true value of a quantity, and the standard deviation of a predicted value expresses its degree of scatter. The smoke detector model has a model bias factor (δ) of 0.61, i.e., the model tends to underpredict the time to activation. The heat detector model has not been evaluated in the FDS Validation Guide, but the sprinkler activation times have been. From the FDS modelling perspective, the heat detectors and sprinklers are almost identical. The sprinkler activation times have a model bias factor (δ) of 1.03, i.e., they can be considered to be quite accurate [2]. The standard deviation of predicted value $(\widetilde{\sigma_M})$ for smoke detector activation time and sprinkler activation time are 0.27 and 0.16, respectively. Other quantities of interest which have played a role in the detection are smoke concentration (δ = 3.73, $\widetilde{\sigma_M}$ = 1.35), ceiling jet temperature (δ = 1.03, $\widetilde{\sigma_M}$ = 0.12) and carbon monoxide concentration (δ = 0.97, $\widetilde{\sigma_M}$ = 0.41). Clearly, with a high bias factor, the overprediction of smoke concentration has contributed to the underprediction of time of activation of smoke detectors. Ceiling jet temperature, which contributes to the activation of heat detectors and linear heat detectors, has a bias factor close to 1 with lower values of standard deviation of predicted value compared to the smoke concentration. The same also holds for the concentration of carbon monoxide, which activates the carbon monoxide sensors on set thresholds. For more details, please refer [2].

B.3.5 Other simulation parameters

Simulations were run as Very Large Eddy Simulations (VLES). Default turbulence models for VLES were used, i.e., a modified Deardorff model for eddy viscosity and constant coefficient Smagorinsky model with van Driest damping for near-wall eddy viscosity [9]. Default parameters were used for other simulation parameters unless otherwise mentioned.

B.4 Simulation results

Main authors of the chapter: Nikhil Verma and Alexandra Tissari, VTT

B.4.1 Open ro-ro space simulations

Various detectors activation times are summarized in Figure 65 and Figure 66. Figure 65 shows the activation time of various detectors with lower activation threshold values, and Figure 66 shows the activation time of various detectors with higher activation threshold values. Both figures have Linear heat detectors with constant temperature activation mode. Details of all types of detectors with top five activation times are provided in appendix A. As discussed in Section B.3.4.6, the bias factor of the smoke detector is considerably lower than 1. The known bias of the model indicates that the activation times with the lower activation threshold are likely to be 13 to 43 seconds short of the adjusted value, excluding the value of scenario S6. For scenario S6, the predicted value is likely to be 97 seconds short of the adjusted value. In general, given the swiftness in which the smoke detectors have responded, the inclusion of the bias factor is not likely to defer the activation time more than a minute for a lower activation threshold. Considering fast detection (which happens with a lower activation threshold) being the main subject of interest, results presented in Figure 66 are discussed below.

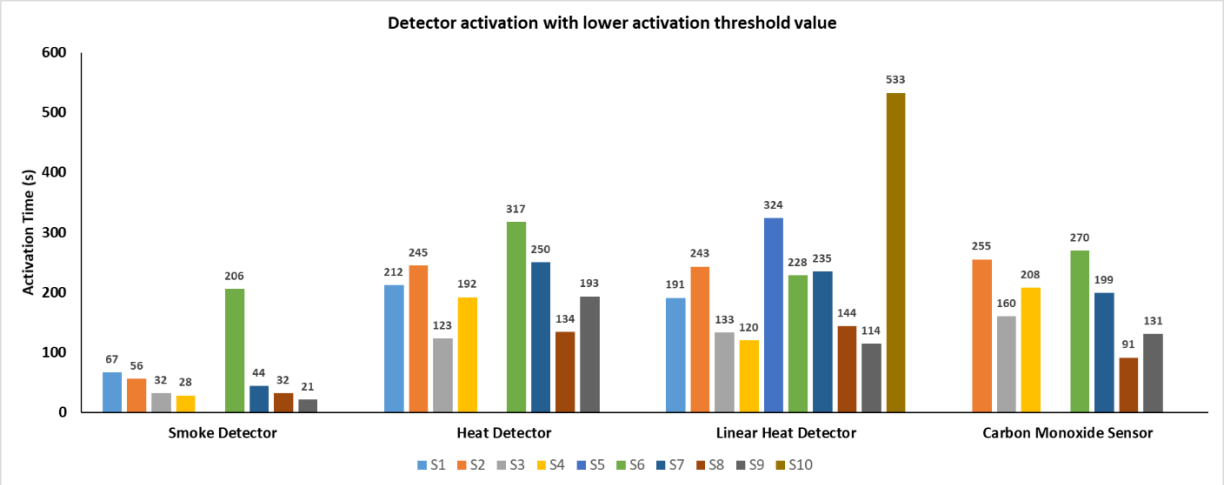

Figure 65. Detector activation times with lower activation threshold values (open ro-ro space).

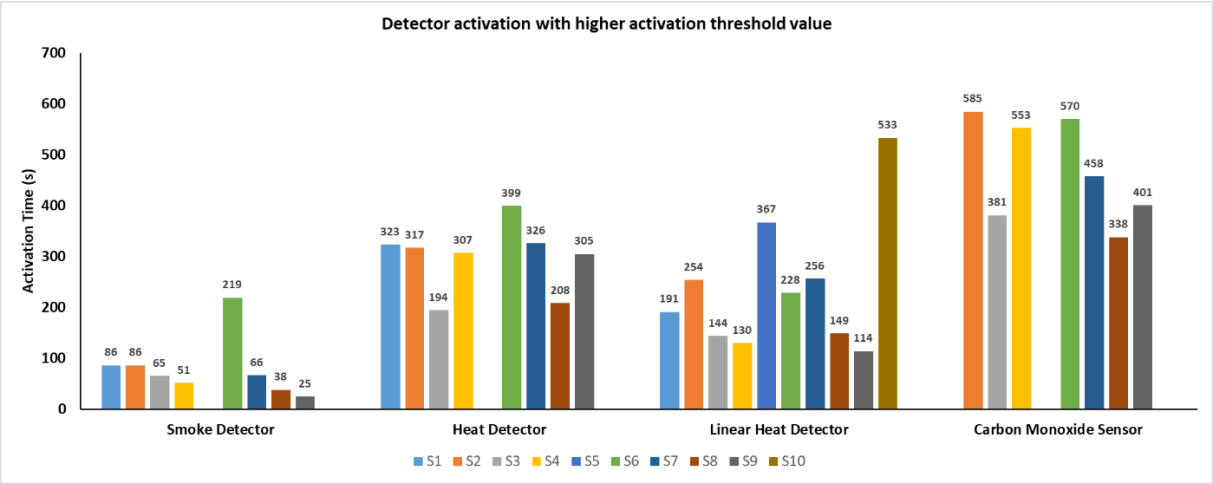

Figure 66. Detector activation times with higher activation threshold values (open ro-ro space).

It can be noted from Figure 66 that in scenarios S5, S6 and S10, either there has been no response from a few detectors, or the response has been among the slowest. In these scenarios, fire is placed near the openings, and the wind from the opposite direction has exhausted the smoke out of the openings without much delay and obstructions. This has led to the decrease in the volume of smoke that could have spread inside the space and thus their concentrations and heat, which could have activated various detectors. Although wind speed is the least in scenario S6, the wind has a lower effect on smoke movement and its characteristics compared to scenarios S5 and S10. In scenarios S2 and S7, fire is also placed near the openings, and the wind directly from the openings has affected the smoke movement and heat transportation by tilting the smoke plume towards the aft side in the simulation. This has affected the response of detectors whose activation are based on thermal properties.

Smoke detectors have been the fastest in the response in the cases where they have detected smoke. However, they failed to detect smoke in scenarios S5 and S10, and detection was very slow in the case of scenario S6. Heat Detectors did not detect fire in scenarios S5 and S10. Although, in scenario S6, heat detectors detected fire, but the detection was the slowest among all other scenarios. The linear heat detector was the only detector that detected fire in all scenarios. Although, it showed the slowest response in scenarios S2, S7 and S10. Moreover, in scenarios S1, S6, S9 and S10, the linear heat detectors have got activated at the same time for lower and upper activation thresholds. The different wind conditions, tilting of the smoke plume, and formation of smoke pockets between the beams appear to have affected the transportation of smoke in bulk. Such accumulation of smoke in pockets might have got fairly uniform high temperature which on reaching linear heat detectors with higher threshold could have triggered them (thus, also triggering the ones with the lower threshold). Carbon Monoxide sensors were the only sensors that failed to detect fire in three scenarios, i.e. S1, S5 and S10.

It can also be noted from Figure 66 that scenarios S2, S5, S6, S7 and S10 have been, in general, difficult for detectors to detect fire when they have a higher threshold for activation.

Figure 67 provides the range of activation times of various detectors. It can be observed that the smoke detector has significantly a smaller range than the other detector types. In comparison between the traditional heat detectors and linear heat detectors, heat detectors seem to have a narrower activation range. However, such range excludes scenarios S5 and S10, where traditional heat detectors have failed to detect fire. Excluding scenarios S5 and S10, linear heat detectors have

given faster response compared to conventional heat detectors. Moreover, Carbon Monoxide sensors have the broadest range of activation time, and they have been non-responsive in scenarios S1, S5 and S10.

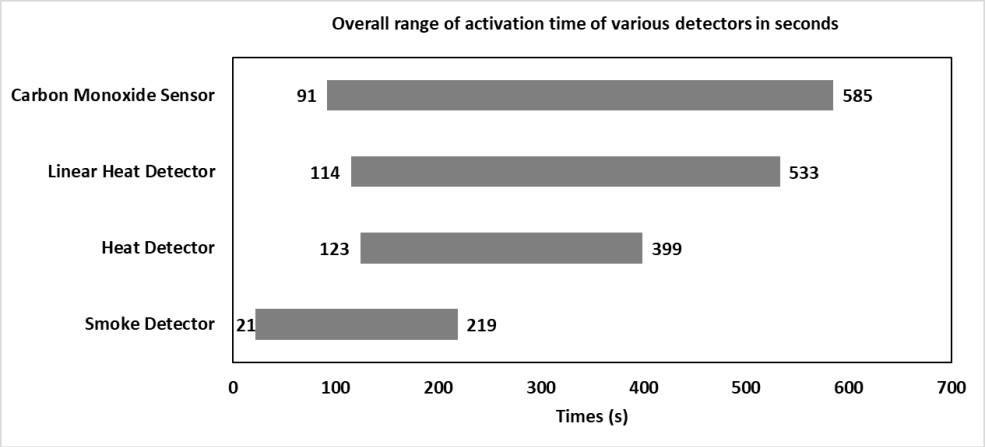

Figure 67. Range of activation time of various detectors based on predicted values (open ro-ro space).*

**For smoke detectors, adjusted values with a known bias will have a range of 34s to 359s covering lower and upper activation thresholds.*

The overall ranges based on predicted values can be used to anticipate the activation time of various detectors with lower bound and upper bound. Given the simplicity of models for detection used in FDS, such a range of values is expected to cover a realistic value of activation time in the light of the uncertainty caused by the sensitivity of detectors towards fire products (smoke particle size and distribution, refractive index etc.), aerodynamic features of the detector, internal complexity of the detector housing, a complex unknown algorithm to reduce the false alarms, etc.

The longitudinal distances between the fire and the first activated detector with each different detection technology are presented in Table 25 and Table 27. The negative sign indicates that the detector is located aft from the fire, and the positive sign indicates that the detector is located forward from the fire. For linear heat detectors, activation times correspond to absolute temperature alarm thresholds. Values are based on the lower activation thresholds. More detailed results are included in Appendix A.

Different wind conditions, along with channelling of smoke by girders, formation of smoke pockets in between girders and immediate obstructions (vehicles, trucks) around the vicinity of fire have affected the smoke movement and transportation and thus the activation of detectors. It can be noted from Table 25 that different wind conditions in different scenarios have differed the distances at which first detectors in various categories were activated. No specific detector can be pointed out to be better than the other for the distances at which they were activated. But, linear heat detectors were activated in all the scenarios and has the least value of the maximum distance at which they were activated, i.e. 11 m, whereas, for the smoke detector, heat detector and CO detector, such distance is 17 m. Images of smoke movement and transportation can be seen in Annex A, where it can be noticed that in scenarios like S1, S2 and S7, wind has strongly pushed the smoke in the aft side, which has considerably protracted the distance at which smoke has started to accumulate at the top level of the deck.

Table 25. Longitudinal distance between the fire and the first activated detector. Negative sign indicates that the detector is located aft from the fire, and positive sign indicates that the detector is located forward from the fire. For linear heat detectors, activation times correspond to absolute temperature alarm thresholds. Values are based on the lower activation thresholds. Abbreviation ND indicates that no detection occurred for the specific detector type in the considered scenario.

ID	Smoke detector	Heat detector	Linear heat detector	CO detector
S1	-17 m	-6 m	-1 m	ND
S2	-17 m	-17 m	-11 m	-6 m
S3	+11 m	+2 m	+5 m	+2 m
S4	+2 m	-5 m	+3 m	+2 m
S5	ND	ND	+1 m	ND
S6	+4 m	+4 m	+1 m	+4 m
S7	-17 m	-17 m	-9 m	-17 m
S8	+11 m	+2 m	+5 m	+2 m
S9	+2 m	-5 m	+3 m	+2 m
S10	ND	ND	+1 m	ND

Activation times for the non-conventional detection technologies, presented in Table 26, were estimated based on the qualitative analysis of simulation results. It was assumed that the video flame detector will activate when the flame is visible above the trucks. Video smoke detector would activate when there is visible smoke above the trucks (optical density value of $0.1 m^{-1}$). Moreover, for flame detector activation, criteria of heat flux greater than 0.5 kW/m^2 above truck is selected. Lastly, for the thermal imaging camera, criteria of gas and surface temperature greater than 200° C above truck is used.

Table 26. Estimated earliest activation times for the non-conventional detection technologies (open ro-ro space).

ID	Video flame detector	Video smoke detector	Flame detector	Thermal imaging camera
S1	350 s	70 s	130 s	210 s
S2	440 s	70 s	120 s	240 s
S3	240 s	30 s	220 s	150 s
S4	220 s	60 s	210 s	140 s
S5	360 s	140 s	130 s	240 s
S6	360 s	90 s	90 s	190 s
S7	460 s	40 s	140 s	250 s
S8	260 s	30 s	230 s	160 s
S9	220 s	20 s	230 s	140 s
S10	320 s	150 s	140 s	250 s

Video flame detectors are, in general, the slowest in response compared to all other non-conventional detectors. Scenario wise, their responses were slowest in scenarios S2 and S7. In both scenarios, the fire was adjacent to the opening with the incoming wind. Wind tilted the plume, and flame length got reduced in the vertical direction, which led to a delay in detection. It can be argued that tilting of flame by natural (or even mechanical) ventilation conditions can affect video flame detector performance.

Video smoke detectors, in general, were the fastest in response in most of the scenarios compared to all other non-conventional detectors. Scenario wise, their responses were slowest in scenarios S5 and

S10. In both the scenarios, the fire was adjacent to the opening, and fast wind was blowing to push them directly outside the window without much obstruction. Clearly, the possibility or placement of fire adjacent to openings from where smoke can easily flow out can delay the performance of video smoke detectors.

Flame detectors after video smoke detector were second-fastest in response in scenarios where the fire was adjacent to openings excluding scenarios S5 and S10, where they were the fastest. Scenario wise, in the case of fire placed along the centreline (S3, S4, S8, S9), their responses were the slowest compared to non-centreline fires. It can be argued that if the radiation receiver is assumed to be along sidewalls, then more is the distance of such walls from fire location, the less would be the intensity of radiation being received at the receiver. In such cases, if the weak intensity is received at the flame detector, then detection can fail.

Thermal imaging cameras have performed better than video flame detectors in the simulations. They recorded slower responses in scenarios S2, S5, S7 and S10. In the case of scenarios S5 and S10, fire was adjacent to the opening, and fast wind was blowing to push them directly outside the window without much obstruction. This reduced the spread of smoke inside the space and hence the smoke temperature. In scenarios S2 and S7, the fire was adjacent to the opening with the fast incoming wind, which diluted the smoke and reduced its temperature.

It can be concluded that video smoke detectors are, in general, the fastest in response to the non-conventional detection technologies. To negate the slow response of video smoke detectors in some scenarios, only flame detector could be thought to be used, as other detectors have been slower in response than flame detectors. However, obstructions can also affect the activation of flame detectors as the height of vehicles can come in between the view angle of such detectors.

B.4.2 Closed ro-ro space simulations

Detector activation times with the lower threshold values are shown in Figure 68, and activation times with the higher threshold values in Figure 69. It can be observed that without exception, traditional smoke detector activates fastest. As discussed in Section B.3.4.6, the bias factor of the smoke detector is considerably lower than 1. The known bias of the model indicates that the activation times with the lower activation threshold are likely to be 27 to 65 seconds too short of the adjusted value. In general, given the swiftness in which the smoke detectors have responded, the inclusion of the bias factor is not likely to defer the activation time more than a minute or so for a lower activation threshold. Moreover, the CO detector would activate faster than the smoke detector in scenarios S14 and S15. In the other scenarios, the smoke detector would still remain faster even with accounting for the probable model bias.

The heat detector fails to predict the fire in scenario S16, and in scenarios S17 and S18, it takes more than 10 minutes to detect the fire. Similarly, a linear heat detector takes more than 10 minutes to detect the fire in scenarios S17 and S18, but unlike the traditional heat detector, it does also activate in S16. The carbon monoxide sensor does not activate in scenarios S16 to S18. The scenarios S16 to S18 have fires with slow growth rates.

It can be observed that for all detector types included in the figure, the fire location in the middle leads to delayed detector activation. For smoke and heat detectors, the fire location near the ventilation exhaust gives shorter activation times than the other locations, but for linear heat detectors and CO detectors, the fire closer to the supply point can be detected faster. However, the differences are small and can be due to differences in detector positions.

Similarly, when scenarios S11 and S14 are compared, the differences in detection time are small. The scenarios are otherwise identical, but the fire has been shifted by half a beam span in the scenario S14. Similarly, the only difference between scenarios S11 and S15 is that the openings in girders have been removed in S15. The differences in activation times are quite small, except for the carbon monoxide sensor. The scenarios S11–S14 and S19–S21 are identical except for the CO and soot yields. Based on the results, varying the values at this range does not have a significant effect on the results.

More simulation results are included Annex B.

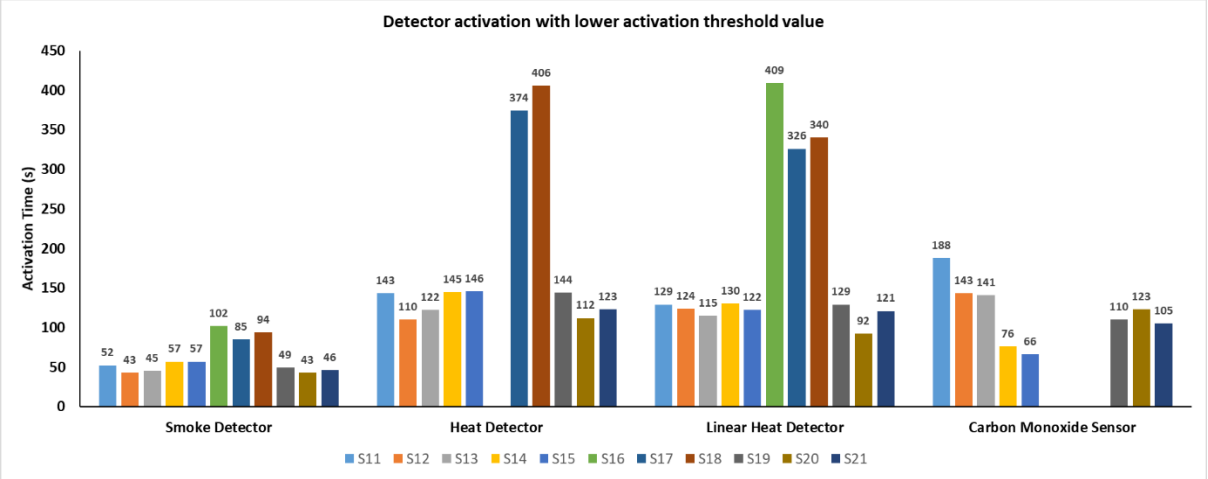

Figure 68. Detector activation times with lower activation threshold values (closed ro-ro space).

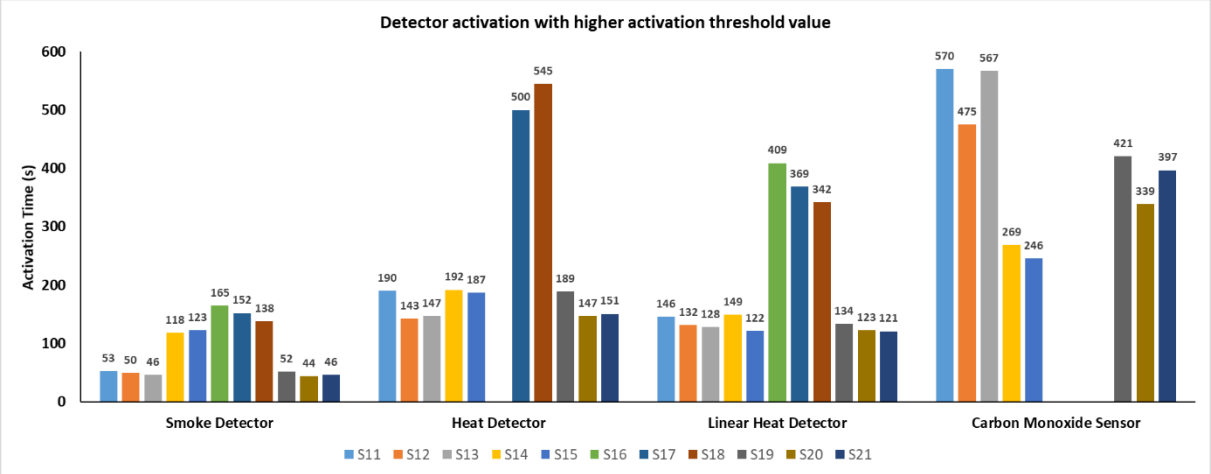

Figure 69. Detector activation times with higher activation threshold values (closed ro-ro space).

The range of activation times for various detectors is shown in Figure 70. It can be observed that the smoke detector has significantly a smaller range than the other detector types. In comparison between the traditional heat detectors and linear heat detectors, the linear heat detectors seem to have a narrower activation range.

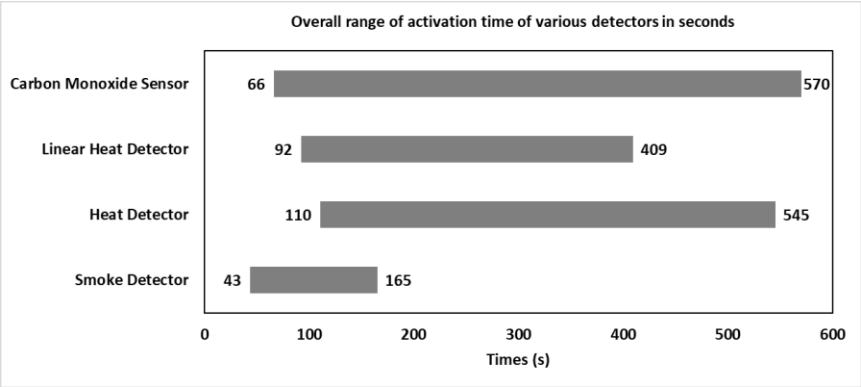

Figure 70. Range of activation times for various detectors (closed ro-ro space).*

**For smoke detectors, adjusted values with known bias, will have range of 70s to 270s covering lower and upper activation threshold.*

The longitudinal distances between the fire and the first activated detector with each different detection technology are presented in Table 27. Negative sign indicates that the detector is located aft from the fire, and positive sign indicates that the detector is located forward from the fire. For linear heat detectors, activation times correspond to absolute temperature alarm thresholds. As the point detectors are simulated at two heights, it's indicated which one would activate first and how much later the other one would activate. Values are based on the lower activation thresholds. More detailed results are included in Annex B, including the results with a rate of rise criteria for applicable detector types. Using the rate of rise criteria led to significantly longer detection times, and in some scenarios, the threshold value was not exceeded during the simulation.

Table 27. Longitudinal distance between the fire and the first activated detector. Negative sign indicates that the detector is located aft from the fire, and positive sign indicates that the detector is located forward from the fire. For linear heat detectors, activation times correspond to absolute temperature alarm thresholds. As the point detectors are simulated at two heights, it's indicated which would activate first and how much later the other one would activate. Values are based on the lower activation thresholds. Abbreviation ND indicates that no detection occurred for the specific detector type in the considered scenario.

ID	Smoke detector	Heat detector	Linear heat detector	CO detector
S11	-5.5 m, lower and upper same time	-5.5 m, lower first, upper +2 s	-3 m	-0.7 m, upper first, lower +10 s
S12	-3 m, lower first, upper +4 s	-3 m, lower first, upper +5 s	-2 m	-3 m, lower and upper same time
S13	-1.8 m, lower first, upper +1 s	-1.8 m, upper first, lower +9 s	-0.6 m	-1.8 m, lower first, upper +7 s
S14	- 6.3 m, upper first, lower +2 s	-6.3 m, lower first, upper +1 s	-3.8 m	-6.3 m, lower and upper same time
S15	-5.5 m, upper first, lower +2 s	-0.7 m, upper first, lower +14 s	-3 m	-5.5 m, lower first, upper +1 s
S16	-5.5 m, lower first, upper +20 s	ND	-3 m	ND
S17	-3 m, lower first, upper +4 s	-3 m, lower first, upper +14 s	-2 m	ND
S18	-1.8 m, upper first, lower +6 s	-1.8 m, upper first, lower +14 s	-0.6 m	ND
S19	-5.5 m, upper first, lower +2 s	-5.5 m, upper first, lower +1 s	-3 m	-5.5 m, lower first, upper +1 s
S20	-3 m, lower first,	-3 m, lower first,	-2 m	-3 m, lower first,

	upper +2 s	upper + 6 s		upper +2 s
S21	-1.8 m, lower first, upper +2 s	-1.8 m, upper first, lower +6 s	-0.6 m	-1.8 m, upper first, lower +8 s

In most scenarios, the first activated detector is the longitudinally closest detector in the same transversal area as the fire, e.g., for scenario S11, the first activated smoke and heat detectors are close to the centreline, similar to the fire. However, in scenario S11, the CO detector which activates first is the longitudinally closest detector located on the portside. In most scenarios, the activated smoke, heat and CO detectors are positioned on the same location both transversally and longitudinally, although the vertical location of the first activated detector can vary. In comparison between scenarios S11 and S15, closure of openings in girders seems to affect which heat detector and CO detector activate first, but not the smoke detector and linear heat detector.

The difference in activation times between the detectors located at different heights does not seem to be significant in the studied cases: for smoke and CO detectors, there seems to be a slight improvement in activation time if the detector is located near the lower edge of the girders rather than closer to the deckhead. For heat detectors, no conclusions can be made, as an equal number of first activated detectors are located in both lower and upper positions. The difference in activation times between the detectors located in lower and upper positions are in most scenarios, less than 10 seconds. The difference is especially small for the smoke detectors, whereas CO detectors have slightly larger differences and the heat detectors the largest.

The development of temperature, CO concentration and visibility through the smoke was monitored at a point inside the exhaust ventilation duct serving the closed ro-ro space. The temperature development in the different simulations is shown in Figure 71. The lowest temperatures, i.e., less than 30 °C at the end of the simulation, in the exhaust duct are obtained when the fire has a slow growth rate or when the fire is located near another exhaust duct. Slightly higher temperatures, i.e., between 40 and 50 °C at the end of the simulation, are obtained when the fire is located in front of a supply point. The highest temperatures in the exhaust duct are obtained when the fire is located near the studied exhaust duct. However, if the same alarm thresholds would be used as for the conveniently located heat detectors, it is evident that the activation times would be excessively long. Furthermore, the temperature does not begin to increase in any of the simulations before 60 seconds has passed after the fire ignition.

The same is true for the development of CO concentration, shown in Figure 72, which does not show any increase before a minute has passed, and for the development of visibility through smoke, shown in Figure 73, which does not reduce in any of the simulations before almost two minutes have passed. The trends which can be observed for the CO concentrations and visibility are very similar as for the temperatures: the increase in concentration and reduction in visibility through smoke seems to be correlated with the location of the fire. Thus, it seems that while detection of the fire from the exhausted gases is possible, much larger delays are observed than with conventionally located detectors. Even if the fire is located near the exhaust vent, the fire products and hot gases are so greatly diluted with fresh air, that quick detection seems rather unlikely even if very low alarm thresholds are used. In addition, the use of very low alarm thresholds would indicate a large number of nuisance alarms, or it would require that the detection system is disabled for cargo operations.

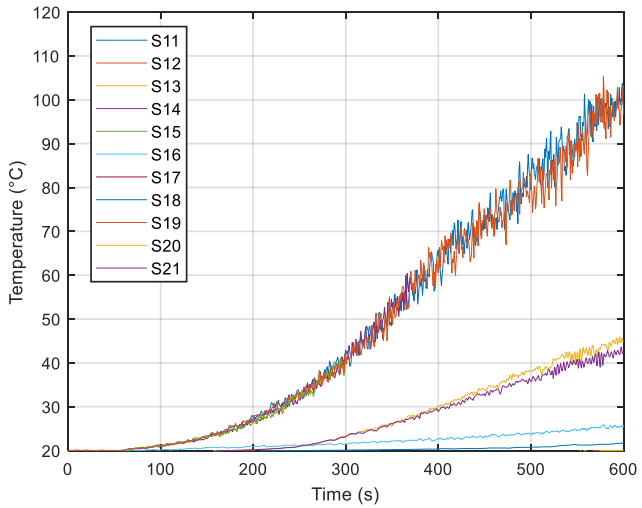

Figure 71. Temperature development at the monitored point inside the exhaust ventilation duct serving the closed ro-ro space.

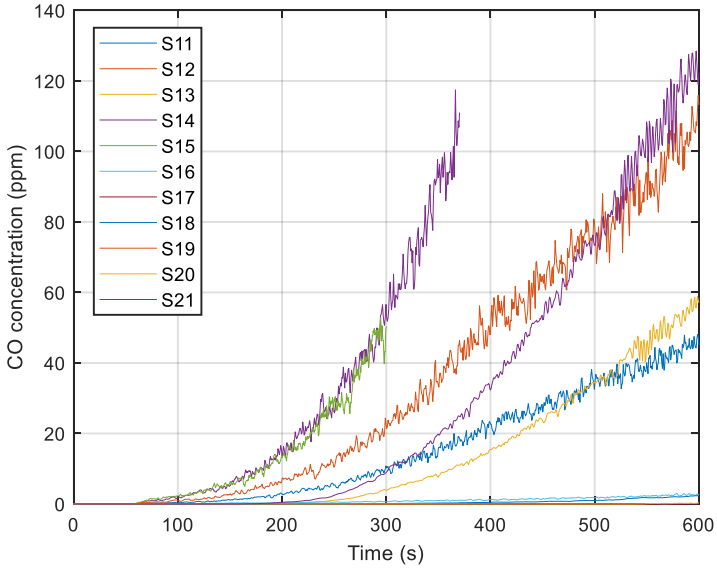

Figure 72. Development of the CO concentration at the monitored point inside the exhaust ventilation duct serving the closed ro-ro space.

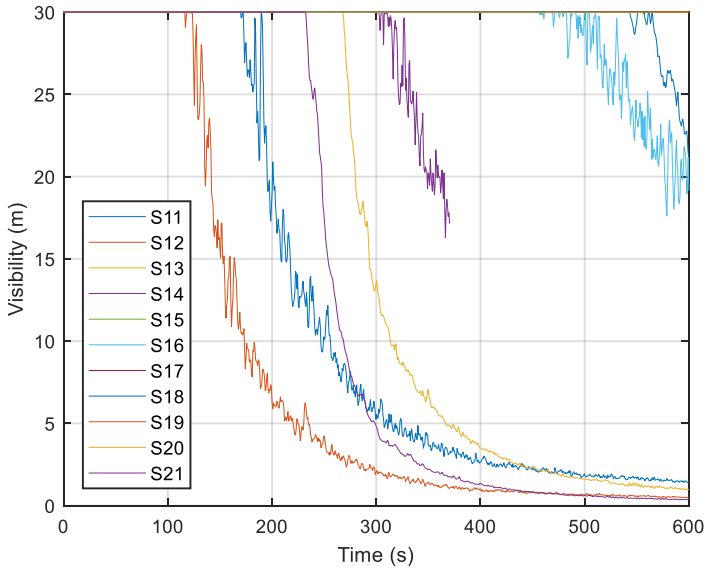

Figure 73. Development of the visibility through smoke at the monitored point inside the exhaust ventilation duct serving the closed ro-ro space.

Activation times were estimated for the other detection technologies using the principles presented in section B.4.1. The estimated earliest activation times for the non-conventional detection technologies in the closed ro-ro space are shown in Table 28.

Table 28. Estimated earliest activation times for the non-conventional detection technologies (closed ro-ro space).

ID	Video flame detector	Video smoke detector	Flame detector	Thermal imaging camera
S11	400 s	70 s	130 s	200 s
S12	300 s	40 s	270 s	200 s
S13	300 s	40 s	160 s	130 s
S14	400 s	120 s	180 s	200 s
S15	400 s	90 s	180 s	200 s
S16	>> 600 s	160 s	570 s	>> 600 s
S17	>> 600 s	80 s	400 s	>> 600 s
S18	>> 600 s	100 s	530 s	>> 600 s
S19	300 s	50 s	130 s	170 s
S20	300 s	40 s	270 s	200 s
S21	300 s	40 s	160 s	130 s

When the fire is in the middle location, the flames are strongly tilted due to ventilation and not visible above trucks, which does not favour video flame detection. Similarly, while there is high temperature gas above the trucks earlier than clearly visible smoke, still relatively long times are required both by conventional flame detectors and thermal imaging cameras.

When the fire is located near the ventilation outlet, the flames are less tilted, but the hot gases are exhausted more efficiently out of the space, which leads to less radiation to the surroundings. When the fire is located near the ventilation inlet, the flames are leaning towards a wall. The ventilation strongly circulates and dilutes the smoke and the gases.

When the fire growth rate is slow, there are no visible flames or very high temperature gases above trucks (scenarios S16–S18).

The effect of the local ventilation environment seems to be significant, as the small change in fire location between scenarios S11 and S14 changes the video smoke detector and flame detector activation times by 50 seconds.

The approach used here is very approximative, but for many scenarios, it seems that the video smoke detector could have similar activation rates as a traditional smoke detector. For the video flame detector, the environment seems quite challenging, as it often takes a relatively long time before the flames become visible. Similarly, the flame detector requires a relatively long time to activate, as there are large obstructions between the fire and the detectors. The thermal imaging camera could, in theory, obtain relatively small detection times if the alarm threshold is set to a low value to compensate for the dilution by the ventilation. However, this could lead to a large number of nuisance alarms, especially if the detection system is not disabled during loading and unloading operations.

B.5 Conclusion

Main author of the chapter: Alexandra Tissari, VTT

CFD simulations of fire detection in closed and open ro-ro spaces have been performed using the FDS software. Both traditional and non-conventional detection technologies have been included in the simulations. Different fires, fire locations and ventilation conditions were studied.

In almost all the simulations, the traditional smoke detectors detected the fire fastest, although this assumes that the smoke detectors are fully functional. This is while point detectors tend to get

damaged easily especially in open ro-ro spaces. A smoke detector failed to detect the fire only in one open ro-ro space simulation where the linear heat detector succeeded in detection.

In the closed ro-ro space simulations, it was noted that while the fire growth rate remains the same and other factors are varied, the differences in activation times remain small. However, for the open ro-ro space simulations, an unfavourable combination of fire location and wind condition could lead to fire not being detected by some detection technologies or could lead to very long activation times. Based on the results, it seems that the fire in the ro-ro space could also be detected from an exhaust ventilation duct serving the space, but much larger delays are expected than with conventionally located detectors. It was observed from the closed ro-ro space simulations that the detectors located longitudinally closest to the fire would activate first in all scenarios. The detectors were also positioned at two different heights in otherwise equal positions in the closed ro-ro space simulations: based on the results, the difference in activation times between the detectors located in lower and upper positions was in most scenarios less than 10 seconds. The results are dependent on the ship arrangement, and results for spaces with different ventilation or girder arrangements could be significantly different.

In the open ro-ro spaces, the video smoke and flame detectors seemed to be the most promising non-conventional technologies. However, the success of the flame detectors is dependent on their location in the ro-ro space. Both video flame detectors and thermal imaging cameras could have challenges in detecting fires when the fire location and wind conditions are unfavourable.

Of the non-conventional detection technologies, the video smoke and linear heat detectors seem to be the most promising technologies for the closed ro-ro spaces. Based on the qualitative assessment, the obstructed spaces might not be the best working environment for the video flame detectors and flame detectors, but similarly, as for the open ro-ro spaces, the result is highly dependent on the fire location and the existing environmental conditions during the fire. The use of thermal imaging cameras should also be further considered: their use for effective fire detection seems to be dependent on how low their alarm threshold can be set without an excessive number of nuisance alarms in normal use, as the high ventilation rates can effectively dilute the hot gases closer to ambient level. The thermal imaging cameras can also activate based on hot surfaces, which could enable noticing possible fires before ignition. However, the crowded ro-ro spaces can make noticing hotspots quite challenging, as the cameras cannot see most of the cargo.

For open ro-ro spaces, the fire is most difficult to detect in scenarios where the fire is located near the side openings. In such cases, linear heat detectors and video smoke detectors were the most promising new technologies based on the simulations.

The key function of this report is to assess the capabilities of different detection technologies to detect fires in open and closed ro-ro spaces. Challenging scenarios for different detection technologies have been examined to explore the detectors that may be suitable in one scenario over another. The methods used in this report are approximative, and many assessments have been made in a qualitative manner due to a lack of information about exact working principles and activation mechanisms of different detection technologies. The lack of information has led to using a large number of estimates in this work. Detectors from different manufactures could have properties and capabilities which are significantly different from those which have been assumed here. The results presented in this report are dependent on the used geometries and the assumptions made. The activation times presented in this report should not be used as a design basis of any kind.

B.6 References

[1] K. McGrattan, S. Hostikka, R. McDermott, J. Floyd, C. Weinschenk, and K. Overholt, “Fire Dynamics Simulator, Technical Reference Guide, Volume 1: Mathematical Model, NIST Special Publication 1018-1.” National Institute of Standards and Technology, Gaithersburg, Maryland, 2020.

[2] K. McGrattan, S. Hostikka, J. Floyd, R. McDermott, and M. Vanella, “Fire Dynamics Simulator, Technical Reference Guide, Volume 3: Validation, NIST Special Publication 1018-3.” National Institute of Standards and Technology, Gaithersburg, Maryland, 2020.

[3] J. Wikman *et al.*, “Study investigating cost effective measures for reducing the risk from fires on ro-ro passenger ships (FIRESAFE), EMSA/OP/01/2016,” 2016. [Online]. Available: http://www.emsa.europa.eu/emsa-documents/latest/item/2931-study-investigating-cost-effective-measures-for-reducing-the-risk-from-fires-on-ro-ro-passenger-ships-firesafe.html.

[4] M. K. Cheong, M. J. Spearpoint, and C. M. Fleischmann, “Calibrating an FDS simulation of goods-vehicle fire growth in a tunnel using the Runehamar experiment ,” *Journal of fire protection engineering* , vol. 19, no. 3. SAGE PUBLICATIONS LTD , LONDON , pp. 177–196, 2009, doi: 10.1177/1042391508101981.

[5] M. K. Cheong, M. J. Spearpoint, and C. M. Fleischmann, “Design fires for vehicles in road tunnels,” in *Proc. 7th International Conference on Performance-Based Codes and Fire Safety Design Methods*, 2008, pp. 229–240.

[6] N. Iqbal and M. H. Salley, “Fire Dynamics Tools (FDTs): Quantitative Fire Hazard Analysis Methods for the U.S. Nuclear Regulatory Commission Fire Protection Inspection Program, Final Report (NUREG-1805),” Washington, DC, 2004.

[7] B. Karlsson and J. Quintiere, *Enclosure fire dynamics*. CRC press, 1999.

[8] M. J. Hurley, “Thermophysical Property Data,” in *SFPE Handbook of Fire Protection Engineering*, M. J. Hurley, D. Gottuk, J. R. Hall, K. Harada, E. Kuligowski, M. Puchovsky, J. Torero, J. M. Watts, and C. Wieczorek, Eds. Springer New York, 2016, pp. 3425–3475.

[9] K. McGrattan, S. Hostikka, J. Floyd, R. McDermott, and M. Vanella, “Fire Dynamics Simulator, User’s Guide, NIST Special Publication 1019.” National Institute of Standards and Technology, Gaithersburg, Maryland, 2020.

[10] European Committee for Standardization, *EN 1993-1-2:2005 Eurocode 3: Design of steel structures. Part 1-2: General rules. Structural fire design*. 2005.

[11] W. Zhang, J. Harff, and R. Schneider, “Analysis of 50-year wind data of the southern Baltic Sea for modelling coastal morphological evolution – a case study from the Darss-Zingst Peninsula ,” *Oceanologia* , vol. 53, no. 1-. Elsevier Urban & Partner Sp. z o.o , SOPOT , pp. 489–518, 2011, doi: 10.5697/oc.53-1-TI.489.

[12] A. Pena Diaz *et al.*, “South Baltic Wind Atlas: South Baltic Offshore Wind Energy Regions Project,” 2011.

[13] M. Rahimpour and P. Oshkai, “Experimental investigation of airflow over the helicopter platform of a polar icebreaker ,” *Ocean engineering* , vol. 121. Elsevier Ltd , OXFORD , pp. 98–111, 2016, doi: 10.1016/j.oceaneng.2016.05.023.

[14] M. Naumann *et al.*, “Hydrographic-hydrochemical assessment of the Baltic Sea 2017,” 2018.

[15] A. Omstedt, C. Pettersen, J. Rodhe, and P. Winsor, “Baltic Sea Climate: 200 Yr of Data on Air Temperature, Sea Level Variation, Ice Cover, and Atmospheric Circulation,” *Climate Research - CLIMATE RES*, vol. 25, pp. 205–216, Jan. 2004, doi: 10.3354/cr025205.

[16] K. Bradtke, A. Herman, and J. Urbanski, “Spatial and interannual variations of seasonal sea surface temperature patterns in the Baltic Sea,” *Oceanologia*, vol. 52, Sep. 2010, doi: 10.5697/oc.52-3.345.

[17] G. Heskestad and R. G. Bill Jr, “Quantification of thermal responsiveness of automatic sprinklers including conduction effects ,” *Fire safety journal* , vol. 14, no. 1–2. pp. 113–125, 1988, doi: 10.1016/0379-7112(88)90049-5.

[18] International Maritime Organization (IMO), *FSS-Code (Fire Safety Systems Code) - Res. MSC.98(73)*. 2014.

[19] Underwriters Laboratories Inc., “UL 521. Heat Detectors for Fire Protective Signaling Systems,” p. 78, 2010.

[20] International Organization for Standardization, “EN 54-22:2015. Fire detection and fire alarm systems. Resettable line-type heat detectors,” p. 83, 2015.

[21] World Health Organisation, “WHO Guidelines for Indoor Air Quality: Selected Pollutants.” World Health Organisation, Geneva, 2010.

[22] Occupational Safety Health Organisation, “OSHA Fact Sheet, Carbon Monoxide Poisoning (DSG FS-3522),” 2012.